ROLE OF COAGULATION IN XENOBIOTIC-INDUCED LIVER INJURY

By

Bradley Paul Sullivan

Submitted to the graduate degree program in Pharmacology, Toxicology and Therapeutics and the Graduate Faculty at the University of Kansas Medical Center for the partial fulfillment of the requirements for the degree Doctor of Philosophy

_____
Chairperson: Bruno Hagenbuch

_____
Mentor: James P. Luyendyk

_____
Hartmut Jaeschke

_____
Partha Kasturi

_____
John Wood

_____: Date Defended

The Dissertation Committee of Bradley Paul Sullivan certifies that this is the approved version of the following dissertation.

ROLE OF COAGULATION IN XENOBIOTIC-INDUCED LIVER INJURY

_____
Chairperson: Bruno Hagenbuch

_____
Mentor: James P. Luyendyk

_____: Date Approved

Abstract

The liver is a common target for xenobiotic-induced toxicity. Of importance, synthesis of soluble coagulation factors by the liver plays an essential role in hemostasis. Blood coagulation cascade activation is evident in both human patients and in animal models of liver injury. Several studies have shown that coagulation is not merely a process reactive to toxicity, but rather a critical determinant of liver disease pathogenesis. Previous studies have utilized global anticoagulation as a strategy to investigate the role of coagulation in liver injury. Currently, our understanding of the mechanisms whereby individual coagulation proteases contribute to hepatotoxicity is inadequate.

Blood coagulation is initiated by tissue factor (TF), a transmembrane cellular receptor for the coagulation factor VII/VIIa. The TF:VIIa complex initiates a serine protease cascade, which culminates in the generation of the serine protease thrombin. Thrombin cleaves circulating fibrinogen to initiate fibrin clot formation. Additionally, thrombin signals to multiple cell types through activation of protease activated receptors (PARs), which can promote inflammation and platelet aggregation. The procoagulant response is balanced by several anticoagulant proteins and fibrin clot degradation is catalyzed by plasmin, the main endogenous fibrin degradation enzyme. The aim of this dissertation was to determine the role of several blood coagulation cascade components in the responses elicited by two model hepatotoxicants; α-naphthylisothiocyanate (ANIT) a toxicant that damages bile duct epithelial cells (BDECs), and acetaminophen (APAP), a common analgesic that causes centrilobular hepatocellular necrosis at high doses.

We found that TF-dependent generation of thrombin contributed to the progression of chronic ANIT-induced hepatic inflammation and fibrosis by a mechanism requiring PAR-1. PAR-1 activation amplified TGF-β1-induced αVβ6 integrin expression by BDECs, and activation of TGF-β signaling *in vivo*. This suggests a novel feed-forward mechanism whereby coagulation can promote fibrogenesis. In contrast, PAR-1 was not required for the acute hepatotoxic effects of ANIT. Rather, ANIT-induced liver

injury occurred by a mechanism involving activation of PAR-4 on platelets and fibrin(ogen). The results highlight a differential contribution of thrombin signaling in acute and chronic cholestatic liver injury.

Previous studies identified the primary inhibitor of fibrinolysis, plasminogen activator inhibitor-1 (PAI-1), as a key hepatoprotective factor in APAP-induced liver injury. Indeed, hepatic fibrin deposition is a prominent feature of APAP-induced hepatocellular necrosis. To our surprise, fibrin(ogen) did not contribute to acute APAP-induced liver injury. Of importance, plasminogen deficiency reduced APAP hepatotoxicity. Taken together, the results suggest that plasmin(ogen) promotes APAP-induced liver injury in a fibrin independent manner.

Overall, these studies revealed novel pathways whereby elements of the coagulation cascade promote liver injury induced by two classical hepatotoxicants. The results suggest that individual coagulation cascade components may play divergent roles in different models of liver injury and potentially at different time points during injury development. Further studies systematically evaluating individual coagulation factors in animal models and human disease are required to fully understand the dynamic contribution that coagulation cascade proteins play in liver injury.

Acknowledgements

First and foremost I would like to recognize the amazing support that I received from my Ph.D. research mentor Dr. James P. Luyenyk. Jim was a source of scientific passion and excitement at all times regardless of whether specific assays or experiments were working. Jim also provided an array of projects to choose from in the lab, so I would never get bored by sticking with just one project or get stuck at a scientific dead end. Indeed, this was probably part of the formula for my success as a graduate student. Furthermore, I also have to acknowledge Jim's patience, as he had the privilege of reviewing my scientific manuscripts, of which some went through numerous rounds of editing. In addition to being a mentor, friend, and colleague Jim was also a great teacher of which I learned several Ph.Ds. worth of information from.

In addition to Jim, several other members of the Luyendyk laboratory made day to day activities a little bit easier. The first member is Dr. Karen Kassel, who was a postdoctoral research fellow for several years during my tenure. Karen always came to work in a joyful mood and was extremely pleasant to work with. Karen also had a thing for being organized, which seemed to be a necessary counterbalance to the Luyendyk lab, although Jim would tell you that we were organized. Next is Ruipeng Wang, also known as Frank. Frank was a great research technician who could cut any tissue on the cryostat and subsequently immunostain that same tissue with almost any antibody combination you would like. In addition, Frank's unique passion to farm, fish, and "hunt" always evoked a fresh smile (or laugh) from the lab. Steph Bishop, another graduate student in the lab was also another avenue to discuss science or just escape the current research thought and talk about something that really matters……bikes! I would also like to give a combination thank you to both Steph and Karen, who both seem to have eagle eyes for all things grammar, which on numerous occasions helped to straighten out the "Bradisms" that sometimes appeared in manuscripts and presentations. Huina Cai was a master of the mouse colony. Her dedication to the care of all the animals helped to keep experiments on track and appropriately controlled with the correctly genotyped animals. In addition to the KUMC Luyendyk lab, I would also like to recognize the

Michigan State University crew. The new MSU lab has helped make my transition to Michigan a little smoother. My success as a graduate student rests on the dedication and collaboration of this entire team.

I would also like to thank my graduate student committee, which has given me both general support and helpful advice on the progression of my scientific projects and writing. In particular, I would like to thank Dr. Bryan Copple for his generous support, scientific collaboration, and unique scientific insights. Bryan served on my committee prior to his acceptance of a new position at Michigan State University and also served as a rotation research mentor in my first year of the IGPBS program. I would also like to thank both the current and past members of the Pharmacology, Toxicology and Therapeutics department at the University of Kansas Medical Center. Between all of the students, post docs, and faculty there was always a solution to a technical problem, reagent shortage, or just someone to talk through the science. Additionally, the staff within the department always had a time saving solution to whatever administrative challenge I was facing at the time. Thanks.

Last, but not least is my family and friends. First my parents, who have given me the background experiences and knowledge that were an essential foundation to both complete an undergraduate degree and to pursue an advanced Ph.D. degree. Additionally, family functions and dinners within the last few years have proven essential vectors for entertainment and relaxation. I would also like to thank my in-laws for their unconditional support and endless list of activities at the Phillips Farm. Of importance, I would also like to thank two of my most trusted social scientist collaborators, my loving wife Kayla and her soul mate and fellow social scientist Tara Turpin for the extensive in depth scientific discussions that have lead to numerous discoveries. And of course my wife Kayla and our two dogs who can always be trusted to take the headache out of any long day at work.

Financial support for this endeavor was granted through the National Institutes of Health, P20RR021940, T32ES007079, R01 ES017537, R01 DK087886 and from the University of Kansas Medical Center Biomedical Research Training Program (BRTP).

Table of Contents

List of abbreviations

ALP	Alkaline phosphatase
ALT	Alanine aminotransferase
ANIT	Alpha-naphthylisothiocyanate
APAP	Acetaminophen
asTF	alternatively spliced tissue factor
αVβ6	AlphaVbeta6 integrin
BDEC	Bile duct epithelial cell
BDL	Bile duct ligation
BSA	Bovine serum albumin
cDNA	Complimentary deoxyribose nucleic acid
Col1a1	Collagen Type 1 alpha 1
CHX	Cycloheximide
CK-19	Cytokeratin 19
CTGF	Connective tissue growth factor
DMSO	Dimethyl sulfoxide
ELISA	Enzyme-linked immunosorbant assay
Fbg	Fibrinogen
FBS	Fetal bovine serum
flTF	Full length tissue factor
FXR	Farnesoid X receptor
GAPDH	Glyceraldehyde 3-phosphate dehydrogenase
H&E	Hematoxylin and eosin stain
HPC	Hepatocyte
ICAM-1	Intracellular adhesion molecule-1
IgG	Immunoglobulin
i.p.	Intraperitoneal
Itgb6	Integrin beta 6
MAPK	Mitogen activated protein kinase
MCP-1	Monocyte chemotatic protein-1 (CCL2)
MMP	Matrix metalloproteinase
MPO	Myeloperoxidase
mRNA	Messanger ribonucleic acid
NAPQI	*N*-acetyl-*p*-benzoquinone imine
OCT	Optimal cutting temperature compound
PAI-1	Plasminogen activator inhibitor-1
PAR	Protease activated receptor
PBC	Primary biliary cirrhosis
PBS	Phosphate buffered saline
PCA	Procoagulant activity
Plg	plasminogen
p.o.	per os (oral gavage)
PSC	Primary sclerosing cholangitis
qPCR	Quantitative polymerase chain reaction
RLU	Relative light unit
r.o.	retro-orbital
SAA1	Serum amyloid A1
SEC	Sinusoidal endothelial cell
SEM	Standard error mean
siRNA	Small inhibitory ribonucleic acid

SMAD	Mothers against decapentaplegic homologue
TA	Tranexamic acid
TAT	Thrombin anti-thrombin
TF	Tissue factor
TGF-β	Transforming growth factor beta
TIMP-1	Tissue inhibitor of metalloproteinase-1
TNK	Tenecteplase
tPA	tissue-type plasminogen activator
TPP	Thrombocyopenic purpura
uPA	Urokinase-type plasminogen activator

List of Figures

Chapter 1

Introduction

1.1 Background

The liver plays an essential role in the homeostasis of multiple biological processes and is a major site of metabolism for both endogenous and exogenous (xenobiotic) molecules (Casarett et al., 2008). A majority of this metabolic capacity is generated by the high expression levels of metabolizing enzymes such as cytochrome P450 enzymes, conjugation enzymes, and transport proteins expressed by hepatocytes (HPCs). HPCs are also known as liver parenchymal cells and represent approximately 80% of the liver mass (Casarett et al., 2008). The expression of these particular proteins in HPCs allows for the rapid transport, exchange, and metabolism of compounds into and out of the blood plasma. As the liver is the first organ to receive blood from the intestine via the portal vein, this extensive metabolic capacity serves as an effective protective mechanism to eliminate hazardous compounds out of the diet before they enter systemic circulation (Jacquot, 1978). However, these same features also make the liver more susceptible to some drug-induced hepatotoxicities, resulting in a major factor for molecule abandonment during the drug development process and various drug-drug interactions that can lead to withdrawal of therapeutic treatment in the clinic (Navarro and Senior, 2006).

1.2 Functions and zonation of the liver

Examining the basic functional architecture of the liver can serve as a good reference point to help illuminate some features and mechanisms of drug-induced liver injury. The most basic unit of the liver is the hepatic sinusoid, which resembles a large complex capillary lined by sinusoidal endothelial cells, which separate the HPCs from blood. In contrast to other organs, the hepatic sinusoidal endothelial cells create a fenestrated (porous) barrier (McCuskey, 2000), which allows for HPCs to be chronically bathed in plasma proteins from the blood and creates a site that allows for relatively free exchange of molecules and proteins between HPCs and blood. Additionally, there are other non-parenchymal cells dispersed throughout the liver such as kupffer cells, stellate cells, bile duct epithelial cells (BDEC), and other resident immune cells that perform various functions (Casarett et al., 2008). Blood enters the sinusoid from the hepatic portal vein and the hepatic artery. These two sources meet in the sinusoid at a

region called the portal area, also known as zone 1 within the liver lobule, and directional perfusion proceeds through the midzonal (zone 2) and centrilobular (zone 3) regions exiting the liver through the central vein (Casarett et al., 2008). This unidirectional blood flow in the hepatic sinusoid creates an oxygen tension gradient between these three zones, having the highest oxygen levels in zone 1 and the least in zone 3. Additionally, intracellular levels of glutathione and expression of conjugation enzymes are highest in zone 1 of the hepatic lobule. Interestingly, zone 3 has the highest expression levels of cytochrome P450, which makes this region of the liver lobule more susceptible to injury from compounds requiring bioactivation by these enzymes (Lindros, 1997).

Another function of HPCs is the synthesis and secretion of bile, which is used to aid in absorption of fat and fat soluble compounds (Casarett et al., 2008). As blood perfuses the liver, bile acids are actively taken up from HPCs and transported into the biliary tree. The biliary tree is made up of both small and large bile ducts, which are channels that guide bile out of the liver emptying into a storage vessel called the gall bladder. After a meal, bile leaves the gall bladder through the common bile duct where it drains into the intestine to help break down lipid droplets by forming smaller micelles. The micelles can then be readily taken up into the small intestine and transported to the liver via the hepatic portal vein completing the cycle. Disruption of this bile flow out of the liver is termed cholestasis and can occur through multiple mechanisms. One mechanism whereby cholestasis can occur is through a decrease in bile acid uptake transporter expression and/or activity on the sinusiodal membrane of HPCs. Alternatively, several mechanisms exist whereby biliary excretion may be disrupted at the canalicular membrane in HPCs (Glaser et al., 2010; Wagner et al., 2010; Padda et al., 2011). Additionally, direct injury to BDECs causes an increase in bile duct permeability and subsequently causes cholestasis originating from the portal area.

1.3 Mechanisms and models of liver injury

1.3.1 Mechanisms of liver injury

Exposure to some xenobiotics can cause direct cellular injury, which can be exemplified in APAP-induced hepatotoxicity. Treatment of purified cultured HPCs with APAP causes direct cytotoxicity as indicated by increase release of intracellular enzymes such as lactose dehydrogenase into the cellular medium (Yan et al., 2010). Similarly, high exposure of other compounds such as bile acids can cause cell death by apoptosis in cultured HPCs (Reinehr et al., 2003). However, during *in vivo* pathogenesis of liver injury, additional factors are present that can promote injury secondary to the original insult. For example, in bile duct ligation (BDL), primary injury is mediated by increased biliary pressure and spilling of bile acids into the liver parenchyma; however, the injury during the secondary injury progression stage is reduced in mice that are deficient in CD18, an essential cellular receptor for neutrophils (Gujral et al., 2003). This secondary injury can also be seen in models of hepatic ischemic reperfusion injury, where initial injury is limited, but secondary inflammation associated with this model promotes further hepatocellular death (Eltzschig and Eckle, 2011). Insofar as human patients enter the clinic at different stages of injury development, the ability to separate primary and secondary drug-induced liver injuries may help predict the overall outcome of hepatoxicity and may help to improve recovery by pharmacologically targeting specific key players during different phases of the injury progression.

Another contributor to the extent of liver injury is the ability of healthy HPCs to proliferate and replenish damaged or dying parenchymal cells. This is classically exemplified in partial hepatectomy, where 3/5 of a mouse liver is removed and the subsequent cellular division causes the liver to "grow" back to its normal size in several weeks (Rabes, 1976). This is also true for xenobiotic-induced liver injury such as in APAP-hepatotoxicity where complete resolution of APAP-induced liver injury can be observed in a matter of days for mice and a matter of weeks for surviving patients (Bernal et al., 2010; Jaeschke et al., 2011). Inhibition of key components that promote HPC proliferation can lead to severe liver injury and delayed normalization of liver function.

Several liver diseases and drugs such as ethyl alcohol, methotrexate, isoniazid, and others can chronically injure the liver, which can cause a viscous cycle of tissue injury, inflammation, and repair. During acute wound healing, several profibrotic genes, such as transforming growth factor beta-1 (TGF-B1) and Type-I collagen help stabilize the damaged area and provide a temporary "Band-aid" by increasing the deposition of extracellular matrix (ECM) in the injured area. Additionally, ECM remodeling proteins such as matrix metalloproteinases (MMPs), and tissue inhibitor of metalloprotinases (TIMPs), help coordinate the breakdown and reconstruction of the ECM during the recovery phase of injury. During chronic liver injury, this beneficial Band-aid can eventually develop into excessive ECM deposition termed fibrosis. Uncontrolled fibrosis can limit hepatic function by developing into cirrhosis through constant synthesis and deposition of ECM proteins and by inhibiting the pathways that naturally break down and remodel the ECM (Bataller and Brenner, 2005). Generally, the activated myofibroblast is considered the main cell type responsible for liver fibrosis as it contributes substantially to the production of type-I collagen, a main fibrotic component of extracellular matrix (Bataller and Brenner, 2005; Friedman, 2008). Within the liver, activated myofibroblasts may come from several pools of cells including quiescent stellate cells, portal fibroblasts, and fibroblast like cells of bone marrow origin (Bataller and Brenner, 2005; Friedman, 2008; Dranoff and Wells, 2010). Importantly, several key profibrogenic molecules that promote liver fibrosis have been identified. One of which is platelet derived growth factor B (PDGF-B), which is a potent mitogen for stellate cells (Bataller and Brenner, 2005; Friedman, 2008). Additionally, transforming growth factor beta (TGF-β) has been shown to stimulate quiescent stellate cells and portal fibroblasts to promote their transition into activated myofibroblasts and is one of the most potent inducers of ECM synthesis in activated myofibroblasts (Friedman, 2008). Identifying ways to limit liver fibrosis could help delay the development of cirrhosis in some patients and may be beneficial in limiting the number of liver transplantations needed in patients with chronic liver diseases.

1.3.2 Examples of drug-induced liver injury in zone 1

Injury initiating in zone 1 of the liver is frequently associated with cholestasis and can be seen after exposure to several xenobiotics including 4,4'methylene dianyline (MDA), flucloxacillin, and alpha-naphthylisothiocyanate (ANIT) (Becker and Plaa, 1965; Kopelman et al., 1966; McNeil et al., 1999; Dietrich et al., 2001; Giouleme et al., 2011). MDA is a curing agent for epoxy resins for the use in manufacture of polyurethane foams and has occupational exposure relevance. MDA toxicity was first observed in 1965 when 84 people consumed MDA contaminated bread in Great Britain, which resulted in jaundice and liver injury (Kopelman et al., 1966). Similarly, ANIT is also toxic to BDECs causing cholestasis, which is dependent upon ANIT transport into the bile to exert its toxic affect (Dietrich et al., 2001). This model toxicant has been used to identify mechanisms and mediators of liver injury initated by BDEC injury. Injury to BDECs can also be seen in patients with an acute biliary obstruction or in rodents subject to bile duct ligation due to an increase in biliary pressure. In response to BDECs injury, bile ducts begin to lose integrity, which allows high concentrations of bile acids to seep out into the surrounding liver parenchyma, which promotes local inflammation and injury (Stang-Voss and Appell, 1981; Dietrich et al., 2001).

In contrast to acute drug-induced liver injury, chronic injury to BDECs by ANIT or extended BDL also can elicit cholestasis, inflammation, and can promote biliary fibrosis. Similarly, several liver diseases also promote chronic BDEC injury, cholestasis, and fibrosis such as in patients presenting with primary billiary cirrhosis (PBC), primary sclerosing cholangitis (PSC), and patients with genetic polymorphisms in the phospholipid transporter multidrug resistance protein 3 (familial cholestasis) (Bhandari et al., 2011; Lindor, 2011; Morotti et al., 2011). Understanding the mechanisms of chronic BDEC injury on the development of fibrosis could play an essential role in developing drug targets to prevent cirrhosis and liver failure in these patients.

1.3.2 Examples of drug-induced liver injury in zone 3

APAP is a classical hepatotoxicant, which is estimated to be responsible for more than 24,000 hospitalizations and approximately 500 deaths per year. Overdose of this drug also represents the most

common cause of drug-induced liver failure in the United States (Blackford et al., 2011). The toxicity of this compound is completely dependent on the ability of cytorchrome P450s to metabolize this drug into the reactive metabolite N-acetyl-p-benzoquinone imine (NAPQI) which is rapidly detoxified through sulfation, glucuronidation, and glutathionylation conjugation pathways at therapeutic doses (Jaeschke et al., 2011). At supratherapeutic doses, the sulfation and glucuronidation detoxification pathways are overwhelmed and glutathione conjugation becomes the dominant detoxification pathway. In APAP poisoning, the depletion of hepatocellular glutathione levels becomes the rate limiting step required for hepatotoxicity. Subsequently, as centrilobular HPCs have the highest expression levels of CYP450 enzymes, zone 3 hepatocytes are the most susceptible to develop hepatocellular necrosis after APAP poisoning (Lindros, 1997). Injury initiating from this zone can also be seen in exposure to several other compounds such as the model toxicant carbon tetrachloride and the anti-cancer agent cyclophosphamide, which both require CYP450 bioactivation (Raucy et al., 1993; Gut et al., 2000).

APAP-induced hepatotoxicity can be modeled in rodents, of which mice are the predominant species due to the increased availability of genetically modified animals and a higher sensitivity to the toxic effects of APAP poisoning when compared to rats (Jaeschke et al., 2011). In relationship to human patients, the mouse model of APAP-induced hepatotoxicity develops much faster. Human patients begin to develop clinical signs of liver injury such as elevated serum transaminase levels around 24 hours after ingestion and peak injury is generally seen between 24-72 hours in surviving patients. Depending on dose, liver injury assessed by both histology and serum transaminase activity levels in most mouse models of APAP-induced toxicity can be seen as early as 2 hours and peak injury is observed between 16-24 hours after administration. Additionally, complete recovery in surviving mice is generally seen by 72 hours, whereas human patients that are treated in the clinic receiving therapies such as N-actetylcysteine to limit liver injury, may take 96 hours or more to fully recover (Ganey et al., 2007; Blackford et al., 2011; Jaeschke et al., 2011). These time course discrepancies between humans and mice are important observations to consider when trying to translate animal data into human relevance.

In addition to HPC cell death, other cell types have also been suggested to be a direct target of APAP-induced hepatotoxicity. One such cell type is the sinusoidal endothelial cell. Patients presenting with APAP-overdose have elevated serum levels of hylauronic acid, a molecule generally cleared by the SECs and considered a general marker of SEC injury in some models (Williams et al., 2003). Interestingly, APAP-toxicity in mice is associated with red blood cell infiltration into the Space of Disse in areas adjacent to injured hepatocytes. Sinusiodal hemorrhage has been suggested to be a consequence of SEC damage, as similar hemorrhage is seen in several classical models of SEC toxicity such as in monocrotaline- and cyclophosphamide-induced liver injury (Gismondi et al., 1980; Copple et al., 2006). Furthermore, SECs have been shown to express CYP450 enzymes, and APAP can be directly toxic to SECs that express high levels of CYP450 in cell culture models (DeLeve et al., 1997). However, the affect of APAP on SECs and the role that these cells and others may play in the progression of APAP-induced liver is still a field of intense study.

1.4 Blood coagulation in liver disease

1.4.1 Overview of the blood coagulation cascade

The blood coagulation cascade is an essential pathway composed of several serine proteases, cellular receptors, and soluble mediators (Fig. 1.1). In healthy subjects, blood coagulation is regulated at the level of activation, as most coagulation proteins are synthesized as zymogens and require an activation step to reveal enzymatic activity. Normally, the coagulation cascade pathway is kept in an inactive, but "ready to go" state so that in response to harmful stimuli such as tissue damage, the blood coagulation cascade can be rapidly activated to prevent hemorrhage (Mackman, 2004). The coagulation cascade is composed of two procoagulant pathways, the intrinsic and the extrinsic pathways, the latter acting as the major activator of blood coagulation. The extrinsic pathway is initiated by tissue factor (TF), a cell surface receptor for the coagulation factor VII/VIIa (Mackman, 2004). The physical expression pattern of TF represents a unique regulatory mechanism to keep hemostasis in balance (Drake et al., 1989; Mackman, 2004). Expression of TF has been described as a "hemostatic envelope" having high

expression levels on cells adjacent to, but not on endothelial cells, therefore restricting the contact of TF with blood (Drake et al., 1989). When tissue injury occurs, loss of vascular integrity and increased vascular permeability can cause blood and coagulation factors to leak out of the vasculature, which brings TF into contact with its ligand; coagulation factor VIIa. The TF:VIIa complex initiates the coagulation serine protease cascade activating several proteases culminating in the generation of thrombin, the distal serine protease (Mackman, 2004).

As TF expression is a major contributor to the regulation of its pro-coagulant activity, it is interesting to note that the expression of TF activity is present in liver, albeit relatively low levels when compared to other organs such as the brain and heart (Drake et al., 1989; Ganey et al., 2007). A recent study has shown that BDECs express TF, which contributes to TF-dependent coagulation cascade activation during liver injury in ANIT-induced toxicity (Luyendyk et al., 2009). Of importance, previous studies have also shown that purified HPCs express a procoagulant form of TF (Stephenne et al., 2007). This poses a unique regulatory challenge to the liver microcirculation as the liver both receives a large volume of blood and is also the primary site of coagulation factor synthesis (Casarett et al., 2008). This suggests that TF activity must be regulated by a secondary mechanism within the liver to prevent pathologic clot formation.

A previous study suggested that the majority of TF staining in HPCs was intracellular, suggesting a physical division between TF and coagulation factors within the perfusing plasma. However, additional intracellular barriers would also have to be in place to prevent TF-VIIa interactions within the cell at the site of protein synthesis. However, an alternative hypothesis would be that TF is held in an inactive non-procoagulant state until some "trigger" activates this protein. This has been shown in several cell culture models where TF expression is not procoagulant until cells are stimulated with a calcium ionophore, which reveals TF-dependent procoagulant activity suggesting an additional mechanism of regulation in addition to expression levels (Bach, 2006). Other studies have suggested that modification of certain amino acids in TF can render it incapable of initiating a procoagulant response, however, the localization and regulation of TF in HPCs is not completely understood.

In addition to regulating the expression and activation of TF to control blood coagulation cascade activation, the procoagulant response is also balanced by anticoagulant pathways in order to prevent excessive pathologic clotting and to localize the procoagulant response at the site of injury. These pathways are initiated by several endogenous inhibitors and feedback loops. One such example of an endogenous feedback inhibitory pathway is initiated by the interaction of the procoagulant serine protease factor X and tissue factor pathway inhibitor (Mackman, 2004; Mackman, 2005). Together these two proteins can limit coagulation by locally inhibiting the action of the TF:VIIa complex and therefore limiting the procoagulant response. In similar fashion, the procoagulant serine protease thrombin can also activate protein C, another anticoagulant protein. When bound to thrombomodulin, this complex can inhibit activated factors V and VIII (Mackman, 2004; Mackman, 2005). Furthermore, thrombin and to a lesser extent factor X has its own direct inhibitor, anti-thrombin III, which can bind both of these proteins rendering them inactive (Mackman, 2004; Mackman, 2005). Anti-thrombin III is a clinically relevant target for anticoagulant therapy and can be targeted by the use of heparins, another class of anticoagulants that act by increasing the affinity of anti-thrombin III for thrombin and factor X (Soff, 2012). Additionally, thrombin anti-thrombin complexes are commonly used as a stable clinical marker of coagulation cascade activation, as the half life of activated thrombin is relatively short in plasma (~30 seconds) due to its high affinity and rapid binding to anti-thrombin III (Abildgaard, 1969; Abildgaard et al., 1974). Together, these anticoagulant pathways help modulate and fine tune the extent of coagulation in response to injury and help limit coagulation to the local site of injury (Mackman, 2004; Mackman, 2005).

1.4.2 Downstream functions of coagulation cascade activation

A main downstream effect of coagulation is the formation of a rigid fibrin clot, which forms a physical barrier in the injured tissue and prevents hemorrhage. In addition to being a physical barrier, several proteins have also been shown to physically bind fibrin clots such as the gpIIb/β3 (GPIIb/IIIa), MAC-1 (αMβ2) and αVβ3 integrins, which can contribute to local infiltration of platelets and

inflammatory cells in the injured tissue (Kubo et al., 2001; Mosesson, 2003). The stability of these fibrin clots are regulated by several mechanisms including their size, density, the extent of crosslinking of the fibrin polymers, which is performed by a transglutaminase factor XIII (Mackman, 2004; Mackman, 2005). Additionally, the stability of these clots are also determined by the activity of the fibrinolytic pathway, a series of enzymes responsible for fibrin degradation (Schaller and Gerber, 2011). Plasmin is the main enzyme responsible for direct dissolution of fibrin clots (Schaller and Gerber, 2011). Plasmin, similar to most other coagulation factors, is a zymogen and is kept in an inactive state (plasminogen), but can be converted to an active protease by cleavage from the plasminogen activators: urokinase-type plasminogen activator (uPA) and tissue-type plasminogen activatior (tPA) (Schaller and Gerber, 2011). The fibrinolytic pathway is also regulated by inhibitory pathways, and can be inhibited at the level of the plasminogen activators by plasminogen activator inhibitor 1 (PAI-1) while plasmin can be directly inhibited by α2-macroglobulin and α2-antiplasmin (Schaller and Gerber, 2011). In addition to fibrin clot dissolution, components of the fibrinolytic pathway have been shown to contribute to several repair mechanisms during wound healing. For example, cleavage of plasminogen creates two products, active plasmin and a peptide called angiostatin; the latter is a potent inhibitor of angiogenesis (O'Reilly et al., 1994). Additionally, fibrin degradation products produced by plasmin have also been shown to promote angiogenesis in endothelial cells (Bootle-Wilbraham et al., 2001). Furthermore, additional targets have been identified for the protease tPA, such as hepatocyte growth factor, an essential molecule in liver regeneration, (Mars et al., 1993) further suggesting that the fibrinolytic pathway is essential in proper resolution of liver injury.

Outside of classical clot formation, thrombin can contribute to hemostasis by regulating the activity of platelets by activating the cell surface G-protein coupled receptors protease activated receptor 1 (PAR-1) and PAR-4 (Kahn et al., 1998; Coughlin, 1999). Importantly, a species difference exists on the expression pattern of PAR receptors between humans and mice. Humans express both the high affinity thrombin receptor PAR-1 and the lower affinity PAR-4 on platelets whereas mouse platelets express PAR-4 and PAR-3; the latter acts as a high affinity co-receptor for thrombin/PAR-4 interaction

(Kahn et al., 1998; Coughlin, 1999; Sambrano et al., 2001). Activation of these PARs on platelets enhances their activation and aggregation capacity. Importantly, PAR stimulation on platelets causes a conformational change in the fibrin/fibrinogen receptor gpIIb/β3 to promote platelet intercalation into the fibrin clot, which stabilizes the clot and further prevents hemorrhage (Kahn et al., 1998). Additionally PAR-1 and PAR-4 have also been shown to be expressed by numerous cell types other than platelets such as liver stellate cells which may contribute to liver injury and fibrosis (Fiorucci et al., 2004; Rullier et al., 2006).

Several other components of the procoagulant pathway also have signaling functions outside of classical fibrin clot formation and platelet activation. For example, TF can activate PAR-2 when bound to factor VIIa and factor X has been shown to activate both PAR-1 and PAR-2 under certain conditions (Borensztajn and Spek, 2011; Rothmeier and Ruf, 2012). Furthermore, PAR-1, PAR-2, and PAR-4 have been shown to be expressed by several cell types within the liver and have been shown to participate in the pathogenesis of multiple liver injuries (Copple et al., 2003; Fiorucci et al., 2004; Martinelli et al., 2008; Luyendyk et al., 2010). The mechanism whereby PARs contribute to drug induced toxicities is most likely through the regulation of the local inflammatory response. However, as with platelets, stimulation of PAR-1 on fibroblasts is thought to cause changes in the cytoskeleton that may activate certain cellular receptors such as the profibrotic αVb6 integrin which contributes to a model of drug-induced pulmonary injury (Munger et al., 1999). Additionally, stimulation of PAR-1 or PAR-4 causes stellate cell contraction and thrombin can induce endothelial cell contraction (Fiorucci et al., 2004; Kolozsvari et al., 2009). Contraction of these two cell types is an essential determinant of portal pressure in the liver and may help limit or coordinate blood flow within the injured liver. Furthermore, during chronic liver injury and fibrosis, excessive portal pressure may lead to esophageal varices (Bari and Garcia-Tsao, 2012). However, the specific mechanisms whereby PARs contribute to the different phases of injury seem to be greatly diverse and model dependent.

In addition to PAR signaling, alternative signaling functions for several coagulation proteins have also been described. For example, TF can also interact with several integrins and can promote

angiogenesis in some cell types (Dorfleutner et al., 2004). Similarly, alternative substrates for the protease plasmin have been found, such as the matrix metalloproteinases (MMP) MMP-2 and MMP-9 and have been shown to play a role in several models of drug induced toxicity (Shanmukhappa et al., 2006; Schaller and Gerber, 2011). Additionally uPA can signal through ligation of its receptor uPAR, which can alter its enzymatic activity (Ngo et al., 2011). Taken together, the blood coagulation cascade is a highly dynamic pathway that prevents hemorrhage and is kept in check by an anticoagulant and fibrinolytic pathway. Several protein components of this pathway have multiple functions outside of classical coagulation cascade through interaction with cellular receptors. These receptors contribute to disease pathology through regulating other non-hemostatic functions such as local inflammation, cellular signaling, and extracellular matrix remodeling. Further studies are required to understand the specific cell types and mechanisms whereby effecter molecules affect different liver injuries in patients.

1.5 Coagulation in liver injury and disease

1.5.1 Background

In addition to performing essential metabolic and detoxification processes, the liver is also the primary site for synthesis of new coagulation factors and the site for exchange of consumed coagulation factors (Mammen, 1992; Casarett et al., 2008). Controlling appropriate plasma concentrations and synthesis of coagulation factors by the liver represents an essential primary regulatory mechanism to control coagulation. A prime example of this hepatic regulatory feature has been exploited in the clinic by the use of the common anti-coagulant drug warfarin. Warfarin works as a vitamin K epoxide reductase inhibitor, an essential enzyme in the maturation step of several procoagulant coagulation factors including factor II, VII, IX, and X (Ansell et al., 2008). In the clinical application, a mild synthesis defect can lower systemic coagulation factor levels and has an anticoagulant effect which can be beneficial for some patients. However, these patients must be carefully monitored as moderate failure of the liver to regulate the synthesis of these factors can lead to unbalanced hemostasis resulting in severe and potentially fatal hemorrhage (Zareh et al., 2011). Insofar as warfarin therapy can cause life threatening

hemorrhage, several other hepatic diseases and drug-induced hepatotoxicities have been associated with reduced coagulation factor levels and decreased hemostatic function (Mammen, 1992; Segal et al., 1997; Copple et al., 2002b; Kerr et al., 2003; Ganey et al., 2007; Luyendyk et al., 2010).

1.5.2 The role of coagulation on liver injury in zone 1 of the hepatic lobule

Acute zone 1 induced liver injury in rodents has identified several abnormalities in hemostasis. ANIT-induced hepatotoxicity is associated with TF-dependent coagulation cascade activation indicated by increased plasma TAT levels and hepatic fibrin deposition (Luyendyk et al., 2009). Reduction in coagulation and hepatic fibrin deposition in TF-deficient mice is associated with reduced liver injury 48 hours after ANIT administration, indicated by a decrease in serum ALT, ALP, and serum bile acid levels (Deng et al., 2009). Similarly, in models of acute MDA hepatotoxicity and biliary obstruction fibrin deposition is evident in the injured liver (Santa Cruz et al., 2007; Wang et al., 2007c); however, the role of hepatic fibrin and coagulation on acute injury in these two models of zone 1 induced liver injury is not known.

One mechanism whereby the coagulation cascade could contribute to acute ANIT-induced liver injury is through the activation of protease activated receptors on platelets as ample coagulation cascade activation and thrombin generation is present by this time. Platelets have been shown to be involved in several models of liver injury (Kuroda and Shiohara, 1996; Hisakura et al., 2010). Interestingly, liver injury was reduced 24 hours after ANIT administration in rats that were depleted of platelets (Bailie et al., 1994). Similarly, mice depleted of platelets had reduced liver injury 12 hours after BDL (Laschke et al., 2008). In that same study, administration of a neutralizing p-selectin antibody also reduced liver injury to a similar extent, suggesting that platelets are involved in the early injury after BDL (Laschke et al., 2008). In contrast to acute cholestasis, mice genetically deficient in platelets had increased fibrosis after bile duct ligation, suggesting that platelets may play a second role in liver injury outside of the initial insult phase and may contribute to the repair process in this model. As decreased platelet counts have been observed in patients with PBC/PSC, this could suggest that platelet therapy might attenuate liver fibrosis during

chronic cholestasis (Pihusch et al., 2002; Kodama et al., 2010). However, whether the coagulation system is responsible for the activation of platelets and the mechanisms whereby they contribute to cholestatic induced liver injury is not known.

Another mechanism whereby coagulation may contribute to liver injury during cholestasis is through activation of PAR-1, which has been shown to contribute to several models of liver injury and is expressed by several cell types within the liver (Copple et al., 2003; Fiorucci et al., 2004; Jesmin et al., 2006; Ganey et al., 2007; Luyendyk et al., 2010). Rats given a PAR-1 antagonist had reduced liver injury and fibrosis 31 days after BDL (Fiorucci et al., 2004). This reduction in liver injury could be due to a decreased inflammatory response as monocyte chemotactic protein 1 (MCP-1) was reduced in this model. Of importance, MCP-1 is influential in attracting circulating monocytes and lymphocytes, the latter are thought to be essential for injury progression in cholestasis-induced liver injury (Dahm et al., 1991; Roth and Dahm, 1997; Gujral et al., 2003; Seki et al., 2009). As PAR-1 expressing fibroblasts contribute to liver injury in this zone, other cell types that express PAR-1 should also be evaluated in this model of liver injury.

During chronic cholestasis, several components of the fibrinolytic pathway are altered such as increased PAI-1 levels and decreased levels of plasminogen and a2-antiplasmin (Segal et al., 1997). Additionally, components of the fibrinolytic pathway have been shown to contribute to liver injury after BDL. For example, mice that are deficient in PAI-1, the main endogenous inhibitor of fibrinolysis, have reduced levels of liver injury after BDL and consequentially these mice also have reduced levels of fibrosis, suggesting that enhanced PA activity and potentially enhanced clearance of fibrin clots may be protective in this model (Bergheim et al., 2006). In agreement with these results, deficiency in tPA led to increased liver injury after BDL (Wang et al., 2007c). As expected, liver injury in these mice was also associated with an increase in hepatic fibrin deposition and increased neutrophil accumulation which promotes liver injury in BDL (Wang et al., 2007c). As CD18 is a component of the fibrin binding MAC-1 integrin and is essential for liver injury in BDL, these data might suggest that fibrin promotes liver injury in cholestatic-induced liver injury by promoting neutrophil accumulation in areas of fibrin

deposition (Gujral et al., 2003; Flick et al., 2004). However, fibrinogen-deficiency was associated with both increased liver injury and hepatic neutrophil accumulation in ANIT-induced liver injury suggesting a different role for fibrin between these two models (Luyendyk et al., 2011a). Additional studies are required to identify the mechanisms whereby fibrin and fibrinolysis contribute to cholestatic liver injury and fibrosis.

1.5.3 The role of coagulation in liver injury in zone 3 of the hepatic lobule

APAP is a well known classical zone 3 hepatotoxicant and several alterations in coagulation parameters are evident in patients presenting with APAP-induced toxicity (Gazzard et al., 1975; Kerr et al., 2003; Ganey et al., 2007). Patients that present with APAP-induced hepatotoxicity have increased plasma levels of TAT complexes suggesting that coagulation is activated in these patients. Furthermore, increased TAT is also associated with decreased levels of coagulation factors II, V, VII, and X, while factors IX and XI are relatively normal in these patients (Gazzard et al., 1975; Kerr et al., 2003). This suggests that the liver has the capacity to synthesize sufficient levels of these proteins and that these patients are potentially suffering from a consumptive coagulopathy (Gazzard et al., 1975; Kerr, 2003). Additionally, thrombocytopenia is also observed in human patients suffering from APAP-induced hepatotoxicity, and the severity of liver injury is inversely proportional to the patients' platelet count (Skokan et al., 1973; Fischereder and Jaffe, 1994). Interestingly, these same phenomena can be reproduced in mice given a single hepatotoxic dose of APAP, which is accompanied by a decrease in circulating plasma fibrinogen levels, increased hepatic fibrin deposition, and decreased platelet counts, suggesting that the mouse model of APAP-induced liver injury recapitulates some of the hemostatic defects seen in human patients (Ganey et al., 2007; Bougie et al., 2010). The majority of coagulation in this model is TF-dependent as thrombin generation is dramatically reduced in TF-deficient mice given a hepatotoxic dose of APAP (Ganey et al., 2007). Of importance, TF-deficient mice or wild type mice pretreated with the anticoagulant heparin have reduced liver injury and hepatic fibrin deposition 6 hours after APAP administration (Ganey et al., 2007). Taken together this suggests that coagulation cascade

activation is present in both mice and patients suffering from APAP-hepatotoxicity and that coagulation contributes to the progression of APAP-induced liver injury.

Another classical zone 3 hepatotoxicant is carbon tetrachloride. Carbon tetrachloride was once widely used as an industrial solvent, but has since been phased out due to its hepatotoxicity effects and its role in ozone depletion (Recknagel, 1967; Hutzinger, 1980). Similar to APAP, carbon tetrachloride is also metabolized to a reactive intermediate by the cytochrome P450s (Raucy et al., 1993). Early studies with this compound identified numerous effects on the blood coagulation cascade in rats given hepatotoxic doses of carbon tetrachloride including increased thrombin times, hepatic hemorrhage, and increased hepatic fibrinogen deposition (Scott and Howell, 1964; Rake et al., 1973). Similar to APAP, thrombocytopenia is also observed in rats given a hepatotoxic dose of carbon tetrachloride (Yamashita et al., 2000). This could suggest that in both of these models, coagulation cascade activation could contribute to thrombocytopenia by activating platelets and promoting their aggregation in the injured liver, however, whether coagulation activates platelets in these two models is not known.

Another mechanism whereby coagulation activation could contribute to both APAP and carbon tetrachloride hepatotoxicity is through activation of PAR-1. PAR-1-deficiency reduced early APAP-induced liver injury, however, PAR-1 deficiency did not alter the extent of acute liver injury in carbon tetrachloride toxicity (Ganey et al., 2007; Rullier et al., 2008). Although there was no difference in liver injury, PAR-1 promoted liver fibrosis in the chronic model of carbon tetrachloride induced liver injury (Rullier et al., 2008). The decrease in hepatic fibrosis in PAR-1-deficient mice was associated with a decrease in a-smooth muscle actin, a marker for activated fibroblasts, the main collagen producing cell types within the liver (Friedman, 2008; Rullier et al., 2008). Furthermore, FV Leiden mice, which carry a mutation in FV and are hypercoagulable, develop enhanced fibrosis, whereas mice treated with the anticoagulant warfarin develop less fibrosis after chronic tetrachloride induced liver injury (Anstee et al., 2008). PAR-1 signaling has been shown to affect several cell types within the liver including stimulating stellate cells to produce collagen (Fiorucci et al., 2004), which is probably the main cell type responsible

for liver fibrosis in the carbon tetrachloride model of liver fibrosis, however, the important hepatic cellular sources of contributing PAR-1 in acute APAP-induced liver injury is not known.

As thrombocytopenia is induced in both APAP and carbon tetrachloride-induced liver injury (Yamashita et al., 2000; Bougie et al., 2010), another mechanism whereby coagulation cascade activation could contribute to liver injury is through thrombin-dependent activation of platelets by PARs. A recent study has suggested that mice given prostacyclin, an inhibitor of platelet activation, protects against APAP-induced liver injury (Cavar et al., 2009). Similarly, several studies have identified prostacyclins and several prostacyclin derivatives to be protective after carbon tetrachloride induced liver injury (Divald et al., 1985). Other studies have shown that inhibiting platelets by giving either aspirin or platelet activating factor receptor antagonists, reduced liver injury in rodent models of APAP-induced hepatotoxicity (Grypioti et al., 2006; Imaeda et al., 2009). Furthermore, as there is abundant thrombin and hepatic fibrin generated after APAP-induced toxicity, this could stimulate platelets locally to promote their aggregation and release of granules in the liver. However, another group showed that administration of low dose aspirin did not protect against APAP-induced liver injury (Williams et al., 2011). Further, studies are required to identify whether platelets contribute to the progression of acute APAP and carbon tetrachloride-induced liver injury. Additionally, platelets should be evaluated in the chronic model of carbon tetrachloride induced liver fibrosis, as platelets have been shown to contribute to liver fibrosis after BDL. Furthermore, studies should be performed to identify whether the thrombocytopenia is dependent on coagulation cascade activation in these two models.

Similar to zone 1-induced liver injury, the fibrinolytic system also contributes to xenobiotic-induced liver injury progression and resolution. In contrast to BDL where enhanced fibrinolytic activity seems to have a protective effect in liver injury, PAI-1 deficiency in the mouse model of APAP-induced toxicity is associated with increased hepatocellular injury, sinusoidal hemorrhage, and mortality (Bajt et al., 2008). PAI-1-deficiency was also associated with an increase in liver injury and an increase in liver fibrosis in mice treated with carbon tetrachloride (von Montfort et al., 2010). However, tPA-deficient mice had increased liver fibrosis in this model (Hsiao et al., 2008). Interestingly, in the acute carbon

tetrachloride model, uPA-deficiency did not protect against liver injury, but significantly delayed the repair and regeneration of liver injury (Shanmukhappa et al., 2006). Interestingly, this result was completely independent of both its receptor uPAR or tPA activity. These studies clearly identify a role for several components of the fibrinolytic pathway in both acute and chronic liver injury in this zone of the liver. However, the role of both uPA and tPA should be explored in both the acute and resolution phases of APAP-induced liver injury. Furthermore, as both PAI-1- and tPA-deficient mice had increased fibrosis, this suggests that these two proteins contribute to liver fibrosis through different mechanisms. Further studies are needed to understand the mechanisms whereby uPA, tPA, and PAI-1 contribute to both acute and chronic liver injury after carbon tetrachloride.

1.6 Figures

Figure 1.1

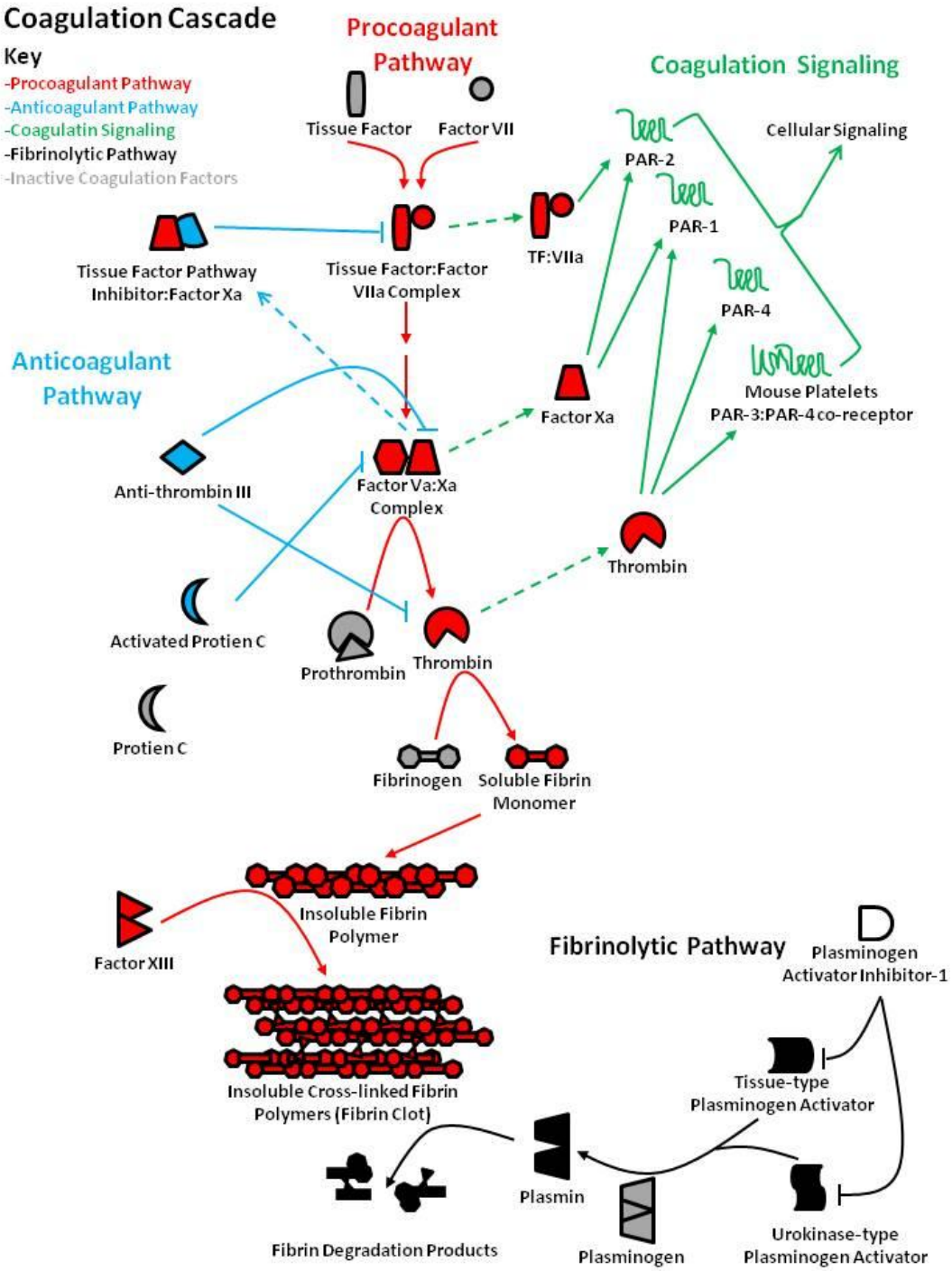

Figure 1.1: A summary of the blood coagulation cascade

The blood coagulation cascade is tightly controlled by both procoagulant (red) and anticoagulant (blue) proteins, which regulate the extent of coagulation cascade activation and subsequent fibrin clot formation. Fibrin clot dissolution is also regulated by enzymes in the fibrinolytic pathway (black). Additionally, several coagulation factors such as thrombin and factor Xa have extracellular signaling functions by activating protease activated receptors (PARs; green), G-protein coupled receptors that can promote platelet aggregation and local inflammation.

1.7 Summary and overview of dissertation

In summary, the liver plays an essential primary role in hemostasis by regulating the synthesis of coagulation factors. The location and function of the liver also predisposes this organ to drug-induced liver injury by xenobiotics, which can cause altered hemostasis in patients through several mechanisms. Furthermore, multiple components of the blood coagulation system have been shown to contribute to drug-induced hepatotoxicity, however, these mechanisms seem to be various and model-dependent. Understanding how components of the blood coagulation system contribute to drug-induced liver injury could help identify novel targets for therapeutic intervention to limit injury and fibrosis in some patients. Additionally, as some components of the fibrinolytic pathway contribute to liver repair and regeneration, pharmacologically targeting this pathway might be beneficial to speed up recovery times in patients with acute liver injury.

Inasmuch as coagulation is associated with liver injury, we utilized two model hepatotoxicants to evaluate the role of several components of the coagulation cascade in drug-induced liver injury originating from two different zones of the liver. The first half of the dissertation describes how the coagulation cascade contributes to zone 1 related hepatotoxicity by the use of ANIT, a selective BDEC toxicant that causes cholestasis. When looked at from a short term perspective, using a rodent model of ANIT toxicity can help identify mechanisms whereby the coagulation cascade can participate in direct hepatotoxicity in response to BDEC damage. In addition, this model hepatotoxicant can be used to study

mechanisms associated with fibrosis during chronic injury to BDECs and we further explore the role of PAR-1 activation on the regulation of several profibrogenic genes in a cell culture model using BDECs. The second part of the dissertation describes the role of coagulation in APAP-induced hepatotoxicity, a classical zone 3 hepatotoxicant and a drug that commonly causes acute liver failure.

Chapter 2

Protective and damaging effect of platelets in acute cholestatic liver injury revealed by depletion and inhibition strategies.

Bradley P. Sullivan[1], Ruipeng Wang[1], Ossama Tawfik[2], and James P. Luyendyk[1]

[1]Department of Pharmacology, Toxicology and Therapeutics and [2]Pathology and Laboratory Medicine, The University of Kansas Medical Center, Kansas City, KS

This article was published in Toxicological Sciences 2010 May;115(1):286-94.

2.1 Abstract

Alpha-naphthylisothiocyanate (ANIT) causes cholestatic hepatitis characterized by intrahepatic bile duct epithelial cell (BDEC) injury and periportal hepatocellular necrosis. The progression of ANIT-induced hepatocyte injury is reported to involve extrahepatic cells including platelets. We showed recently that the procoagulant protein tissue factor (TF) is essential for ANIT-induced coagulation and contributes to ANIT-induced liver necrosis. Platelets have been shown to express TF and can contribute to coagulation cascade activation. To this end, we tested the hypothesis that platelet-dependent coagulation contributes to ANIT-induced liver injury. In ANIT (60 mg/kg)-treated mice, activation of the coagulation cascade occurred prior to a decrease of platelets in the blood. Immunostaining for glycoprotein IIb (CD41) revealed platelet accumulation along the borders of necrotic foci in livers of ANIT-treated mice. Antibody-mediated platelet depletion did not affect coagulation, but markedly affected liver histopathology in ANIT-treated mice. Platelet depletion induced marked pooling of blood within necrotic lesions consistent with parenchymal-type peliosis as early as 24 hours after ANIT treatment. In contrast, treatment with the $P2Y_{12}$ inhibitor clopidogrel significantly reduced ANIT-induced hepatocyte necrosis and serum ALT activity, but did not exaggerate bleeding into necrotic foci. Clopidogrel also reduced hepatic neutrophil accumulation but did not affect induction of ICAM-1 or KC/Groα mRNA expression in liver. The data indicate that ANIT-induced coagulation is platelet-independent and that platelets contribute to ANIT-induced hepatocyte necrosis by promoting neutrophil accumulation. In contrast, severe thrombocytopenia induces parenchymal-type peliosis in the livers of ANIT-treated mice, a rare hepatic lesion associated with pooling of blood in the liver.

2.2 Introduction

Acute intrahepatic cholestatic liver injury is modeled by administration of the xenobiotic alpha-naphthylisothiocyanate (ANIT), which selectively injures intrahepatic bile duct epithelial cells (BDECs) after oral administration (Plaa and Priestly, 1976). Damage to bile ducts causes the release of high concentrations of bile acids into the liver sinusoids. Although bile acids are cytotoxic to hepatocytes

(Perez and Briz, 2009), several studies suggest that the progression of acute cholestatic liver injury involves multiple mediators. For example, neutrophil depletion or deficiency in the β2 integrin CD18 reduced liver necrosis induced by bile duct ligation (BDL) or ANIT treatment (Dahm et al., 1991; Gujral et al., 2003; Kodali et al., 2006). The coagulation cascade also contributes to BDL- and ANIT-induced liver injury (Abdel-Salam et al., 2005; Luyendyk et al., 2009). Platelets also appear to contribute to cholestatic liver injury (Bailie et al., 1994; Laschke et al., 2008). Taken together, these studies indicate an important role of elements of blood in cholestatic liver injury.

Previous studies using BDL as a model of obstructive cholestasis indicated that platelets contribute to cholestatic liver injury by promoting induction of chemotactic factors and the accumulation of neutrophils in the liver (Laschke et al., 2008). However, it is not clear whether this mechanism is shared in other models of cholestatic injury. It is possible that platelets contribute to cholestatic liver injury via other mechanisms. For example, we have shown that ANIT-induced liver injury is reduced in mice deficient in the procoagulant protein tissue factor (TF), suggesting that the coagulation cascade contributes to the pathogenesis (Luyendyk et al., 2009). Activated platelets possess a thrombogenic surface capable of propagating coagulation cascade activation (Ofosu, 2002). Platelets have been shown to express TF via a functional spliceosome (Schwertz et al., 2006). Accordingly, platelet activation and accumulation in the liver of ANIT-treated mice could contribute to liver injury by activating the coagulation cascade. However, the role of platelets in the procoagulant response induced by cholestatic liver injury has not been evaluated.

Interestingly, in addition to the potential for damaging effects of platelets during acute liver injury, they may also serve a protective function. Some studies implicate the release of serotonin by platelets as a mediator of liver regeneration and repair after partial hepatectomy (Lesurtel et al., 2006), although this is not necessarily true for other types of liver injury (Nocito et al., 2007; Lang et al., 2008). Other studies have suggested that mediators released by platelets, such as sphingosine-1-phosphate and serotonin, can affect sinusoidal endothelial cell (SEC) fenestration and inhibit SEC injury (Braet et al.,

1995; Zheng et al., 2006)). It is also possible that platelets limit hemorrhage secondary to SEC damage during early cholestasis, although this possibility has not been investigated.

We sought to clarify the role of platelets in the procoagulant response and hepatocyte damage elicited by acute xenobiotic-induced cholestatic liver injury utilizing both platelet depletion (i.e., anti-CD41 antibody) and inhibition (i.e., clopidogrel) strategies. Biomarkers of coagulation, liver injury, and inflammatory cell accumulation were assessed. The results indicate divergent effects of platelet depletion and platelet inhibition on the progression of acute cholestatic liver injury.

2.3 Materials and Methods:

2.3.1 Mice and treatment models: Male, wild type C57Bl/6J mice used for these studies were purchased from the Jackson Laboratory. Mice were maintained in an Association for Accreditation and Assessment of Laboratory Animal Care International (AAALAC)-accredited facility at the University of Kansas Medical Center. Mice were housed at an ambient temperature of 22°C with alternating 12-h light/dark cycles, and allowed water and rodent chow ad libitum (Teklad 8604; Harlan, Indianapolis, IN). All animal procedures were performed according to the guidelines of the American Association for Laboratory Animal Science and were approved by the KUMC Institutional Animal Care and Use Committee.

After removal of food overnight, mice were given ANIT (Sigma-Aldrich, St. Louis, MO) (60 mg/kg, po) in a volume of corn oil determined by the weight of the mouse (i.e., 10 ml/kg body weight) or an equivalent volume of corn oil (vehicle control). Various times after ANIT treatment the mice were anesthetized with isoflurane and blood collected from the caudal vena cava into citrate (for thrombin-antithrombin (TAT) determination), EDTA (for platelet quantification) or an empty syringe for the collection of serum. Plasma and serum were collected by centrifugation. Sections of liver from the left lateral lobe were fixed in 10% neutral-buffered formalin for 48 hours. The right medial lobe was affixed to a cork with OCT and frozen for 3 minutes in liquid nitrogen-chilled isopentane. The remaining liver was snap frozen in liquid nitrogen. For platelet depletion studies, mice were given a single dose of endotoxin- and azide free anti-CD41 antibody (clone, MWReg30) (1 mg/kg in sterile PBS) custom

prepared by BioLegend (La Jolla, CA) or 1mg/kg isotype control rat IgG (BioXCell, West Lebanon, NH) 16 hours before ANIT administration. For platelet inhibition studies, clopidogrel (Axxora, San Diego, CA) dissolved in sterile PBS or sterile PBS was given 8 hours (30 mg/kg, ip) after ANIT treatment, followed by additional injections every 12 hours (30 mg/kg, ip) until completion of the experiment.

2.3.2 Histopathological analysis and immunofluorescent staining: Formalin-fixed livers were processed routinely, embedded in paraffin, sectioned at 5 microns, and stained with hematoxylin and eosin. Slides were evaluated by light microscopy by a Board-certified pathologist (O.T.). Liver specimens were carefully evaluated for evidence of inflammation, steatosis, fibrosis, necrosis and peliosis. Necrosis was scored as 0 to 4 based on extent of necrosis as described previously (Luyendyk et al., 2009). Areas without necrosis were scored as 0 and areas with extensive necrosis are scored as 4. Multiple cyst-like, blood-filled cavities of variable sizes, shapes and numbers within liver parenchyma characteristically known as "peliosis" were noted in several mice with different treatments as discussed below. In none of the cases was "phlebectatic peliosis," characterized by histologic features of regular blood filled cavities lined by endothelial cells identified. Instead, the only type of peliosis that was noted was of the "parenchymal-type", where various blood or fibrin filled irregular cystic parenchymal spaces were identified surrounded and intermixed with necrotic, degenerated hepatocytes. The extent of this parenchymal peliosis was graded into rare (rare minute microscopic foci of peliosis), moderate (moderate-sized, multiple areas of peliosis) or severe (multiple, large-sized, coalescent foci). For platelet and fibrin staining, frozen sections cut at 8 microns were fixed in 4% neutral-buffered formalin for 10 minutes at room temperature, washed 3 times with PBS, and blocked with 10% goat serum in PBS (block buffer) for 1 hour. Sections were incubated with the primary antibodies rabbit anti-human fibrinogen (1:5000; Dako, Carpinteria, CA) and/or rat anti-mouse CD41 (1:1000; Serotec, Raleigh, NC) diluted in block buffer for 2 hours at room temperature. The slides were washed and incubated with Alexa 488- and Alexa 594-conjugated secondary antibodies (Invitrogen, Carlsbad, CA) diluted in block buffer +2% mouse serum for 2 hours. The slides were then washed with PBS and fluorescent staining of the livers sections was visualized using an Olympus BX41 microscope (Olympus, Lake Success, NY). Images were captured

using an Olympus DP70 and merged using the Olympus DP Manager software. Quantification of CD41 area was performed utilizing Scion Image as described previously (Yee et al., 2003).

2.3.3 Clinical chemistry, platelet quantification in blood and thrombin-antithrombin measurement: The serum activities of alanine aminotransferase (ALT) and alkaline phosphatase (ALP) were determined using commercially available reagents (Pointe Scientific, Canton, MI). Thrombin-antithrombin levels in plasma were determined using a commercially available ELISA kit (Siemens Healthcare Diagnostics, Deerfield, IL). Quantification of platelets was performed on EDTA-anticoagulated whole blood utilizing a Beckman Coulter LH 780.

2.3.4 RNA isolation, cDNA synthesis, and real-time PCR: RNA was isolated from 75 mg of snap-frozen liver using TRI reagent (Molecular Research Center, Inc., Cincinnati, OH) according to the manufacturer's protocol. One microgram of RNA was utilized for the synthesis of cDNA using a High Capacity cDNA Reverse Transcription kit (Applied Biosystems, Foster City, CA) and MyCycler thermal cycler (Bio-Rad, Hercules, CA). Levels of Cxcl1 (KC), ICAM-1 and 18S mRNA were determined using TaqMan gene expression assays and TaqMan gene expression master mix (Applied Biosystems, Foster City, CA) on an StepOnePlus sequence detection system (Applied Biosystems, Foster City, CA). The expression of KC and ICAM-1 mRNA was normalized relative to 18S expression levels, and relative expression level determined using the comparative Ct method.

2.3.5 Tissue myeloperoxidase (MPO) activity: Neutrophil accumulation in liver was estimated by measuring liver homogenate MPO activity. 100 mg of frozen liver was homogenized in a buffer containing 0.5% hexadecyl trimethyl ammonium bromide, 10 mM EDTA and 50 mM Na_2PO_4, pH 5.4 and subjected to 3 freeze-thaw cycles followed by centrifugation at 12,000 x g for 15 minutes at 4°C. MPO activity in the supernatant was determined by addition of 50 mM Na_2PO_4 containing 0.167 mg/ml *o*-dianisidine dihydrochloride (Sigma, St. Louis, MO) and 0.0005% hydrogen peroxide (Sigma, St. Louis, MO) in 50 mM phosphate buffer (pH 6.0). MPO activity was expressed as the change in absorbance measured at 460 nm per mg of protein in the liver homogenate. The concentration of protein in liver homogenate was determined using a BCA assay (Pierce).

2.3.6 Statistics: Comparison of two groups was performed using Student's *t*-test. Comparison of 3 or more groups was performed using one-way analysis of variance and Student-Newman-Keul's post-hoc test. Where data were not normally distributed comparisons were made by ANOVA on ranks and Student-Newman-Keul's post-hoc test. The criterion for statistical significance was $P<0.05$.

2.4 Results

2.4.1 Time course of ANIT-induced hepatic platelet accumulation, coagulation, and liver injury.

First, we determined the relative time course of thrombocytopenia, coagulation cascade activation and liver injury in mice treated with ANIT. Serum ALT and ALP activity were slightly elevated in ANIT-treated mice at 24 hours and injury progressed further by 48 hours (Fig. 2.1A-B). In agreement with our previous study (Luyendyk et al., 2009), plasma TAT concentration increased dramatically at 24 hours and increased further by 48 hours (Fig. 2.1C). An increase in TAT in the plasma indicates generation of the coagulation protease thrombin. Interestingly, the increase in plasma TAT concentration preceded a decrease in platelets in the blood. A decrease in platelets in blood was observed at 48 hours after ANIT treatment (Fig. 2.1D). Of importance, the results indicate that coagulation precedes the decrease in platelets in blood of ANIT-treated mice. Scattered CD41-positive (i.e., platelet) staining consistent with localization to the sinusoids and larger vessels was observed in liver sections from vehicle-treated mice (Fig. 2.2A) and within larger vessels. In agreement with previous studies (Yee et al., 2003; Luyendyk et al., 2009), fibrin staining in livers from vehicle treated mice was restricted to the intima of larger vessels (Fig. 2.2B-C). The marked decrease in blood platelets in ANIT-treated mice at 48 hours was associated with increased platelet accumulation within areas of hepatic necrosis (i.e., bile infarcts) (Fig. 2.2D). Fibrin deposition also occurred within areas of necrosis in ANIT-treated mice (Fig. 2.2E-F).

2.4.2 Effect of platelet depletion on ANIT-induced coagulation and liver injury. Platelet depletion was accomplished using an anti-CD41 antibody, clone MWReg30. Previous studies have utilized this antibody to specifically deplete platelets in mice (Lesurtel et al., 2006). Platelet depletion with the anti-CD41 antibody alone did not cause liver injury (data not shown). Pretreatment with the anti-CD41

antibody dramatically reduced blood platelets in ANIT-treated mice at 24 hours and at 48 hours (Fig. 2.3A). Interestingly, platelet depletion did not affect ANIT-induced coagulation, as indicated by increased plasma TAT concentration at 24 hours and 48 hours (normal levels <5 ng/mL) (Fig. 2.3B). This is in agreement with our finding that coagulation preceded a decrease in platelets in the blood in ANIT-treated mice. Platelet depletion did not affect serum ALP activity in ANIT-treated mice at either 24 hours or 48 hours (Fig. 2.3C). Interestingly, serum ALT activity was substantially increased by platelet depletion in ANIT-treated mice at 24 hours (Fig. 2.3D). While serum ALT activity did not increase further in platelet-depleted mice given ANIT, serum ALT activity increased further by 48 hours in ANIT-treated mice given control antibody (Fig. 2.3D).

2.4.3 Effect of platelet depletion on liver histopathology in ANIT-treated mice. Liver necrosis induced by ANIT is characterized by areas of periportal necrosis containing bile and is associated with marked inflammatory cell accumulation (Becker and Plaa, 1965; Plaa and Priestly, 1976). We have described the liver histopathology associated with high dose ANIT administration previously (Luyendyk et al., 2009). Of importance, these so-called "bile infarcts" were evident in the livers of ANIT-treated mice given control IgG at 24 hours (Fig. 2.4A) and the size and frequency of necrotic lesions increased in these mice by 48 hours (Fig. 2.4D) (Table 2.1). Red blood cell infiltration of necrotic areas was evident in mice given ANIT and control IgG and this was somewhat increased at 48 hours (Table 2.1). Interestingly, platelet depletion increased the severity of necrotic lesions in ANIT-treated mice at 24 hours and this was associated with substantial pooling of blood within areas of necrosis, a lesion consistent with parenchymal-type peliosis (Tsokos and Erbersdobler, 2005). Peliosis was evident both in proximity to periportal necrosis (Fig. 2.4B) and in regions of the liver several hepatocytes separated from damaged bile ducts (Fig. 2.4C). Peliosis was also prominent in these mice at 48 hours (Fig. 2.4F), and in contrast to mice given control IgG, the severity of necrosis did not substantially increase between 24 and 48 hours (Table 2.1).

2.4.4 Inhibition of platelet activation reduces ANIT-induced liver injury: evidence for platelet-dependent neutrophil accumulation. As opposed to depleting all platelets, we next utilized the $P2Y_{12}$

receptor antagonist clopidogrel to inhibit platelet activation. Administration of clopidogrel alone did not affect serum ALT activity (data not shown) or liver histopathology (Table 2.2). Clopidogrel administration did not affect serum ALT activity in ANIT-treated mice at 24 hours (902 ± 204 U/L [ANIT+Veh] vs. 748 ± 226 U/L [ANIT+clopidogrel]). In contrast, at 48 hours clopidogrel administration significantly reduced serum ALT activity in ANIT-treated mice (Fig. 2.5A) but did not affect increases in serum ALP activity (Fig. 2.5B). Clopidogrel treatment reduced hepatic platelet accumulation (Fig. 2.5C-G) in ANIT-treated mice and reduced the severity of necrosis (Table 2.2), but did not increase red blood cell accumulation within necrotic lesions. Clopidogrel did not affect ICAM-1 or KC induction in the livers of ANIT-treated mice (Fig. 2.6A-B). In contrast, clopidogrel substantially reduced hepatic neutrophil accumulation, as indicated by reduced liver homogenate MPO activity (Fig. 2.6C).

2.5 Discussion

Platelets have been implicated in the pathogenesis of multiple types of liver damage including viral hepatitis (Lang et al., 2008), ischemia-reperfusion (Yadav et al., 1999), bile duct ligation (Laschke et al., 2008), and injury induced by xenobiotics including concanavalin (Miyazawa et al., 1998; Massaguer et al., 2002), and lipopolysaccharide (Pearson et al., 1995). Our data agree with a previous study showing that platelet depletion in rats (Bailie et al., 1994) reduces ANIT-induced liver necrosis. Both platelet depletion and inhibition strategies reduced the severity of liver necrosis in ANIT-treated mice. However, platelet depletion exacerbated a perhaps underappreciated lesion in ANIT-treated mice characterized by pooling of blood in areas of necrosis (i.e., peliosis). The data support the hypothesis that platelets have both protective and damaging effects in ANIT-induced liver injury.

Our previous work indicated that ANIT-induced coagulation cascade activation is TF-dependent, and that TF contributes to the progression of ANIT-induced liver injury. Insofar as platelets can express TF and contribute to activation of the coagulation cascade (Ofosu, 2002; Schwertz et al., 2006), we examined their involvement in this capacity in ANIT-induced liver injury. The results presented herein indicate that blood platelets are reduced after coagulation cascade activation and platelet depletion did not

affect thrombin generation. This indicates that coagulation cascade activation is not dependent on platelets in ANIT-treated mice, and that another cell type expressing TF is important for coagulation in this model. Indeed, we have shown that BDECs express TF (Luyendyk et al., 2009), and the initial destruction of these cells by ANIT may cause TF-dependent coagulation. Moreover, TF expressed by other cells in the liver such as hepatocytes (Stephenne et al., 2007) could contribute to ANIT-induced coagulation.

Platelets appear to modify hepatocellular injury in ANIT-treated mice by impacting hepatic accumulation of inflammatory cells. Clopidogrel treatment reduced neutrophil accumulation in the livers of ANIT-treated mice. Of importance, platelet depletion did not significantly reduce liver homogenate MPO activity 48 hours after ANIT treatment (71 ± 15 vs. 130 ± 62), although direct comparison of these results is complex as leukocyte infiltration may be driven by additional mechanisms under conditions of peliosis induced by complete platelet deficiency. It has also been shown after BDL that platelet depletion reduced neutrophil accumulation in liver, as well as hepatic ICAM-1 and KC/Groα mRNA levels (Laschke et al., 2008). In contrast, clopidogrel treatment did not affect hepatic expression of ICAM-1 or KC mRNAs in ANIT-treated mice. Adhesion molecules on the surface of activated platelets, including GPIIb/IIIa and P-selectin, interact directly with integrins and selectins on the surface of neutrophils (Zarbock et al., 2007). Of interest, a P-selectin antibody decreased the accumulation of neutrophils in liver after BDL (Laschke et al., 2008). Interactions between platelets, neutrophils and sinusoidal endothelial cells may be critical for promoting neutrophil accumulation in the livers of ANIT-treated mice.

The mechanisms by which platelets are recruited and activated in the livers of ANIT-treated mice have not been determined. While we sought to evaluate the role of platelets in activating the coagulation cascade, the time course of coagulation and of platelet activation suggests the possibility of the opposite relationship. That is, that the coagulation cascade is a mediator of platelet activation during cholestatic liver injury. Thrombin is a potent activator of platelets via protease activated receptors (PARs). Thrombin

activation of human platelets requires PAR-1 (Trejo et al., 1996), whereas in mice, PAR-3 and PAR-4 are required (Kahn et al., 1998). In addition to eliciting intracellular signaling in platelets, the interaction of these cells with cross-linked fibrin (Lupu et al., 2005) within areas of necrosis in ANIT-treated mice could be an important mechanism for platelet accumulation. Indeed, platelets colocalized with fibrin in areas of necrosis in livers of ANIT-treated mice. Additional studies clarifying the role of thrombin and fibrin in the platelet activation observed in ANIT-treated mice are required.

Previous studies have implicated platelets as mediators of liver damage during cholestasis (Bailie et al., 1994; Laschke et al., 2008). Depletion of platelets in rats limited the progression of ANIT-induced hepatocellular injury, but did not affect biomarkers of biliary injury (Bailie et al., 1994). The present results agree with those described previously, insofar as a pharmacologic inhibitor of platelet activation (i.e., clopidogrel) reduced hepatocyte necrosis in ANIT-treated mice, but did not impact serum ALP activity, an indicator of cholangiocyte damage. However, in striking contrast to platelet depletion in rats, platelet depletion in ANIT-treated mice exacerbated the pooling of blood within necrotic lesions, consistent with parenchymal type peliosis (Tsokos and Erbersdobler, 2005). This variant of peliosis is typified by pooling of blood within or adjacent to necrotic tissue, and the lesions are not necessarily bordered by endothelium or fibrotic material, the latter being a hallmark of another peliosis variant called phlebectatic peliosis (Tsokos and Erbersdobler, 2005). The basis for this lesion in our study but not in platelet-depleted ANIT-exposed rats is not clear, but could relate to multiple factors including differences in species, fasting, severity of liver injury, or use of whole antiserum vs. anti-CD41 antibody. Of importance, the anti-CD41 (GP11bIIIa) antibody commonly utilized to examine the role of platelets in tissue injury has systemic effects, including transient induction of hypothermia and lung injury (Nieswandt et al., 1999; Nieswandt et al., 2000). Moreover, complexes of this antibody and platelets accumulate in the liver after administration and may be cleared by Kupffer cells (Bagchus et al., 1989). This could impact normal hepatic homeostasis.

Peliosis hepatis in patients is a relatively rare clinical finding associated with a variety of diseases and treatment with various drugs including 6-mercaptopurines and steroids (Tsokos and Erbersdobler,

2005). Peliosis in the liver has also been described in rodent models of exposure to xenobiotics including TCDD (Niittynen et al., 2003), cadmium (Habeebu et al., 1998; Tzirogiannis et al., 2006) , hexachlorobenzene (Carthew and Smith, 1994), and anabolic steroids (Stang-Voss and Appell, 1981; Tsirigotis et al., 2007). Interestingly, peliosis has been reported in the context of cholestatic liver injury in rodent models (Romagnuolo et al., 1998; Niittynen et al., 2003) and in patients (Hayward et al., 1991; Russmann et al., 2001). Moreover, in some patients, peliosis in liver and pancreas has been associated with exaggerated coagulation and thrombotic thrombocytopenic purpura (TTP) (Samyn et al., 2004; Belovejdov et al., 2008), a somewhat counterintuitive finding in the context of altered hemostasis in liver. Of importance, peliosis in ANIT-treated mice depleted of platelets occurred in the presence of marked coagulation, as indicated by increased plasma TAT concentration. However, a definitive mechanistic role of either the coagulation cascade or platelets in the pathogenesis of peliosis has not been described.

It is curious in our study that a near complete depletion of platelets caused peliosis in ANIT-treated mice at 24 hours, a time point at which ANIT alone had minimal effect on the number of platelets in the blood. It is possible that the accumulation of very few platelets is required to limit peliosis in the liver during cholestasis. Indeed, although we did not detect a difference in platelet numbers in blood, the number of platelets in the sinusoids increased 24 hours after ANIT treatment (Supplemental Figure 2.1). Indeed, the upregulation of adhesion molecules, such as P-selectin, on the surface of platelets may precede an observable decrease in blood platelets. Additional studies are required to determine the time course of P-selectin upregulation on platelets in this model. The pathogenesis of peliosis has been proposed to stem from perturbed sinusoidal endothelial cell function in the liver (Tsokos and Erbersdobler, 2005; DeLeve, 2007), including induction of cell death, and it is possible that initial platelet accumulation in the liver during cholestasis limits SEC dysfunction that leads to peliosis. Indeed, cholestatic liver injury is associated with SEC dysfunction, and bile acids can activate intracellular signaling pathways in SECs (Yoshidome et al., 2000; Keitel et al., 2007). Platelet release of sphingosine-1-phosphate has been shown to be cytoprotective to endothelial cells (Zheng et al., 2006). Moreover, serotonin released from platelets promotes liver regeneration and has been shown to alter SEC

fenestration (Braet et al., 1995). Another possibility is that the accumulation of platelets at the expanding edge of necrotic lesions constitutes a cellular barrier to limit bleeding into necrotic areas. To this end, severe thrombocytopenia and concurrent cholestasis may be risk factors for developing peliosis. Additional studies are warranted to determine the mechanism whereby platelets can prevent peliosis during cholestasis.

In summary, the results indicate that in ANIT-induced cholestatic liver injury, hepatic platelet accumulation promotes neutrophil accumulation and hepatocyte necrosis, but not coagulation cascade activation. Of importance, the finding of peliosis in livers of ANIT-treated mice after platelet depletion suggests that severe thrombocytopenia may render the liver susceptible to peliosis during cholestasis.

2.6 Figures

Figure 2.1

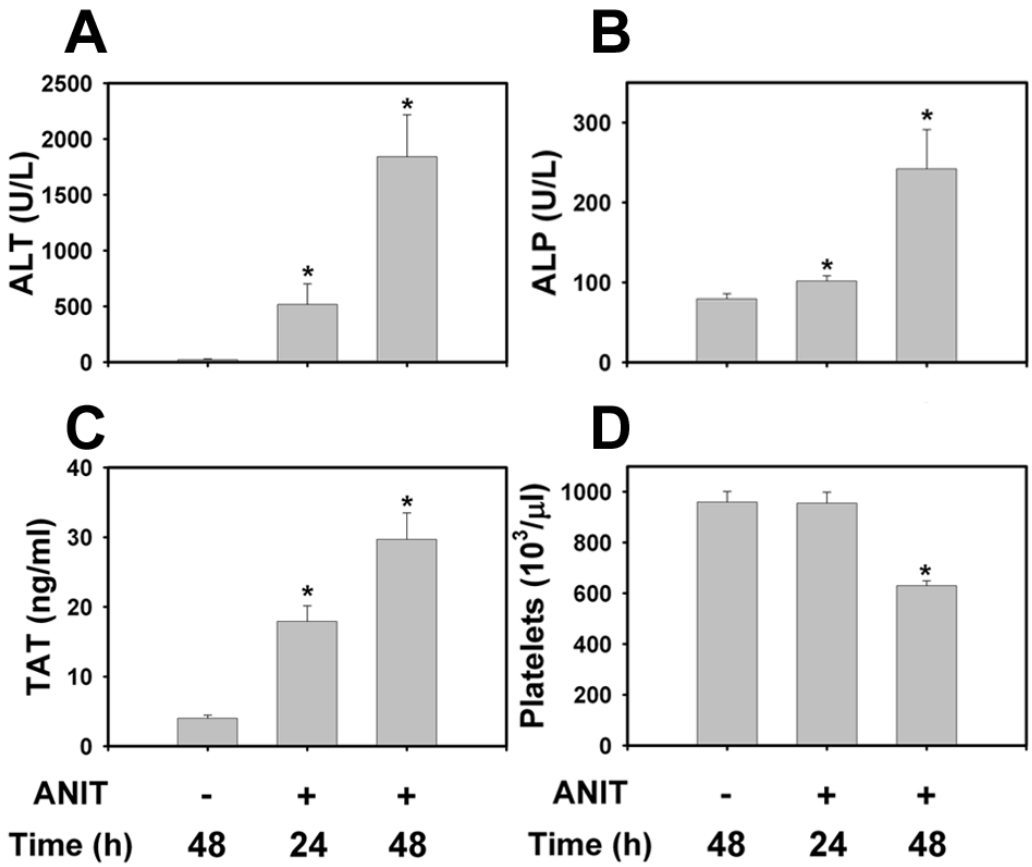

Figure 2.1: Time course of ANIT-induced liver injury, coagulation and blood platelets in mice.

Mice were given ANIT (60 mg/kg, po) or vehicle (corn oil). (A) Serum ALT activity, (B) serum ALP activity, (C) plasma thrombin-antithrombin (TAT) levels, and (D) platelets in EDTA-anticoagulated whole blood were determined 24 and 48 hours after ANIT administration. Levels of all biomarkers in mice given vehicle were not different between 24 and 48 hours. 48 hour data are shown. Data are expressed as mean ± SEM. n=5 mice per group. *Significantly different from Veh-treated mice. $P<0.05$.

Figure 2.2

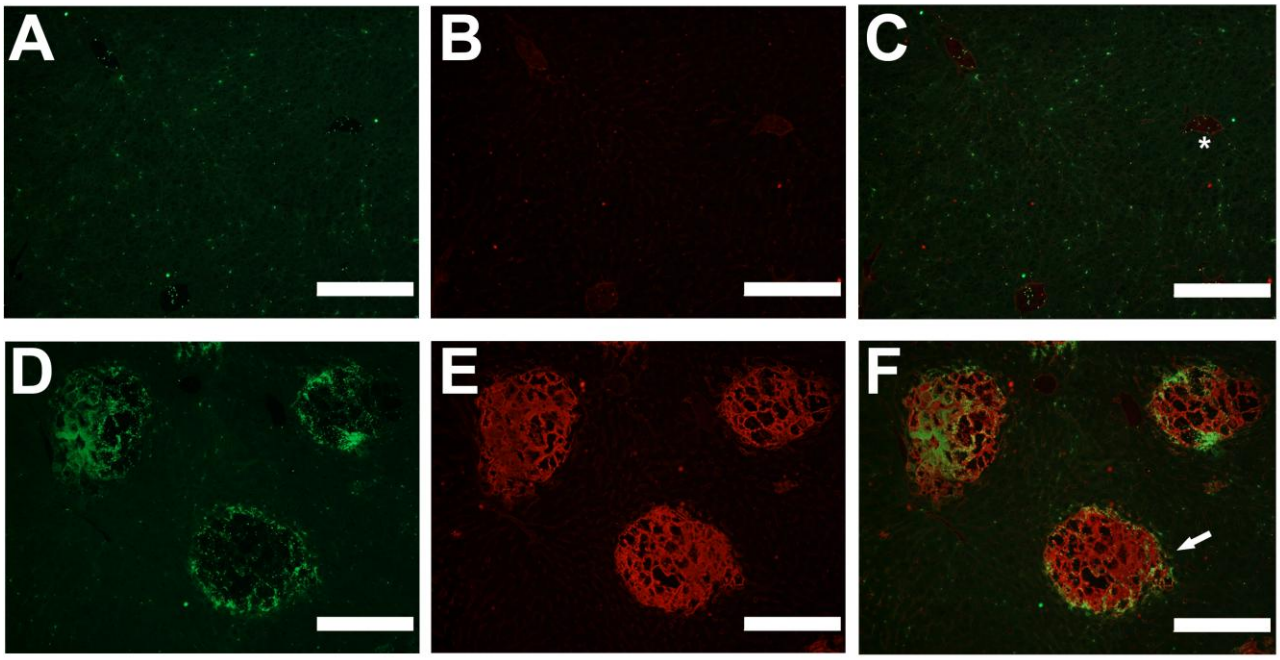

Figure 2.2: Platelet accumulation and fibrin deposition in livers of ANIT-treated mice.

Mice were given ANIT (60 mg/kg, po) or vehicle (corn oil) and livers removed 48 hours later. (A-B) Representative photomicrographs showing (A) CD41 (platelet, green) staining and (B) fibrin (red) staining in a liver section from a vehicle-treated mouse. The digital merge of these images is shown in

panel C. Asterisk indicates fibrin staining (red) outlining the border of a central vein. (D-E) Representative photomicrographs showing marked (D) CD41 (platelet, green) staining and (E) fibrin (red) staining in areas of necrosis in a liver section from a ANIT-treated mouse. The digital merge of these images is shown in panel F. Bar = 20 microns. Arrow indicates an area of hepatic necrosis containing fibrin and bordered by marked platelet accumulation.

Figure 2.3

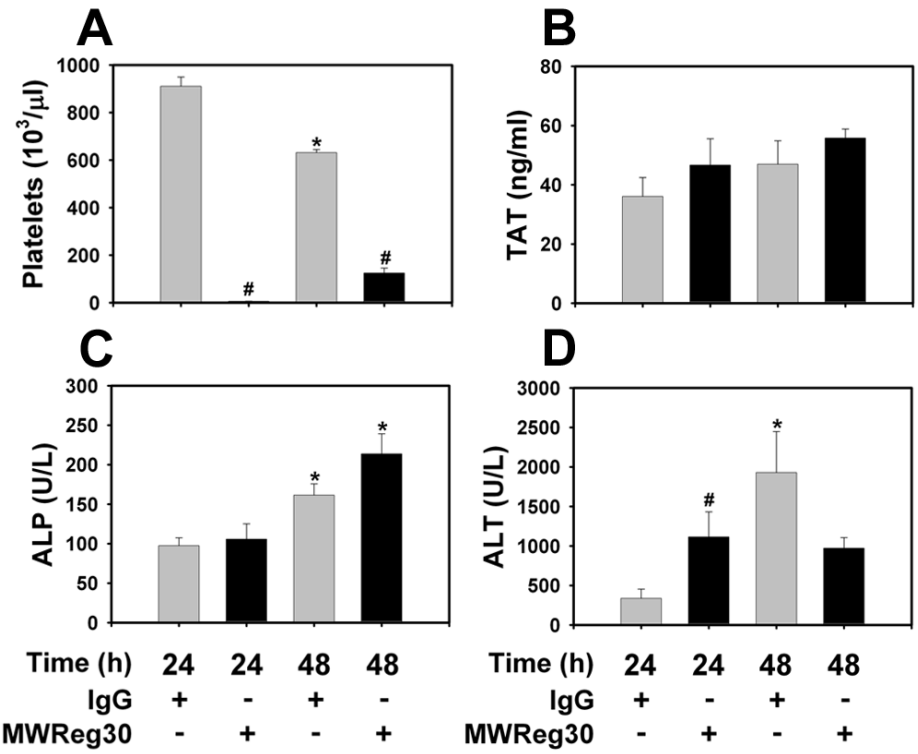

Figure 2.3: Effect of platelet depletion on ANIT-induced coagulation and liver injury.

Mice were given 1 mg/kg of anti-CD41 antibody (MWReg30) or isotype control antibody 16 hours prior to treatment with ANIT (60 mg/kg, po). (A) Platelets in EDTA-anticoagulated whole blood, (B) plasma thrombin-antithrombin (TAT) levels, (C) serum ALP activity, and (D) serum ALT activity were determined 24 and 48 hours later. Data are expressed as mean ± SEM. n=5 mice per group.*Significantly different from the same group of mice at 24 hours. #Significantly different from ANIT-treated mice pretreated with isotype control antibody.

Figure 2.4

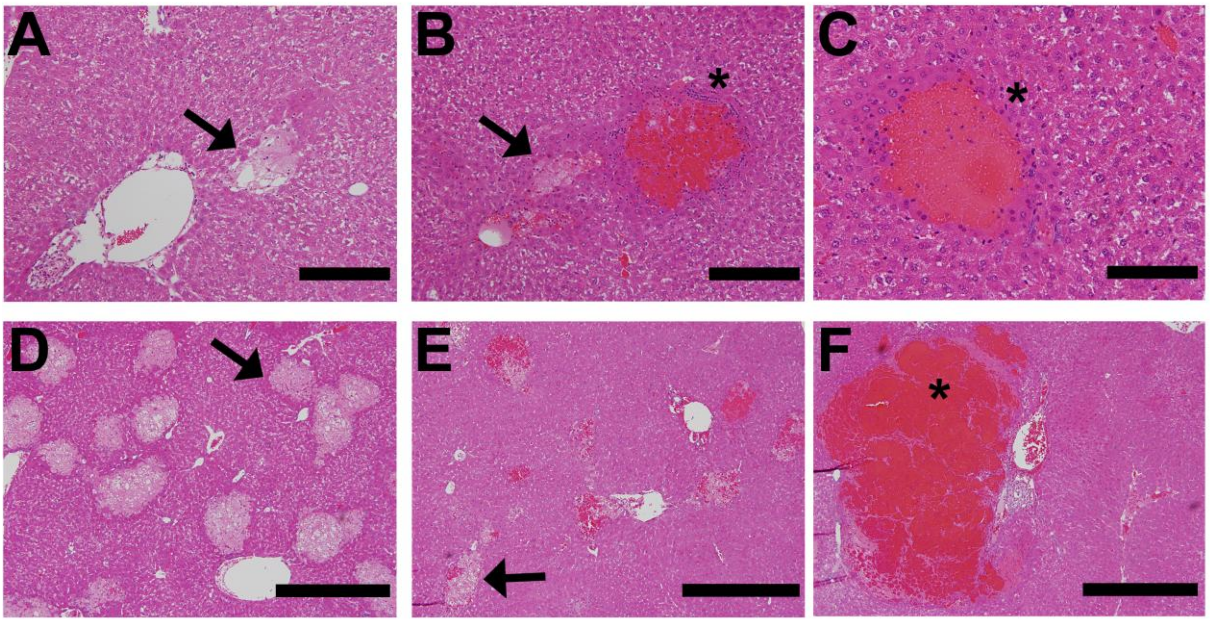

Figure 2.4: Effect of platelet depletion on ANIT-induced liver histopathology.

Mice were given 1 mg/kg of anti-CD41 antibody or isotype control antibody 16 hours prior to treatment with ANIT (60 mg/kg, po). Representative photomicrographs showing H&E-stained liver sections from isotype control antibody-pretreated mice (A) 24 hours and (D) 48 hours after ANIT-treatment, and in anti-CD41 antibody-pretreated mice 24 hours after ANIT treatment (B and C) and 48 hours after ANIT-treatment (E and F). Bar = 20 microns (A and B), 10 microns (C), 50 microns (D-F). Arrows indicate areas of periportal hepatocellular necrosis. Asterisks are near areas of parenchymal-type peliosis.

Figure 2.5

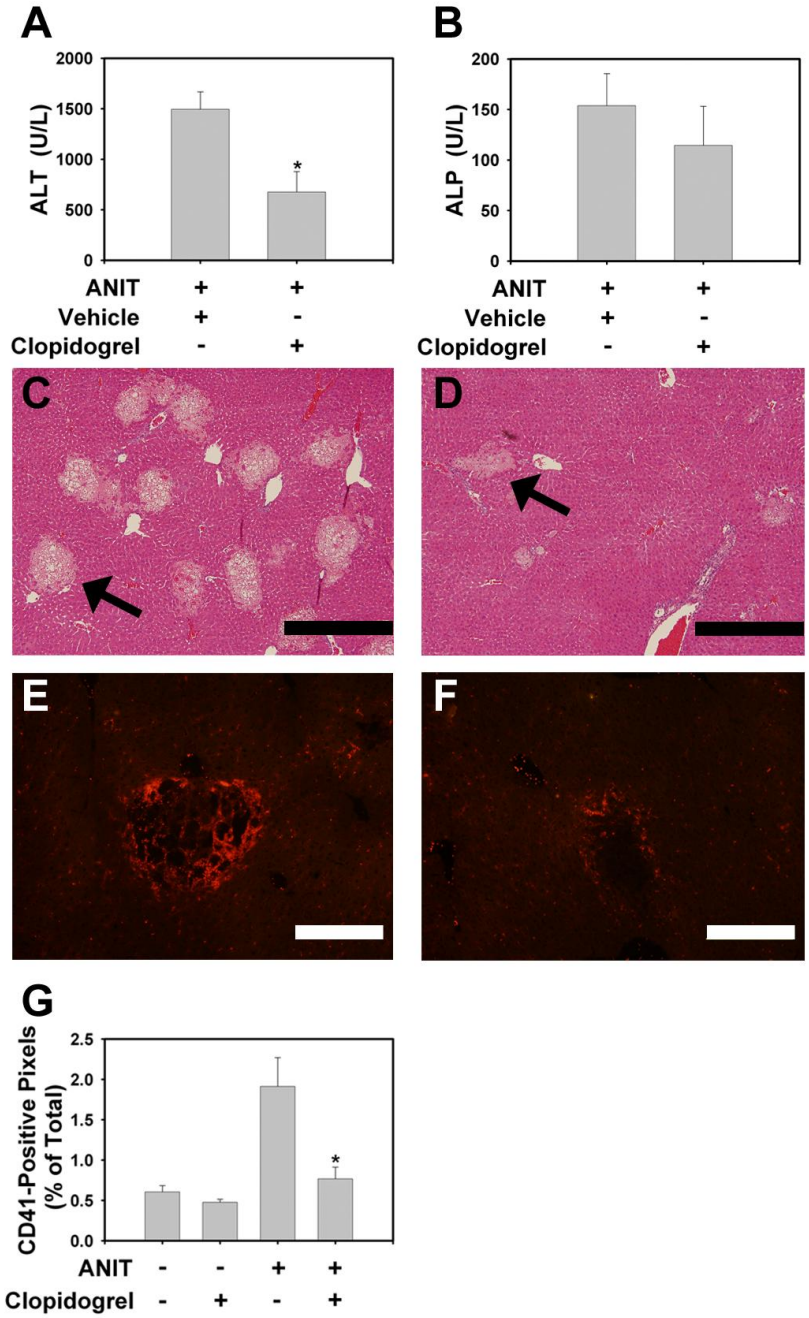

Figure 2.5: Effect of clopidogrel treatment on ANIT-induced liver injury.

Mice were treated with ANIT (60 mg/kg, po), then subsequently with clopidogrel (30 mg/kg, ip) or sterile PBS 8, 20, and 32 hours later. Serum (A) ALT activity and (B) ALP activity were determined 48 hours

later. Representative photomicrographs showing H&E-stained (C and D, Bar=50 microns) and anti-CD41 (platelet, red) stained (E and F, Bar= 20 microns) liver sections from ANIT-treated mice given vehicle (C and E) or clopidogrel (D and F). (G) Quantification of CD41-positive staining (platelets) in liver sections from each group of mice. Data are expressed as mean ± SEM. n=3-6 mice per group. *Significantly different from ANIT-treated mice given sterile PBS. P<0.05. Arrows indicate areas of periportal hepatocellular necrosis.

Figure 2.6

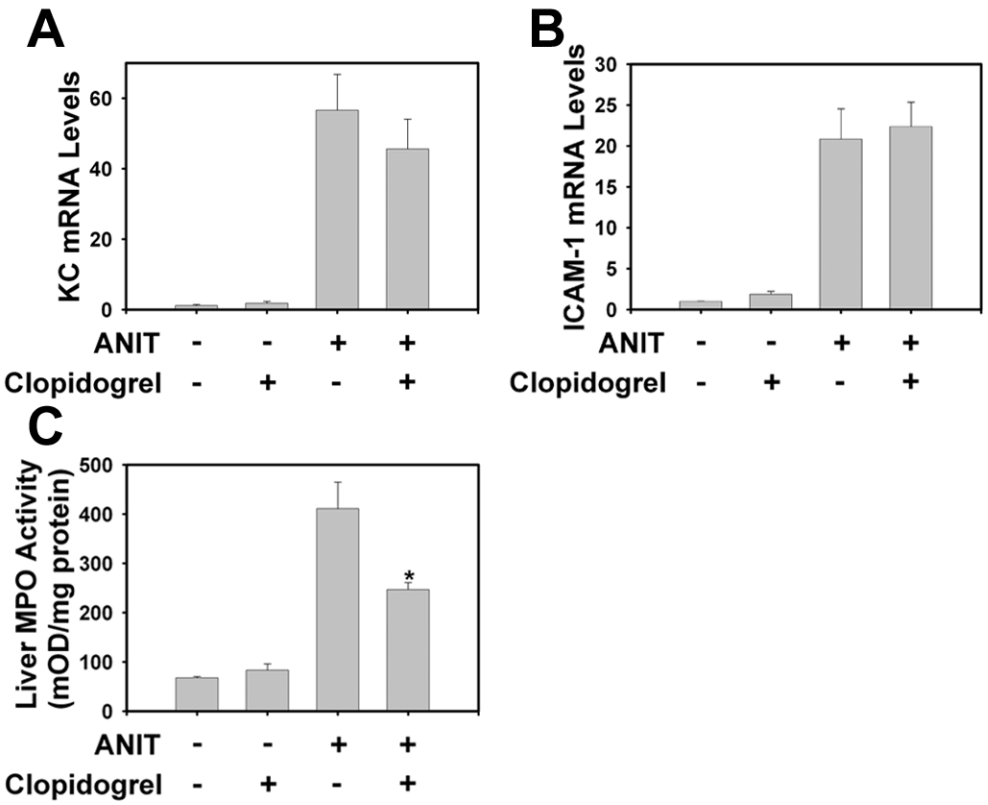

Figure 2.6: Effect of clopidogrel treatment on indicators of neutrophil accumulation.

Mice were treated with ANIT (60 mg/kg, po), then subsequently with clopidogrel (30 mg/kg, ip) or sterile PBS 8, 20, and 32 hours later. Hepatic KC (A) and ICAM-1 (B) mRNA levels were determined 48 hours later. (C) Liver homogenate myeloperoxidase (MPO) activity was measured 48 hours after ANIT

treatment. Data are expressed as mean ± SEM. n=3-6 mice per group. *Significantly different from ANIT-treated mice given sterile PBS. P<0.05.

2.7 Supplemental Figures

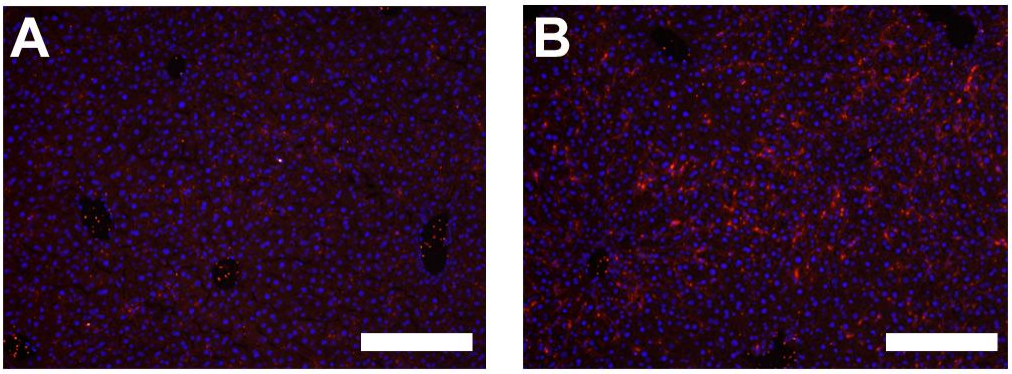

Supplemental Figure 2.1: Hepatic accumulation of platelets 24 hours after ANIT treatment.

Wild type mice were given ANIT (60 mg/kg, po) or vehicle (corn oil) and livers removed 24 hours later. Representative photomicrographs showing CD41 (platelet, red) staining in liver sections from a mouse treated with vehicle (A) for 24 hours or ANIT (B) for 24 hours. Sections were counterstained with DAPI. Bar= 20 microns

2.8 Tables

Table 2.1

	ANIT 24 hours		**ANIT 48 hours**	
	IgG	**MWReg30**	**IgG**	**MWReg30**
Necrosis (score)	1.4 (0,1,2,2,2)	3 (3,3,3)	4 (4,4,4,4,4)	3.6 (3,3,4,4,4)
Peliosis (grade)	A (2), R (3)	M (1), P (2)	R (2), M (3)	M (3), P (2)

Table 2.1: Effect of platelet depletion on ANIT-induced liver necrosis and parenchymal-type peliosis.

Mice were given 1 mg/kg of anti-CD41 antibody (MWReg30) or isotype control antibody 16 hours prior to treatment with ANIT (60 mg/kg, po) and livers were collected 24 or 48 hours later. The severity of necrosis in liver sections was assigned a score from 0-4, increasing in severity as described in Methods. Average necrosis scores and the score for each animal are shown. Parenchymal-type peliosis in liver sections was categorized as absent (A) rare, microscopic foci (R), multiple lesions moderate in size (M) or multiple large sized coalescent foci (P).

Table 2.2

	Vehicle	**Clopidogrel**
Vehicle	0 (0,0,0)	0 (0,0,0)
ANIT	2.7 (3,3,3,3,2,2)	2.0 (1/2,2,2,2,2,3)

Table 2.2: Effect of platelet depletion on ANIT-induced liver necrosis.

Mice were treated with ANIT (60 mg/kg, po), then subsequently with clopidogrel (30 mg/kg, ip) or sterile PBS 8, 20, and 32 hours later. Livers were collected 48 hours after ANIT treatment and the severity of necrosis in liver sections was assigned a score from 0-4, increasing in severity as described in Methods. Average necrosis scores and the score for each animal are shown.

Chapter 3

Role of Fibrinogen and protease-activated receptors in acute xenobiotic-induced cholestatic liver injury.

James P. Luyendyk[1], Nigel Mackman[2] and Bradley P. Sullivan*[1]

[1] Department of Pharmacology, Toxicology and Therapeutics, The University of Kansas Medical Center, Kansas City, KS

[2] Division of Hematology/Oncology, Department of Medicine, University of North Carolina, Chapel Hill, NC

*Bradley Sullivan made significant contributions to this work.

This article was published in Toxicological Sciences. 2011 Jan;119(1):233-43.

3.1 Abstract

Alpha-naphthylisothiocyanate (ANIT)-induced cholestatic liver injury causes tissue factor (TF)-dependent coagulation in mice and TF-deficiency reduces ANIT-induced liver injury. However, the mechanism whereby TF contributes to hepatotoxicity in this model is not known. Utilizing pharmacologic and genetic strategies, we evaluated the contribution of fibrinogen and two distinct receptors for thrombin, protease activated receptor-1 (PAR-1) and PAR-4, in a model of acute ANIT hepatotoxicity. ANIT administration (60 mg/kg, po) caused a marked induction of the genes encoding the three fibrinogen chains (α, β, and γ) in liver, an increase in plasma fibrinogen, and concurrent deposition of thrombin-cleaved fibrin in liver. Partial depletion of circulating fibrinogen with ancrod did not impact ANIT hepatotoxicity. However, complete fibrin(ogen)-deficiency significantly reduced serum ALT activity and hepatocellular necrosis in ANIT-treated mice. ANIT-induced hepatocellular necrosis was similar in PAR-$1^{-/-}$ mice compared to PAR-$1^{+/+}$ mice. Interestingly, the progression of ANIT-induced hepatocellular necrosis was significantly reduced in PAR-$4^{-/-}$ mice, and by administration of an inhibitory PAR-4 pepducin (P4Pal-10, 0.5 mg/kg, sc) to wild type mice 8 hours after ANIT treatment. Interestingly, a distinct lesion, parenchymal-type peliosis, was also observed in PAR-$4^{-/-}$ mice treated with ANIT, and in mice that were given P4Pal-10 prior to ANIT administration. The results suggest that fibrin(ogen), but not PAR-1, contributes to the progression of ANIT hepatotoxicity in mice. Moreover, the data suggest a dual role for PAR-4 in ANIT hepatotoxicity, both mediating an early protection against peliosis, and contributing to the progression of hepatocellular necrosis.

3.2 Introduction

Acute chemical-induced cholestatic liver injury can be modeled in rodents by administration of alpha-naphthylisothiocyanate (ANIT), which achieves micromolar levels in the bile of exposed animals (Jean et al., 1995). This results in bile duct injury and formation of “bile infarcts,” areas of periportal hepatocellular necrosis containing dead/dying hepatocytes, bile, and inflammatory cells, which have been described in detail previously (Plaa and Priestly, 1976). Deficiency in the transport of ANIT into the bile

prevents necrosis, suggesting that the cytotoxic disruption of intrahepatic bile ducts is critical for necrosis in this model (Dietrich et al., 2001). In addition, several studies have shown that extrahepatic factors including platelets and neutrophils, as well as tissue factor (TF), the primary activator of the extrinsic pathway of blood coagulation, contribute to necrosis progression (Bailie et al., 1994; Kodali et al., 2006; Luyendyk et al., 2009; Sullivan et al., 2010a).

Acute ANIT hepatotoxicity is associated with activation of the coagulation cascade, as indicated by thrombin generation and deposition of fibrin clots within areas of hepatocellular necrosis. Indeed, coagulation cascade activation occurs in numerous models of chemical-induced hepatotoxicity. TF-deficiency reduced generation of the coagulation protease thrombin and the severity of hepatocellular necrosis in ANIT-treated mice (Luyendyk et al., 2009). However, the mechanism whereby the coagulation cascade contributes to the progression of liver necrosis in this model is not known. Investigation of the role of coagulation in hepatotoxicity is frequently limited to examining the effect of thrombin inhibition (i.e, with anticoagulants) on hepatotoxicity, with the exact mechanism whereby thrombin contributes to liver injury left unanswered.

Thrombin generated by activation of the coagulation cascade has multiple roles. Thrombin cleaves circulating fibrinogen to fibrin monomers, which are cross-linked to form insoluble fibrin clots. Moreover, thrombin can cleave and activate cell-surface G-protein coupled protease activated receptors (PARs) to elicit intracellular signaling (Coughlin, 1999). PAR-1 and PAR-4 are thrombin receptors expressed by nonparenchymal cells in the liver (Copple et al., 2003; Jesmin et al., 2006). Unlike humans, mouse platelets do not express PAR-1; rather, murine platelets are activated by thrombin via cleavage of PAR-4 (Sambrano et al., 2001). Of importance, the involvement of fibrin and PARs in acute ANIT hepatotoxicity has not been evaluated.

Although the role of PAR-1 in liver fibrosis induced by chronic liver injury has been investigated previously (Fiorucci et al., 2004; Rullier et al., 2008; Sullivan et al., 2010b), the role of this receptor in acute hepatotoxicity is less clear. PAR-1-deficient mice were protected from acute acetaminophen hepatotoxicity (Ganey et al., 2007). Activation of PAR-1 contributed to neutrophil activation in

lipopolysaccharide-primed livers (Copple et al., 2003). However, PAR-1-deficiency does not contribute to the acute hepatotoxic effects of other chemicals, such as carbon tetrachloride (Rullier et al., 2008). In comparison to PAR-1, few studies have examined the role of PAR-4 in hepatotoxicity.

Since we have shown previously that genetically reducing coagulation limits ANIT-induced liver injury, the present study tested the hypothesis that PAR-1 and PAR-4 signaling, as well as fibrin clots contribute to acute ANIT-induced hepatotoxicity.

3.3 Materials and Methods

3.3.1 Mice: Male and female mice between the ages of 8-16 weeks were used for these studies. Male wild type C57Bl/6J mice were purchased from The Jackson Laboratory for studies of ancrod and P4Pal-10 administration. PAR-$1^{-/-}$ mice (Connolly *et al.* 1997) and PAR-$1^{+/+}$ mice on an identical genetic background (N8 C57Bl/6J) were maintained by homozygous breeding. Age-matched male PAR-$1^{+/+}$ mice and PAR-$1^{-/-}$ mice were used for experiments. Fbg$\alpha^{-/-}$ ($Fbg^{-/-}$) mice (Suh et al., 1995) were kindly provided by Dr. Jay Degen (Cincinnati Children's Hospital Medical Center, Cincinnati, OH). Female $Fbg^{-/-}$ mice and $Fbg^{+/-}$ mice were used for 4 independent experiments with age-matched mice of each genotype. PAR-$4^{-/-}$ mice (Sambrano et al., 2001) and PAR-$4^{+/+}$ mice were maintained by homozygous breeding. Age-matched male PAR-$4^{+/+}$ mice and PAR-$4^{-/-}$ mice were used for experiments. Mice were maintained in an AAALAC-accredited facility at the University of Kansas Medical Center. Mice were housed at an ambient temperature of 22°C with alternating 12-h light/dark cycles, and allowed water and rodent chow ad libitum (Teklad 8604; Harlan, Indianapolis, IN). All animal procedures were performed according to the guidelines of the American Association for Laboratory Animal Science and were approved by the KUMC Institutional Animal Care and Use Committee.

3.3.2 ANIT hepatotoxicity model and pharmacologic interventions: Fasted mice were treated with ANIT (Sigma-Aldrich, St. Louis, MO) dissolved in corn oil (60 mg/kg, p.o.) or corn oil alone (control [vehicle] treatment) at 10 ml/kg. Food was returned after treatment with ANIT or vehicle. For fibrinogen depletion studies, 1.75U ancrod/mouse (National Institute for Biological Standards and Control,

Hertfordshire, England) or its vehicle (sterile saline) was administered by intraperitoneal injection 2, 12, 24 and 36 hours after ANIT administration. The PAR-4 pepducin P4pal-10 (palmitoyl-SGRRYGHALR-NH2; Genscript, Piscataway, NJ), or its vehicle (PBS), was administered by subcutaneous injection at a dose of 0.5 mg/kg 8 and 24 hours after ANIT treatment. For select studies, an additional dose of P4pal-10 was also given 2 hours prior to ANIT. The mice were then anesthetized using isoflurane 24 or 48 hours after ANIT treatment for the collection of blood and liver samples. Blood was collected from the caudal vena cava into a syringe containing sodium citrate (final concentration, 0.38%) and additional blood was collected into a syringe without anticoagulant. Plasma and serum were collected from this blood by centrifugation. Sections of liver from the left lateral lobe were fixed in 10% neutral-buffered formalin. The right medial lobe was cut into a cube and affixed to a cork using OCT and frozen for 3 minutes in liquid nitrogen-chilled isopentane. The remaining liver was snap frozen in liquid nitrogen.

3.3.3 RNA isolation, cDNA synthesis, and real-time PCR: RNA was isolated from approximately 100 mg of snap-frozen liver using TRI reagent (Molecular Research Center, Inc., Cincinnati, OH). cDNA synthesis was performed using 1 microgram of RNA and a High Capacity cDNA Reverse Transcription kit (Applied Biosystems) and MyCycler thermal cycler (Bio-Rad). Levels of Fbgα, Fbgβ, Fbgγ, serum amyloid A1 (SAA1), and GAPDH mRNA were determined using TaqMan gene expression assays and TaqMan gene expression master mix (Applied Biosystems) and a StepOnePlus (Applied Biosystems). The expression of each mRNA was normalized relative to GAPDH expression levels, and relative expression level determined using the comparative Ct method.

3.3.4 Clinical chemistry, plasma fibrinogen determination, and fibrin western blotting: The serum activities of alanine aminotransferase (ALT) and alkaline phosphatase (ALP) were determined using commercially available reagents (Thermo Scientific). The concentration of bile acids in serum was determined by using a commercial kit (Bio-quant, San Diego, CA). Plasma fibrinogen levels were determined using commercial reagents (Siemens Healthcare Diagnostics, Deerfield, IL) and a STart4 coagulation analyzer (Diagnostica Stago). Levels of fibrin in liver extracts were determined by western blotting as described previously (Luyendyk et al., 2009).

3.3.5 Histopathology: Formalin-fixed livers were subjected to routine processing, sectioned at 5 microns, stained with hematoxylin and eosin, and evaluated by light microscopy for the presence of hepatocellular necrosis, the features of which we have described in detail previously (Luyendyk et al., 2009). Three sections of liver from the left lateral lobe were evaluated from each animal. Each section was evaluated in its entirety. Low magnification (40X) images encompassing each section were captured in a masked fashion. Areas of hepatocellular necrosis in each image were outlined manually using Scion imaging software by J.P.L., and the area of liver occupied by necrotic areas (i.e,. bile infarcts) was measured and compared to the total area of liver in each image. The % necrotic area, number of lesions per 40X field, and average lesion size in square microns was determined.

3.3.7 Statistics: Comparison of two groups was performed using Student's *t*-test. Data resistant to transformation to achieve a normal distribution were compared utilizing the Mann-Whitney Rank Sum Test. Comparison of 3 or more groups was performed using one-way analysis of variance and Student-Newman-Keul's post-hoc test. The criterion for statistical significance was $P<0.05$.

3.4 Results

3.4.1 Induction of fibrinogen expression in ANIT-induced cholestatic liver injury. Compared to vehicle-treated mice, levels of mRNAs encoding the Fbgα, Fbgβ, and Fbgγ genes were significantly increased in livers of ANIT-treated mice (Fig. 3.1A-C). We have shown previously that ANIT treatment activates the coagulation cascade and causes marked deposition of fibrin in the liver (Luyendyk et al., 2009). To this end, we anticipated that ANIT treatment would elicit consumption of circulating fibrinogen. In contrast, and in line with induction of fibrinogen expression in liver, ANIT treatment was associated with a significant increase in plasma fibrinogen concentration (Fig. 3.1D). Interestingly, mRNA levels of SAA1 were dramatically increased in livers of mice treated with ANIT (Fig 3.1E).

3.4.2 Effect of fibrin(ogen)-deficiency on ANIT-induced cholestatic liver injury. To deplete circulating fibrinogen in wild type mice, we utilized ancrod, which enzymatically cleaves fibrinogen. Ancrod partially reduced plasma fibrinogen levels (Fig. 3.2A) and hepatic fibrin deposition (Fig. 3.2B) in

ANIT-treated mice. However, depletion of fibrinogen with ancrod did not significantly affect the increase in serum ALT activity, ALP activity, serum bile acid levels or liver necrosis in ANIT-treated mice (Fig. 3.2C-H). Of importance, in preliminary studies we found that ancrod treatment reduced fibrinogen levels in naïve mice to undetectable levels (data not shown). The induction of fibrinogen expression in ANIT-treated mice prevented complete depletion of fibrinogen with ancrod, with fibrinogen levels in ANIT-treated mice given ancrod resembling normal physiological fibrinogen levels (i.e., compare Fig. 3.2A vs. Fig. 3.1D). To this end, we utilized Fbg$\alpha^{-/-}$ mice ($Fbg^{-/-}$ mice), which lack circulating fibrinogen (Suh et al., 1995). Serum ALT activity was reduced in ANIT-treated $Fbg^{-/-}$ mice compared to ANIT-treated $Fbg^{+/-}$ mice, although this difference did not achieve statistical significance at 48 hours (Fig. 3.3A). However, fibrinogen deficiency did not significantly affect serum ALP activity or bile acid concentration in ANIT-treated mice (Fig 3.3B-C). Interestingly, both the number and average size of necrotic lesions tended to be lower in ANIT-treated $Fbg^{-/-}$ mice compared to ANIT-treated $Fbg^{+/-}$ mice, although these differences did not achieve statistical significance (Fig. 3.3D-E). Of importance, the overall area of necrosis induced by ANIT treatment was significantly reduced in ANIT-treated $Fbg^{-/-}$ mice compared to ANIT-treated $Fbg^{+/-}$ mice (Fig. 3.3F-H).

3.4.3 Characterization of ANIT-induced cholestatic liver injury in PAR-1 deficient and PAR-4 deficient mice. Thrombin can activate intracellular signaling via PAR-1 and PAR-4. To this end, we evaluated the role of these PARs in ANIT hepatotoxicity utilizing PAR-$1^{-/-}$ mice and PAR-$4^{-/-}$ mice. Serum ALT activity, ALP activity, and bile acid levels were similar in PAR-$1^{+/+}$ mice and PAR-$1^{-/-}$ mice 48 hours after ANIT treatment (Fig. 3.4A-C). In agreement, PAR-1-deficiency did not affect necrosis in ANIT-treated mice (Fig. 3.4D-F).

Twenty-four hours after ANIT administration, serum ALT activity was significantly increased in PAR-$4^{-/-}$ mice compared to PAR-$4^{+/+}$ mice (Fig. 3.5A). In contrast, serum ALP activity and bile acid levels were not different between PAR-$4^{-/-}$ mice and PAR-$4^{+/+}$ mice at 24 or 48 hours (Fig. 3.5B-C). Interestingly, within 48 hours after ANIT treatment, serum ALT activity in PAR-$4^{+/+}$ mice achieved levels similar to PAR-$4^{-/-}$ mice (Fig. 3.5A). Minimal necrosis was observed in ANIT-treated PAR-$4^{+/+}$ mice at 24

hours (Fig. 3.5D-G). In striking contrast, significant liver injury occurred in the livers of ANIT-treated PAR-4$^{-/-}$ mice 24 hours after ANIT treatment (Fig 3.5D-F, 3.5H). This injury was characterized by periportal necrosis associated with marked accumulation of red blood cells within the necrotic area, a unique lesion with features resembling parenchymal-type peliosis, which also occured in platelet-depleted mice challenged with ANIT (Sullivan et al., 2010a). Interestingly, in agreement with our previous studies (Luyendyk et al., 2009), ANIT-induced necrosis markedly increased in the livers of PAR-4$^{+/+}$ mice by 48 hours (Fig. 3.5D-F, 3.5I). In contrast, the severity of necrosis did not increase in PAR-4$^{-/-}$ mice between 24 and 48 hours (Fig. 3.5D-F, 3.5J), although the lesions observed at 24 hours appeared to persist at 48 hours (Fig. 3.5J). The results are consistent with the hypothesis that PAR-4 both protects the liver from early necrosis/hemorrhage during the early phase of ANIT-induced cholestasis, but also contributes at later times to the progression of periportal hepatocellular necrosis.

3.4.4 Effect of pharmacological inhibition of PAR-4 on ANIT-induced cholestatic liver injury. The whole-body PAR-4-deficient mice did not allow us to characterize the role of PAR-4 during different phases of ANIT-induced liver injury. To address the contribution of PAR-4 in both the initiation and progression of ANIT-induced cholestatic liver injury, we utilized a selective cell-permeable peptide inhibitor of PAR-4, P4Pal-10 (Covic et al., 2002). The dose selected for these studies has been shown previously to inhibit PAR-4-dependent activation of mouse platelets (Covic et al., 2002) and reduces inflammation in another murine model (Slofstra et al., 2007). The pepducin was administered by subcutaneous injection as this prolongs the half-life of the peptide in rodents (Covic et al., 2002).

To test the hypothesis that PAR-4 contributes to the progression of ANIT hepatotoxicity, we administered P4Pal-10 by subcutaneous injection 8 hours after ANIT treatment. Compared to mice given vehicle, ANIT-induced liver injury was significantly reduced in mice given P4Pal-10, as indicated by a significant reduction in serum ALT activity and the area of hepatocellular necrosis (Fig. 3.6A, 3.6D-F). Interestingly, serum ALP activity tended to be lower in P4Pal-10-treated mice, although this change did not meet statistical significance. Serum bile acids were significantly reduced in P4Pal-10-treated mice given ANIT (Fig. 3.6B-C). Of importance, in mice given pepducin in this paradigm, there was no

evidence of excessive red blood cell accumulation within necrotic lesions compared to mice given vehicle and ANIT (not shown). This result is consistent with an early protective effect of PAR-4, left intact in this paradigm by delaying administration of the PAR-4 inhibitor. In contrast, and mirroring the effect of complete PAR-4-deficiency (Fig. 3.5), when P4Pal-10 was administered to mice 2 hours prior to ANIT, serum ALT activity was significantly increased at 24 hours (Fig. 3.7A). In 50% of the mice given P4Pal-10 prior to ANIT, significant hemorrhage was evident within necrotic areas (Fig. 3.7E), resembling changes observed in PAR-4$^{-/-}$ mice treated with ANIT (Fig. 3.5H). Interestingly, similar to PAR-4$^{-/-}$ mice, no changes in serum ALP activity or levels of bile acids were observed 24 hours after ANIT administration in mice pre-treated with P4Pal-10 (Fig 3.7B-C).

3.5 Discussion

Anticoagulant administration reduced the hepatotoxicity of several xenobiotics in rodents, including lipopolysaccharide (LPS) (Pearson et al., 1996), monocrotaline (Copple et al., 2002b), dimethylnitrosamine (Fujiwara et al., 1988), and acetaminophen (Ganey et al., 2007), as well as the ability of LPS to enhance hepatotoxicity in xenobiotic co-exposure models (Deng et al., 2009). These studies strongly support the hypothesis that the coagulation cascade contributes to hepatotoxic responses, but the mechanism whereby thrombin promotes liver injury in these models has not been investigated in detail. Indeed, thrombin could contribute to hepatotoxic responses via fibrin clot formation as well as signaling through various PARs. ANIT-induced thrombin generation and liver injury were reduced in mice expressing very low levels of TF (Luyendyk et al., 2009). Elaborating on this result, we found that both fibrin(ogen) and PAR-4, but not PAR-1, contribute to acute ANIT-induced cholestatic liver injury in mice.

Circulating fibrinogen protein is comprised of three subunits encoded by different genes (i.e, α,β,γ), which are primarily expressed by the liver. In other models of hepatotoxicity, deposition of cross-linked fibrin occurs in conjunction with consumption of circulating fibrinogen protein (Copple et al., 2002a; Ganey et al., 2007). Of interest, in ANIT-treated mice, fibrinogen gene expression and circulating

fibrinogen concentration increased. This increase in fibrinogen availability could contribute to the marked fibrin deposition within necrotic lesions in ANIT-treated mice (Luyendyk et al., 2009). The dramatic induction of SAA1 suggests a basis for the induction of fibrinogen in ANIT-treated mice as a component of an acute phase response. However, the fibrinogen genes have also been shown to be targets of the nuclear receptor farnesoid X receptor (FXR), a bile acid receptor (Anisfeld et al., 2005). Insofar as bile acid levels increase substantially in the livers of ANIT-treated mice, this could be a plausible mechanism whereby fibrinogen expression increases in this model. Interestingly, FXR-deficiency did not affect basal fibrinogen gene expression in mice, nor did cholic-acid feeding affect Fbg gene induction in mice (Anisfeld et al., 2005). Additional studies are needed to clarify the mechanism of fibrinogen induction in the ANIT model, and comparison with other models of non-cholestatic liver injury may provide further insight into the regulation of the fibrinogen genes.

Fibrinogen depletion with ancrod did not affect ANIT-induced liver injury. However, ancrod administration did not completely deplete circulating fibrinogen or prevent fibrin deposition in ANIT-treated mice, most likely due to parallel fibrinogen gene induction. Of interest, ANIT-induced liver necrosis was significantly reduced in mice lacking fibrinogen. This result is consistent with the hypothesis that fibrin deposition contributes to ANIT hepatotoxicity in mice. One mechanism whereby fibrin could contribute to the progression of liver injury in this model is by causing local hypoxia that promotes hepatocyte injury. Indeed, anticoagulant administration has been shown to reduce liver hypoxia in other models of xenobiotic hepatotoxicity (Luyendyk et al., 2004; Copple et al., 2006). Alternatively, fibrin could promote liver necrosis in ANIT-treated mice by enhancing the recruitment or activation of inflammatory cells. Through interactions with αIIbβ3 and Mac-1 integrins, fibrin(ogen) can direct the accumulation and activation of platelets and neutrophils, respectively (Williams et al., 1995; Flick et al., 2004). Indeed, both of these cell types have been shown to contribute to liver injury in ANIT-treated rodents (Bailie et al., 1994; Kodali et al., 2006; Sullivan et al., 2010a). Of importance, a complete depletion of platelets caused parenchymal-type peliosis in ANIT-treated mice (Sullivan et al., 2010a), and there was no evidence of peliosis or severe hemorrhage in ANIT-treated $Fbg^{-/-}$ mice.

Distinct from its role in generating fibrin clots, thrombin activates intracellular signaling pathways via cleavage of various PARs (Kahn et al., 1998; Coughlin, 1999). Whereas PAR-1 expression was not identified on hepatocytes (Copple et al., 2003), hepatic non-parenchymal cells have been shown to express PAR-1 (Gaca et al., 2002; Copple et al., 2003; Gillibert-Duplantier et al., 2007). The cellular distribution of PAR-4 in liver has not been extensively evaluated, although immunohistochemical staining in one study suggested expression by Kupffer cells (Rullier et al., 2006). Of importance, the cellular distribution of these two receptors is different in mice and humans, with PAR-1 being the principal receptor for thrombin on human platelets, whereas thrombin signaling through PAR-4 is important for the activation of platelets in mice (Sambrano et al., 2001).

Thrombin activation of PAR-1 has been shown to elicit the expression of neutrophil chemokines (Uzonyi et al., 2006) and PAR-1 activation promotes neutrophil-dependent hepatotoxicity in LPS-primed livers (Copple et al., 2003), suggesting a potential avenue for cross-talk between PAR-1 signaling and neutrophil accumulation/activation in cholestatic liver injury. However, PAR-$1^{-/-}$ mice were not protected from ANIT-induced liver injury. Interestingly, a previous study showed that a pharmacologic inhibitor of PAR-1 reduced serum ALT activity after bile duct ligation (Fiorucci et al., 2004), although the inhibitor also prevented fibrinogen consumption, suggesting inhibition of thrombin generation.

Previous work by our group and others has shown that platelets contribute to ANIT-induced liver injury (Bailie et al., 1994; Sullivan et al., 2010a). However, an important dichotomy exists for the role of platelets in this model. Depleting platelets prior to ANIT administration induced parenchymal-type peliosis in ANIT-treated mice. In contrast, delayed inhibition of platelets by treatment with the ADP receptor antagonist clopidogrel (i.e,. 8 hours post ANIT administration) reduced hepatic neutrophil accumulation and necrosis, but did not cause parenchymal-type peliosis (Sullivan et al., 2010a). The parallels between these observations and the current PAR-4 studies are intriguing. Complete PAR-4-deficiency, like platelet-depletion, caused parenchymal type peliosis, but reduced the progression of ANIT-induced periportal necrosis, whereas delayed administration of PAR-4 pepducin significantly reduced the severity of necrosis. Taken together, these results suggest two roles for PAR-4 in the ANIT

model. Initial activation of PAR-4 protects the liver by limiting bleeding into areas of necrosis, resembling parenchymal-type peliosis. Late activation of PAR-4 contributes to the progression of ANIT-induced periportal necrosis. Additional studies may reveal critical crosstalk between thrombin, platelets, and neutrophils required for both protective and damaging processes in the livers of ANIT-treated mice. Examples of potential lines of investigation include evaluating the role of PAR-4 in initiation of liver repair and regeneration and in the accumulation/activation of inflammatory cells, such as neutrophils, which contribute to ANIT hepatotoxicity.

3.6 Figures

Figure 3.1

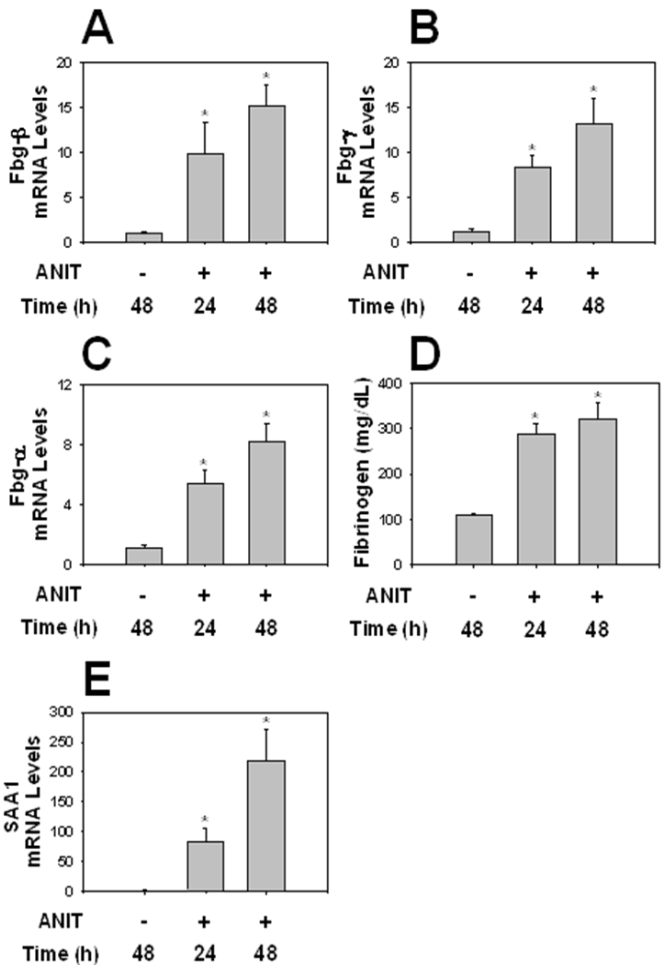

Figure 3.1: Induction of fibrinogen and serum amyloid A1 expression in ANIT-treated mice.

Wild type C57Bl/6J mice were treated with vehicle (corn oil) or ANIT (60 mg/kg, po). Hepatic (A) fbgβ, (B) fbgγ and (C) fbgα mRNA levels, (D) plasma fibrinogen concentration, and (E) SAA1 mRNA expression were determined 24 and 48 hours later. Levels of all biomarkers in mice given vehicle were not different between 24 and 48 hours and were pooled. Data are expressed as mean ± SEM. n=5 mice per group. *Significantly different from vehicle-treated mice.

Figure 3.2

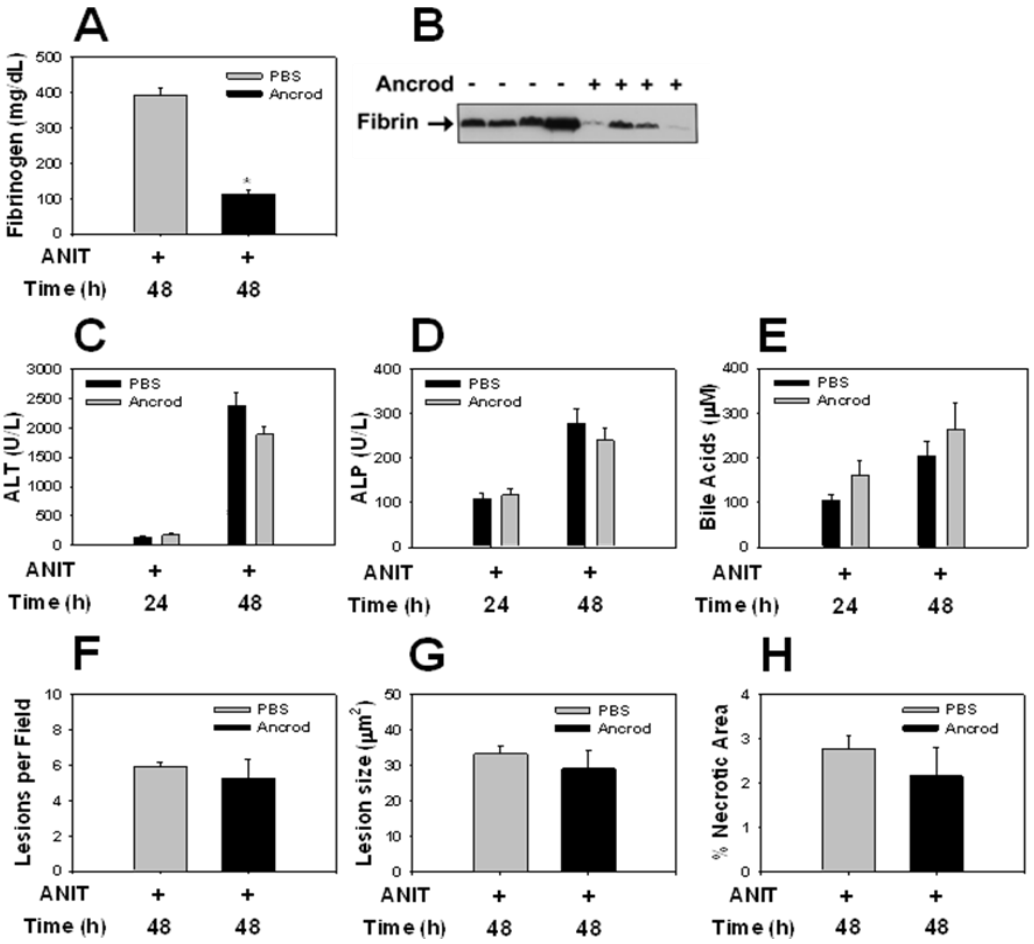

Figure 3.2: Effect of fibrinogen depletion on ANIT-induced liver injury.

ANIT-treated (60 mg/kg, po) wild type C57Bl/6J mice were given multiple injections of ancrod (1.75U/mouse, ip) or PBS as described in Methods. (A) Plasma fibrinogen levels and (B) hepatic fibrin deposition (representative western blot shown) were determined 48 hours after ANIT administration. (C) Serum ALT, and (D) ALP activity, (E) and bile acid levels were determined 24 and 48 hours after ANIT administration. For analysis of liver histopathology, the (F) average number of necrotic lesions per 40X field (G) average lesion size and (H) percentage of necrotic tissue were determined as described in Methods. Data are expressed as mean ± SEM. n=10 mice per group for circulating biomarkers in the blood and 5 mice per group for analysis of liver histopathology. *Significantly different from ANIT-treated mice given PBS.

Figure 3.3

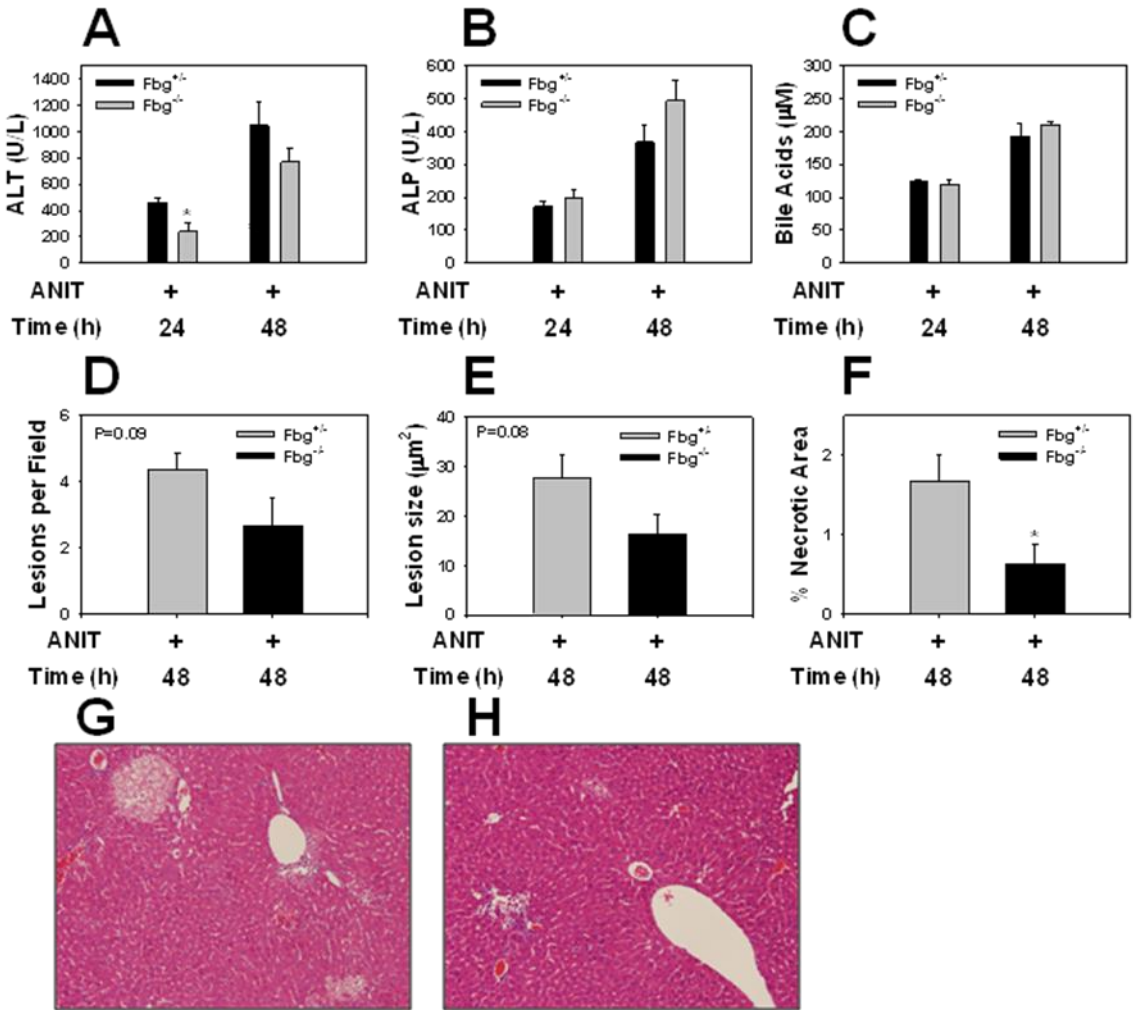

Figure 3.3: Effect of complete fibrinogen deficiency on ANIT-induced liver injury.

$Fbg^{+/-}$ mice and $Fbg^{-/-}$ mice were treated with ANIT (60 mg/kg, po) and (A) serum ALT, and (B) ALP activity, (C) and bile acid levels were determined 24 and 48 hours later. For analysis of liver histopathology, the (D) average number of necrotic lesions per 40X field (E) average lesion size and (F) percentage of necrotic tissue were determined as described in Methods. Data are expressed as mean ± SEM. n=7 $Fbg^{+/-}$ mice and 5 $Fbg^{-/-}$ mice per group at 24 hours, and 11 $Fbg^{+/-}$ mice and 7 $Fbg^{-/-}$ mice per group at 48 hours. *Significantly different from ANIT-treated $Fbg^{+/-}$ mice. Representative

photomicrographs showing H&E-stained liver sections from ANIT-treated (G) $Fbg^{+/-}$ mice and (H) ANIT-treated $Fbg^{-/-}$ mice.

Figure 3.4

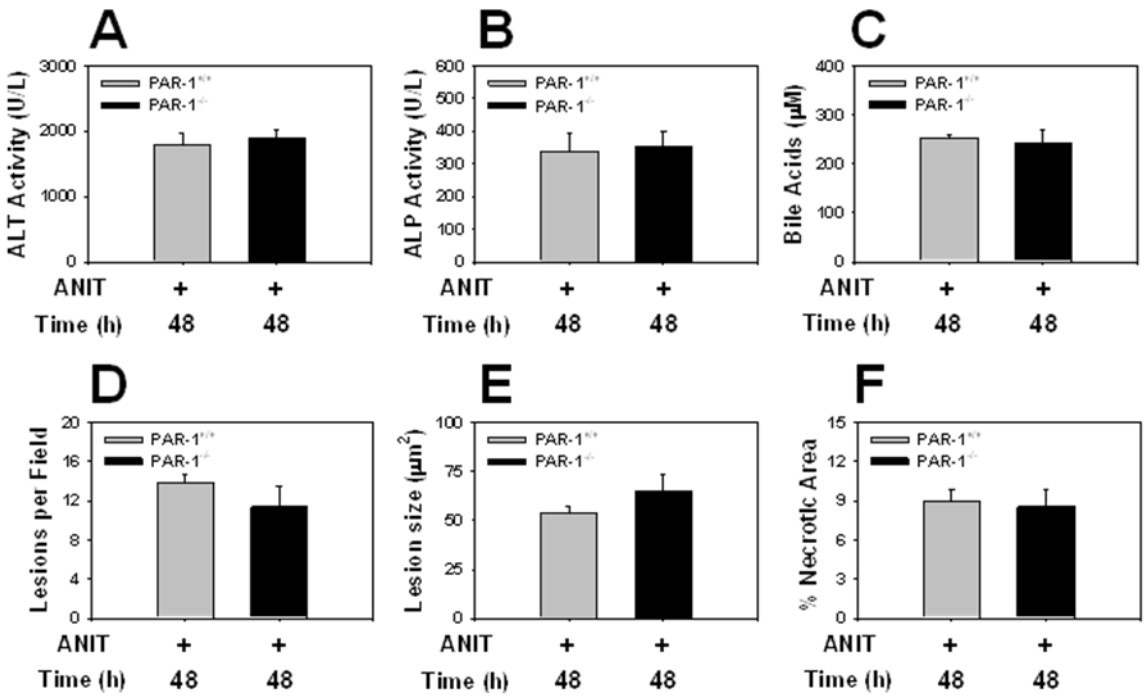

Figure 3.4: Effect of PAR-1 deficiency on ANIT-induced liver injury.

$PAR\text{-}1^{+/+}$ mice and $PAR\text{-}1^{-/-}$ mice were treated with ANIT (60 mg/kg, po) and (A) serum ALT, and (B) ALP activity, and (C) bile acid levels were determined 48 hours later. For analysis of liver histopathology, the (D) average number of necrotic lesions per 40X field (E) average lesion size and (F) percentage of necrotic tissue were determined as described in Methods. Data are expressed as mean ± SEM. n= 8 $PAR\text{-}1^{+/+}$ mice and 7 $PAR\text{-}1^{-/-}$ mice per group.

Figure 3.5

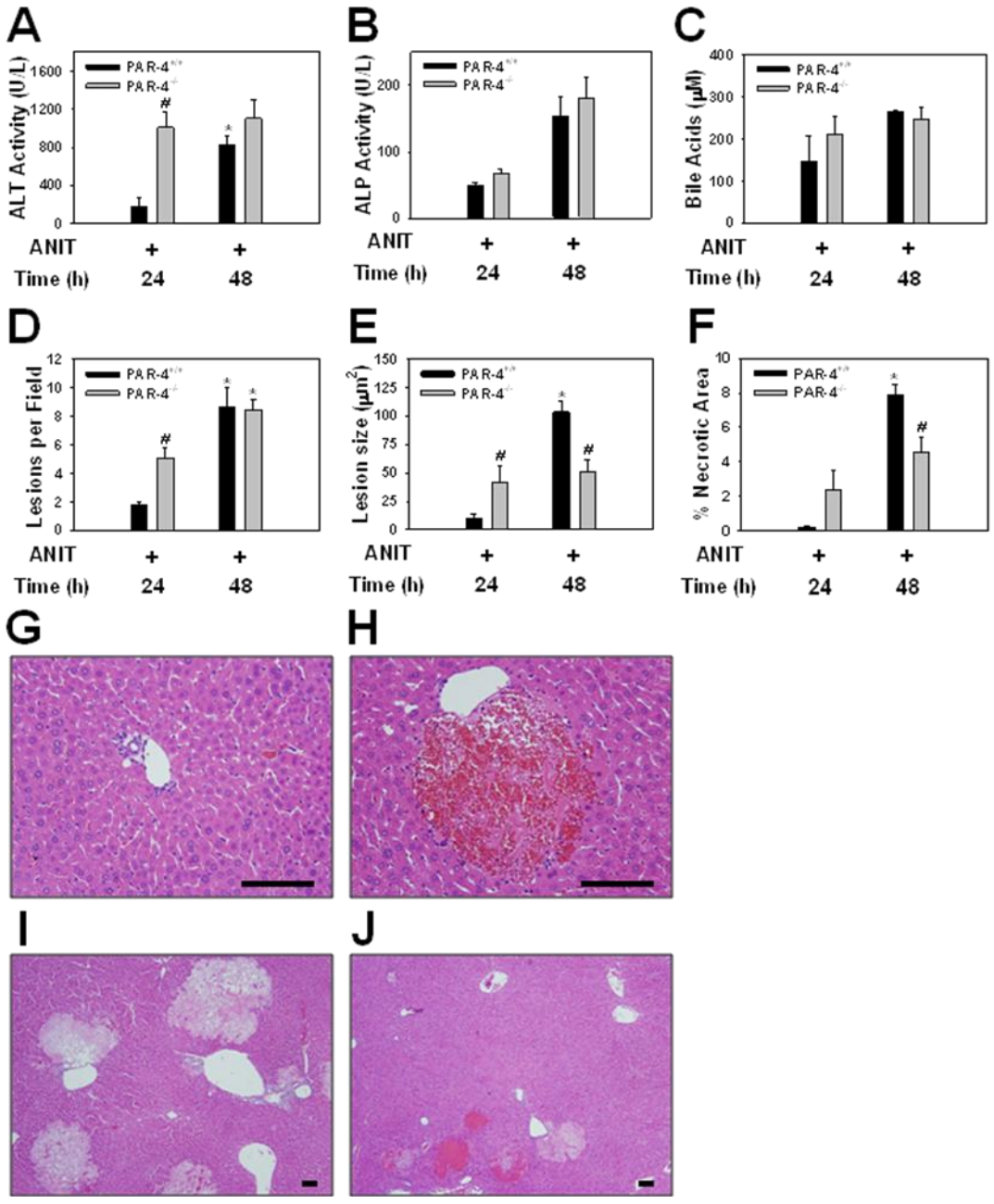

Figure 3.5: Effect of PAR-4 deficiency on ANIT-induced liver injury.

PAR-4$^{+/+}$ mice and PAR-4$^{-/-}$ mice were treated with ANIT (60 mg/kg, po) and (A) serum ALT, and (B) ALP activity, and (C) bile acid levels were determined 24 and 48 hours later. For analysis of liver histopathology, the (D) average number of necrotic lesions per 40X field, (E) average lesion size and (F)

percentage of necrotic tissue were determined as described in Methods. Representative photomicrographs of H&E-stained liver sections from ANIT-treated PAR-$4^{+/+}$ mice at (G) 24 hours and (I) 48 hours, and ANIT-treated PAR-$4^{-/-}$ mice at (H) 24 hours and (J) 48 hours are shown. Bar = 10 microns. Data are expressed as mean ± SEM. n=4 mice per group at 24 hours and 6 mice per group at 48 hours. *Significantly different from mice of the same genotype at 24 hours. #Significantly different from ANIT-treated PAR-$4^{+/+}$ mice at that time.

Figure 3.6

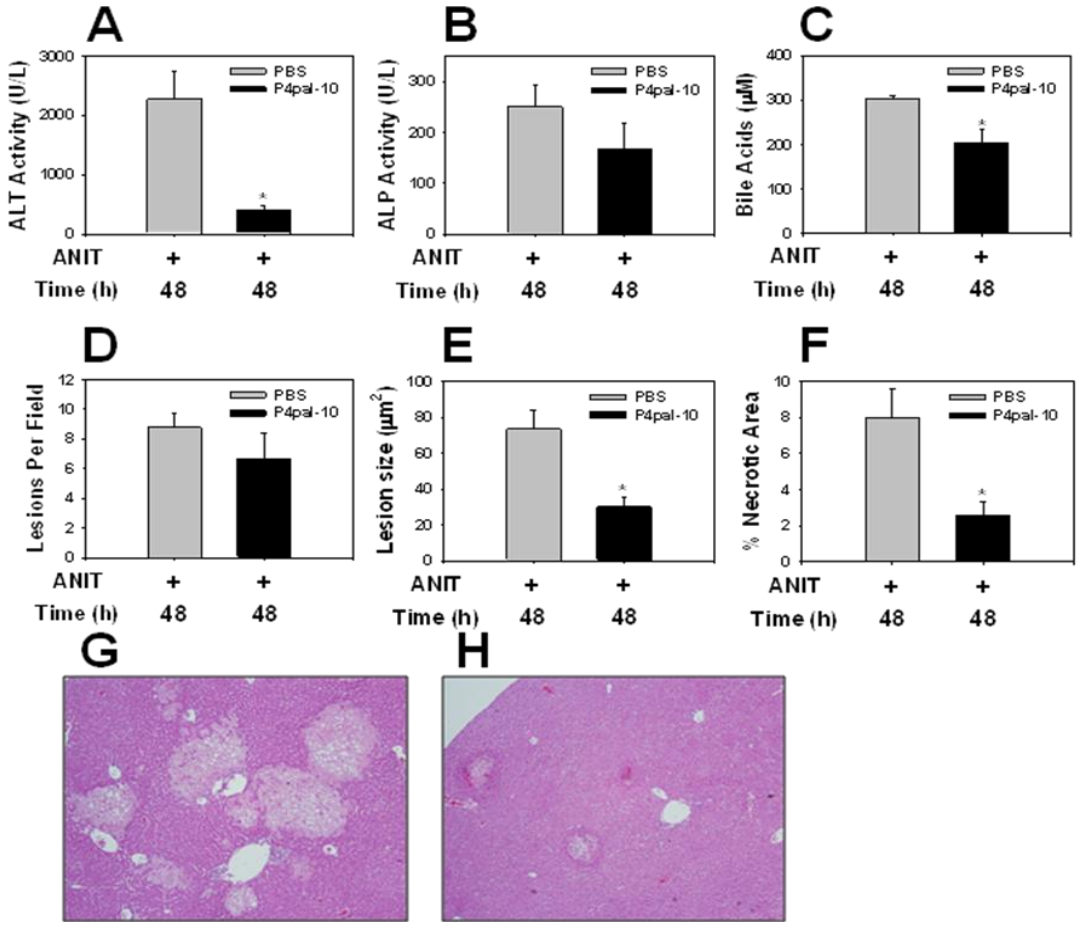

Figure 3.6: Effect of delayed PAR-4 inhibitor treatment on ANIT-induced liver injury.

ANIT-treated (60 mg/kg, po) wild type C57Bl/6J mice were treated with P4Pal-10 (0.5 mg/kg, sc) or PBS 8 and 24 hours after ANIT, as described in Methods. (A) Serum ALT, and (B) ALP activity, and (C) bile

acid levels were determined 48 hours after ANIT administration. For analysis of liver histopathology, the (D) average number of necrotic lesions per 40X field (E) average lesion size and (F) percentage of necrotic tissue were determined as described in Methods. Representative photomicrographs of H&E-stained liver sections from ANIT-treated mice given (G) PBS or (H) P4Pal-10 are shown. Data are expressed as mean ± SEM. n=10 mice treated with PBS and 10 mice treated with P4Pal-10. *Significantly different from ANIT-treated mice given PBS.

Figure 3.7

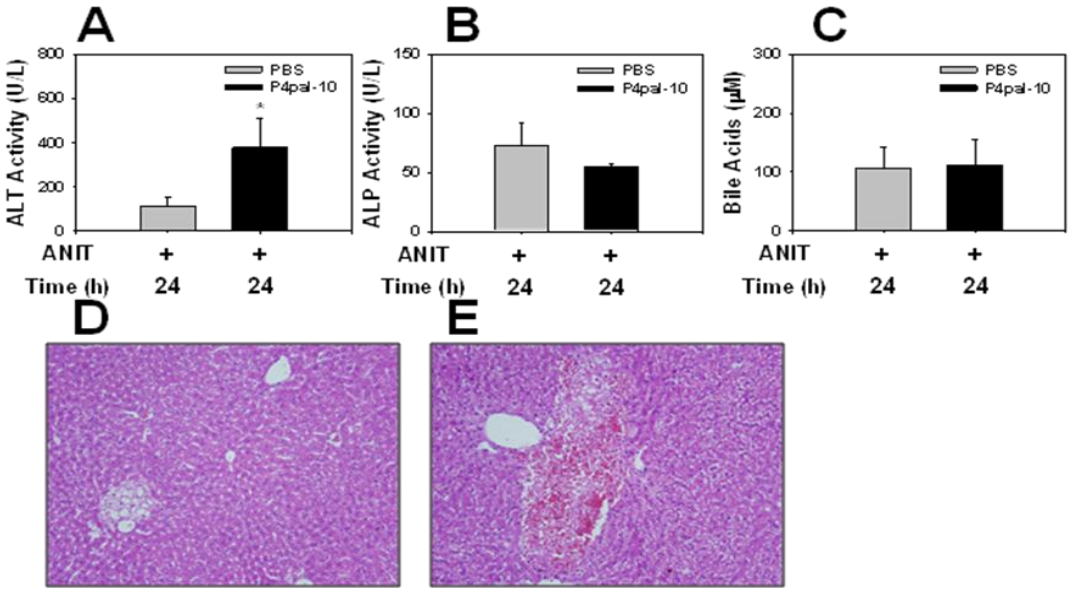

Figure 3.7: Effect of PAR-4 inhibitor pretreatment on ANIT-induced liver injury.

ANIT-treated (60 mg/kg, po) wild type C57Bl/6J mice were given P4Pal-10 (0.5 mg/kg, sc) or PBS 2 hours prior to and 8 hours after ANIT, as described in Methods. (A) Serum ALT, and (B) ALP activity, and (C) bile acid levels were determined 24 hours later. Representative photomicrographs of H&E-stained liver sections from ANIT-treated mice given (D) PBS or (E) P4Pal-10 are shown. n=6 mice per group. *Significantly different from ANIT-treated mice given PBS.

Chapter 4

The coagulation system contributes to alphaVbeta6 integrin expression and liver fibrosis induced by cholestasis.

Bradley P. Sullivan[1], Paul H. Weinreb[2], Shelia M. Violette[3], and James P. Luyendyk[1]

[1]Department of Pharmacology, Toxicology and Therapeutics, The University of Kansas Medical Center, Kansas City, KS [2] Biogen Idec, Inc., and [3] Stromedix Inc.

This article was published in American Journal of Pathology. 2010 Dec;177(6):2837-49.

4.1 Abstract

Chronic injury to intrahepatic bile duct epithelial cells (BDECs) elicits expression of various mediators that promote liver fibrosis, including the αVβ6 integrin. We tested the hypothesis that tissue factor (TF)-dependent thrombin generation and protease activated receptor-1 (PAR-1) activation contribute to liver fibrosis induced by cholestasis via induction of αVβ6 expression. To test this hypothesis, mice deficient in either TF or PAR-1 were fed a diet containing 0.025% alpha-naphthylisothiocyanate (ANIT), a BDEC selective toxicant. In genetically modified mice with a 50% reduction in liver TF activity fed an ANIT diet, coagulation cascade activation and liver fibrosis were reduced. Similarly, liver fibrosis was significantly reduced in PAR-$1^{-/-}$ mice fed an ANIT diet. Hepatic integrin β6 mRNA induction, expression of αVβ6 protein by intrahepatic BDECs, and SMAD2 phosphorylation were reduced by TF-deficiency and PAR-1-deficiency in mice fed the ANIT diet. Treatment with either an anti-αVβ6 blocking antibody or soluble TGF-β receptor type II reduced liver fibrosis in mice fed the ANIT diet. PAR-1 activation enhanced TGF-β1-induced integrin β6 mRNA expression in transformed human BDECs and in primary rat BDECs. Interestingly, TF and PAR-1 mRNA levels were increased in livers from patients with cholestatic liver disease. These results indicate that a TF-PAR-1 pathway contributes to liver fibrosis induced by chronic cholestasis by increasing expression of the αVβ6 integrin, an important regulator of TGF-β1 activation.

4.2 Introduction

Chronic injury to intrahepatic bile duct epithelial cells (BDECs) causes cholestatic liver disease characterized by an increase in toxic bile constituents in the hepatic parenchyma. This elicits inflammation and a profibrogenic response characterized by excessive deposition of extracellular matrix (e.g., collagens), which may lead to liver cirrhosis (Friedman, 2008). The cellular and molecular mechanisms of liver fibrosis caused by intrahepatic BDEC injury are not completely understood. Recent animal studies have clearly demonstrated that αVβ6 is critical for the development of liver fibrosis in two distinct models of cholestasis, and that it promotes fibrosis by activating the profibrogenic growth factor,

TGF-β1 (Wang et al., 2007a; Patsenker et al., 2008). However, the mechanism of αVβ6 upregulation on BDECs during cholestasis is not known.

Injury to intrahepatic BDECs can be modeled in rodents by administration of the xenobiotic alpha-naphthylisothiocyanate (ANIT) (Plaa and Priestly, 1976). Repetitive canilicular transport of an unstable ANIT-glutathione conjugate from hepatocytes into the bile exposes BDECs to toxic concentrations of ANIT (Roth and Dahm, 1997; Dietrich et al., 2001). In animals administered large doses of ANIT, hepatocellular necrosis manifests proximal to damaged bile ducts (Becker and Plaa, 1965) by mechanisms likely involving both high concentrations of hydrophobic bile acids released from damaged bile ducts (Perez and Briz, 2009) and infiltration of inflammatory cells (Kodali et al., 2006). In contrast, rodents fed a small dose of ANIT in their diet (e.g., 0.25-1 gram/kg diet) develop modest BDEC injury associated with BDEC proliferation, periportal inflammation, profibrogenic gene expression, and peribiliary collagen deposition (Tjandra et al., 2000; Lesage et al., 2001; Xu et al., 2004; Moritoki et al., 2006). Consequently, ANIT-induced chronic BDEC injury provides an important model to evaluate the pathogenesis of liver fibrosis stemming from cytotoxic challenge to the intrahepatic BDECs.

Tissue factor (TF) is a transmembrane protein and the principal activator of the extrinsic blood coagulation cascade. It is involved in both physiological hemostasis and the pathogenesis of various diseases (Mackman, 2009). In the liver, TF is expressed by various cells including BDECs (Luyendyk et al., 2009). Previous studies have shown that in rodents the coagulation cascade is activated by obstructive cholestasis and after acute toxic insult to the biliary epithelium (Abdel-Salam et al., 2005; Luyendyk et al., 2009). Similarly, generation of the coagulation protease thrombin is evident in patients with primary biliary cirrhosis (PBC) (Segal et al., 1997; Biagini et al., 2006). Pharmacologic anticoagulation and a protease activated receptor-1 (PAR-1) antagonist reduced hepatic collagen levels after bile duct ligation (Fiorucci et al., 2004; Abdel-Salam et al., 2005), suggesting that thrombin contributes to liver fibrosis during obstructive cholestasis. These experiments demonstrate a role for PAR-1 in fibrosis induced by cholestasis. However, the mechanism of coagulation cascade activation during cholestasis and

downstream consequences of PAR-1 activation that promote liver fibrosis during cholestasis are not known.

In the present studies, we tested the hypothesis that a TF-dependent procoagulant response accompanies intrahepatic BDEC injury and promotes liver fibrosis by a mechanism requiring thrombin-dependent induction of the αVβ6 integrin by BDECs.

4.3 Methods

4.3.1 Mice: All studies were carried out with mice of 8-16 weeks of age. Wild type C57Bl/6J mice were purchased from The Jackson Laboratory (Bar Harbor, MA). Mice heterozygous for murine (m) TF ($mTF^{+/-}hTF^{+}$ mice; hereafter referred to as $TF^{+/-}$ mice) and control mice ($mTF^{+/+}hTF^{+}$ mice; hereafter referred to as $TF^{+/+}$ mice), each expressing a low level (approximately 1%) of human TF (hTF), were kindly provided by Dr. Nigel Mackman (University of North Carolina-Chapel Hill). Age-matched $TF^{+/-}$ mice and $TF^{+/+}$ littermates were used for these studies. PAR-$1^{-/-}$ mice and PAR-$1^{+/+}$ mice on an identical genetic background (N8 C57Bl/6J) were maintained by homozygous breeding. Mice were maintained in an AAALAC-accredited facility at the University of Kansas Medical Center. Mice were housed at an ambient temperature of 22°C with alternating 12-h light/dark cycles, and provided water and rodent chow *ad libitum* (Teklad 8604; Harlan, Indianapolis, IN) prior to feeding custom diets. All animal procedures were performed according to the guidelines of the American Association for Laboratory Animal Science and were approved by the University of Kansas Medical Center Institutional Animal Care and Use Committee.

4.3.2 Diets and sample collection: Diets were prepared by Dyets, Inc (Bethlehem, PA). The ANIT diet was an AIN-93M purified diet containing 0.025% ANIT (Sigma-Aldrich, St. Louis, MO). The control diet was AIN-93M, a purified diet formulated for maintenance of mature rodents. For antibody studies, wild type C57Bl/6J mice were administered once weekly intraperitoneal (ip) injections of isotype control antibody (clone 1E6, 10 mg/kg), recombinant murine TGF-β receptor II-Fc fusion protein (mTGFβRII-Fc, 5 mg/kg) (Wang et al., 2007a) or anti-αVβ6 antibody (Clone 6.3G9, 1 or 10 mg/kg) (Wang et al.,

2007a), each diluted in sterile, endotoxin-free phosphate-buffered saline (PBS). Mice were fed the diets for 2 weeks, subsequently anesthetized with isoflurane, and blood was collected from the caudal vena cava into sodium citrate (final, 0.38%) or an empty syringe for the collection of plasma and serum, respectively. The liver was removed, washed in saline, and the intact gall bladder removed. The left medial lobe of the liver was affixed to a cork with OCT and frozen for 3 minutes in liquid nitrogen-chilled isopentane. Sections of the left lateral lobe were fixed in neutral-buffered formalin for 48 hours prior to routine processing. The remaining liver was cut into 100 mg pieces and flash-frozen in liquid nitrogen.

4.3.3. Biomarkers of injury and coagulation and MCP-1 determination: Serum ALT activity was determined using a commercial assay (ThermoFisher, Waltham, MA). Plasma thrombin-antithrombin (TAT) levels were determined using a commercial ELISA (Siemens Healthcare Diagnostics, Waltham, MA). Supernatant MCP-1 levels were determined using a commercial ELISA (eBioscience, San Diego, CA).

4.3.4 Cell culture and treatments: Transformed human bile duct epithelial cells (MMNK-1 cells) (Maruyama et al., 2004) were kindly provided by Dr. Melissa Runge-Morris (Wayne State University, Detroit, MI), on behalf of Dr. Naoya Kobayashi (Okayama University, Okayama, Japan). The cells were maintained at 37^{o} C at 5% CO_2 in DMEM supplemented with 10% fetal bovine serum (FBS), 10 U/ml Penicillin and 10 µg/ml Streptomycin (Sigma-Aldrich, St. Louis, MO), serum starved for 60 minutes, and then stimulated with recombinant human TGF-β1 (5 ng/ml, Peprotech, Rocky Hill, NJ) or its vehicle (endotoxin-free PBS containing 2 mg/ml BSA), and with human α-thrombin (10 U/ml, Enzyme Research Laboratories, South Bend, IN), 10 µM TFLLRN, 100 µM SFLLRN, 100 µM FSLLRN (AnaSpec, Inc., San Jose, CA) or associated vehicle (endotoxin-free PBS, Sigma-Aldrich). Primary rat BDECs were kindly provided by Dr. Vasanthi Bhaskaran, Dr. Monica Otieno, and Dr. Lois Lehman-Mckeeman (Brisol-Myers Squibb, Princeton, NJ). Rat BDECs were maintained in LYD medium (DMEM/F12 supplemented with 1.2 mg/ml sodium bicarbonate, 5 mg/ml D-glucose, 3 µM forskolin, 1 µM dexamethasone, 5 nM triiodothyronine [Sigma], 10% Nuserum IV, 20 ng/ml epidermal growth factor,

12.5 µg/ ml bovine pituitary extract, 1% ITS premix [BD Biosciences, San Jose CA] and 50 µg/ml Gentamicin [Invitrogen, Carlsbad CA] pH 7.35). The rat BDECs were co-stimulated with TGF-β1 and thrombin as described above.

4.3.5 RNA isolation, cDNA synthesis and real-time PCR: Total RNA was isolated from 100 mg of snap-frozen liver or adherent cells utilizing TRI Reagent (Molecular Research Center, Cincinnati, OH), from which 1 µg of cDNA was synthesized utilizing a high capacity cDNA synthesis kit (Applied Biosystems, Foster City, CA). Subsequent real-time PCR analysis was performed utilizing a StepOnePlus instrument (Applied Biosystems, Foster City, CA) and 2X Taqman Master Mix and Taqman gene expression assays (Applied Biosystems, Foster City, CA). The levels of each gene were adjusted to the levels of 18S RNA for *in vivo* studies and GAPDH for *in vitro* studies and the relative levels of each gene evaluated utilizing the ΔΔCt method.

4.3.6 Detection of phosphorylated SMAD2 in liver homogenate: Approximately 100 mg of liver was homogenized in 1.5 ml of a buffer containing 10 mM HEPES, 10 mM KCl, 300 mM sucrose, 1.5 mM $MgCl_2$, 0.5 mM DTT, 1 mM PMSF, and a protease/phosphatase inhibitor cocktail (Pierce), and subjected to centrifugation at 3600 x g for 10 min at 4°C. The resulting pellet was lysed in 0.2 mL of a buffer containing 20 mM HEPES, 100 mM KCl, 100 mM NaCl, 20% glycerol, 1 mM PMSF, and a protease/phosphatase inhibitor cocktail (Pierce), incubated on ice for 30 minutes, then subjected to centrifugation at 20,800 x g for 15 minutes at 4°C. The supernatant (i.e., nuclear fraction) was collected and protein levels determined using a Bio-rad Dc kit (Bio-Rad). 100 µg of this protein extract was utilized for the detection of phosphorylated SMAD2 (Ser465/467) using a commercially available PathScan ELISA (Cell Signaling Technology).

4.3.7 Immunofluorescent staining and confocal microscopy: For all immunofluorescent staining, 5 micron frozen sections obtained from the isopentane-fixed livers were used. For each staining, the sections were fixed with 4% neutral buffered formalin for 10 minutes. For Type 1 collagen staining, sections were blocked with 10% goat serum in PBS for 1 hour at room temperature and then incubated

with primary antibody (rabbit anti-mouse Type 1 collagen, AB765 Millipore [Temecula, CA]) diluted to 0.5 µg/ml in block buffer overnight at 4°C. The sections were washed with PBS and then incubated with an anti-rabbit Alexa 594-conjugated secondary antibody (Invitrogen, Carlsbad, CA) for 2 hours at room temperature. For αVβ6 staining, sections were blocked with 10% goat serum in PBS for 1 hour at room temperature and then incubated with primary antibody (human/mouse chimeric anti-αVβ6, ch2A1) (Van Aarsen et al., 2008) diluted 1:200 in block buffer overnight at 4°C. The sections were then washed and incubated with a rat anti-mouse CK19 antibody diluted 1:2000 in block buffer for 2 hours at room temperature (clone TROMA-3, Developmental Studies Hybridoma Bank, Iowa City, IA). The TROMA-3 antibody developed by R. Kemler was obtained from the Developmental Studies Hybridoma Bank developed under the auspices of the NICHD and maintained by The University of Iowa, Department of Biology, Iowa City, IA. The sections were then incubated with cross-adsorbed secondary antibodies: Alexa 488-conjugated goat anti-rat IgG and Alexa 594-conjugated goat anti-human IgG (Invitrogen, Carlsbad, CA), each diluted 1:500 in block buffer. Slides were then washed with PBS after secondary antibody addition and fluorescent staining in the livers sections was visualized using an Olympus BX41 microscope (Olympus, Lake Success, NY). Staining protocols for confocal microscopy were similar with substitution of goat anti-human IgG Alexa 546-conjugated antibody. Slides were visualized using a Nikon TE2000-U Motorized Inverted Scope (Nikon Instruments Inc., Melville, NY) outfitted with a 3-laser confocal system. Images were captured using Nikon-EZC1 3.8 confocal imaging software.

Quantification of Type 1 Collagen staining in 10 randomly selected 100X fields per tissue was performed using Scion Image (Scion Corporation, Frederick, MD) as described previously (Kim et al., 2006). Quantification of αVβ6 staining was performed using Scion Image as follows: 1) 10 randomly selected 400X fields containing periportal regions (positive for CK19 staining) were captured per tissue, 2) For each identical field the red fluorescence (positive red αVβ6 staining) was also captured. For each image the area of CK19 staining (positive pixels) and accompanying αVβ6 staining intensity (integrated density) was determined and αVβ6 staining intensity expressed as a ratio of the CK19 area. For

representative photomicrographs, red and green images were merged using the Olympus DP Manager software.

4.3.8 Trichrome staining: Formalin-fixed sections were stained utilizing a Chromaview Gomori Trichrome staining kit (Thermo-Fisher, Waltham, MA) as described by the manufacturer's protocol.

4.3.9 Flow Cytometry: MMNK-1 cells were collected by trypsinization and pelleted by centrifugation at 700 x g for 2 minutes. The cells were then adjusted to a density of $1x10^6$ cells/ml in block buffer (10% goat serum in PBS) and incubated for 20 minutes at 4^oC. Cells were then incubated for 1 hour at 4^oC with anti-mouse PAR-1 antibody (ATAP2, Santa Cruz Biotechnology, Santa Cruz, CA) or IgG2a isotype control (BioLegend, San Diego, CA) at a concentration of 1 µg/10^6 cells. Cells were pelleted by centrifugation at 700 x g and washed 5 times with 2% FBS in PBS. Cells were then incubated with Alexa Fluor 647-conjugated goat anti-mouse secondary antibody at a concentration of 1 µg/10^6 cells for 1 hour at 4^oC. Cells were washed 5 times with 2% FBS in PBS and then fixed in 4% paraformaldehyde (BioLegend) for 20 minutes. Cells were then resuspended in 2% FBS in PBS and 20,000 events were measured on a FACSCalibur (BD Biosciences, San Jose, CA).

4.3.10 Human liver samples: Research involving human livers was reviewed by the University of Kansas Medical Center Human Research Protection Program and the use of de-identified human liver samples was approved. The specimens used in this study were collected by Erik Schadde, M.D, Richard Gilroy, M.D., Bashar Abdulkarim, M.D., Ph.D, Jameson Forster,M.D, Mojtaba Olyaee, M.D., and Atta M Nawabi, M.D., and provided by the KU Liver Center Tissue Bank. The project "Determination of gene expression related to coagulation signaling in liver disease" is sponsored by the Liver Center at The University of Kansas Medical Center. Diseased liver tissue utilized was from patients with primary biliary cirrhosis (4 Females, age 59, 56, 60, 61; 1 Male, age 47) and patients with primary sclerosing cholangitis (3 Males, age 44, 45, 57). Donor liver samples without histological evidence of cholestasis, fibrosis or severe inflammation were selected as control tissues (5 Females, age 41, 48, 56, 52, 66; 5 Males, age 57, 45, 57, 58, 48).

4.3.11 Statistics: Comparison of two groups was performed using Student's t-test. Comparison of 3 or more groups was performed using one- or two-way analysis of variance, as appropriate, and the Student-Newman-Keuls post-hoc test. The criterion for statistical significance was $P<0.05$.

4.4 Results

4.4.1 TF-deficiency reduces coagulation and attenuates liver fibrosis in mice fed the ANIT diet. Heterozygous TF-deficiency ($TF^{+/-}$), which reduces liver TF activity by 50% (Luyendyk et al., 2009), did not affect plasma thrombin-antithrombin (TAT) levels in mice fed the control diet (Table 4.1). Plasma TAT levels increased significantly in $TF^{+/+}$ mice fed the ANIT diet compared to mice fed control diet (Table 4.1), and this increase was largely prevented in $TF^{+/-}$ mice (Table 4.1, $P=0.070$ for the comparison of $TF^{+/-}$ mice fed ANIT diet with $TF^{+/-}$ mice fed control diet.). TF-deficiency did not affect the modest increase in serum ALT activity in mice fed the ANIT diet (Table 4.1). The induction of alpha-1 type I collagen (Col1a1) mRNA in liver was significantly reduced in $TF^{+/-}$ mice fed the ANIT diet compared to $TF^{+/+}$ mice fed the ANIT diet (Fig. 4.1A). Increased periportal deposition of type 1 collagen was evident in the livers of $TF^{+/+}$ mice fed the ANIT diet compared to mice fed the control diet (Fig. 4.1C and G). Similarly, trichrome staining revealed marked periportal collagen deposition in livers of $TF^{+/+}$ mice fed the ANIT diet (Fig. 4.1H). In agreement with the reduction in Col1a1 mRNA levels, collagen deposition was significantly reduced in the livers of $TF^{+/-}$ mice fed the ANIT diet (Fig. 4.1B and G-J).

4.4.2 Role of protease activated receptor-1 in liver fibrosis in mice fed the ANIT diet. One mechanism whereby TF-dependent thrombin generation could contribute to liver fibrosis in mice fed the ANIT diet is by activation of PAR-1. To determine the role of PAR-1 in hepatic injury and fibrosis induced by the ANIT diet we utilized $PAR\text{-}1^{-/-}$ mice. Serum ALT activity increased similarly in $PAR\text{-}1^{+/+}$ mice and $PAR\text{-}1^{-/-}$ mice fed the ANIT diet (data not shown). Reflecting the effect of TF-deficiency on liver fibrosis in mice fed the ANIT diet, Col1a1 mRNA and collagen deposition were significantly reduced in the livers of $PAR\text{-}1^{-/-}$ mice compared to $PAR\text{-}1^{+/+}$ mice fed the ANIT diet (Fig. 4.2A-J).

4.4.3 Effect of TF- or PAR-1-deficiency on induction of fibrogenic genes in the livers of mice fed the ANIT diet. Insofar as both TF-deficiency and PAR-1-deficiency reduced liver fibrosis in mice fed the ANIT diet, we examined similarities in the induction of profibrogenic genes in liver as a prelude to identify the mechanism(s) whereby coagulation protease signaling contributes to liver fibrosis. Both TF-deficiency and PAR-1-deficiency attenuated induction of tissue inhibitor of metalloproteinase-1 (TIMP-1) mRNA in livers of mice fed the ANIT diet (Fig. 4.3A-B). Interestingly, levels of transforming growth factor-β1 (TGF-β1) mRNA in livers of mice fed the ANIT diet were not significantly affected by either TF- or PAR-1-deficiency (Fig. 4.3C-D). However, induction of integrin β6 mRNA was significantly reduced by TF-deficiency and PAR-1-deficiency (Fig. 4.3E-F).

4.4.4 TF and PAR-1 contribute to the αVβ6 integrin expression by bile duct epithelial cells (BDECs) and SMAD2 phosphorylation in livers of mice fed the ANIT diet. The αVβ6 integrin is highly expressed in BDECs in mice subjected to common bile duct ligation (BDL) and in livers of patients with cholestatic liver disease (Wang et al., 2007a). Indeed, we found that integrin β6 mRNA levels increased in the livers of patients with PBC and PSC compared to control livers (data not shown). Recent studies utilizing pharmacologic and genetic strategies indicated a critical role for this integrin in the activation of TGF-β and liver fibrosis induced by chronic cholestasis (Wang et al., 2007a; Patsenker et al., 2008). Of importance, the mechanism whereby αVβ6 integrin expression increases during chronic cholestasis is not known. To determine whether the effect of TF- and PAR-1-deficiency on integrin β6 mRNA levels (Fig. 4.3E-F) was mirrored by changes in the biliary levels of the β6 protein, we utilized immunofluorescent staining. Liver sections from mice fed either control diet or ANIT diet were co-stained for the β6 integrin and cytokeratin 19 (CK19), the latter a biomarker of BDECs in the adult mouse liver. Minimal αVβ6 integrin staining was observed in livers of $TF^{+/+}$ mice and $TF^{+/-}$ mice fed the control diet (Fig. 4.4A and D). An increase in BDEC number, as indicated by an increase in CK19-positive staining, was evident in the livers of $TF^{+/+}$ mice and $TF^{+/-}$ mice fed the ANIT diet (Fig. 4.4H and K). αVβ6 integrin expression increased substantially in $TF^{+/+}$ mice fed the ANIT diet and the staining colocalized with CK19,

indicating αVβ6 expression by BDECs (Fig. 4.4G-I). Visualization of αVβ6/CK19 co-staining by confocal microscopy indicated colocalization of these proteins within the same plane of cells (Supplemental Fig. 4.1). Compared to $TF^{+/+}$ mice fed the ANIT diet, the intensity of αVβ6 staining was significantly reduced in $TF^{+/-}$ mice fed the ANIT diet (Fig. 4.4J and M). Moreover, an analogous pattern of CK19 and αVβ6 staining was observed in liver sections from PAR-$1^{+/+}$ mice and PAR-$1^{-/-}$ mice fed the ANIT diet (Fig. 4.5A-M).

To determine whether αVβ6 expression correlated with activation of TGF-β signaling, we evaluated levels of phosphorylated SMAD-2 in liver. TGF-β signaling culminates in SMAD2 phosphorylation, and this readout has been used previously as an indicator of TGF-β activation (Wang et al., 2007a; Horan et al., 2008). Both TF-deficiency (p=0.058) and PAR-1-deficiency reduced the levels of phospho-SMAD2 in livers of mice fed the ANIT diet, consistent with the reduced αVβ6 protein expression in TF-deficient and PAR-1-deficient mice (Fig. 4.4N and 4.5N).

4.4.5 The αVβ6 integrin and TGF-β contribute to liver fibrosis in mice fed the ANIT diet. The role of αVβ6 and TGF-β1 in the liver fibrosis induced by the ANIT diet has not been described previously. To this end, we evaluated whether TF- and PAR-1-dependent upregulation of αVβ6 could contribute to liver fibrosis in this model. Compared to wild type mice administered an isotype control antibody (1E6), wild type mice administered a function blocking anti-αVβ6 antibody (clone 6.3G9) (Weinreb et al., 2004) and fed the ANIT diet demonstrated a dose-dependent inhibition of TIMP-1 and Col1a1 gene expression (Fig. 4.6A and B) and Type 1 collagen deposition (Fig. 4.6C, E-J) in the liver. Of importance, administration of the anti-αVβ6 antibody significantly reduced SMAD2 phosphorylation in the livers of mice fed the ANIT diet, indicating inhibition of TGF-β activation (Fig. 4.6D). Since αVβ6 led to activation of the TGF-β cytokine (Munger et al., 1999), we evaluated the contribution of TGF-β to liver fibrosis in this model using a recombinant murine TGF-β receptor type II-Fc fusion protein (mTGFβRII-Fc) (2). Administration of mTGFβRII-Fc blocked SMAD2 phosphorylation in liver (Fig. 4.6D) and also significantly reduced TIMP-1 and Col1a1 gene expression (Fig. 4.6A and B) and Type 1 collagen

deposition (Fig. 4.6C, E-F, and K-L) in the livers of wild type mice fed the ANIT diet. These results indicate that αVβ6 contributes to TGF-β activation and liver fibrosis in mice fed the ANIT diet, and are consistent with the hypothesis that a TF-PAR-1-dependent pathway contributes to liver fibrosis by upregulating αVβ6 expression.

4.4.6 Expression of PAR-1 by transformed human bile duct epithelial cells. One possible mechanism whereby PAR-1 could contribute to expression of integrin β6 mRNA is by direct stimulation of BDECs. Although other epithelial cells have been shown to express PAR-1 (Shimizu et al., 2000; Rondeau et al., 2001), the expression of PAR-1 by BDECs has not been described. To address this question we selected MMNK-1 cells, a transformed human bile duct epithelial cell line shown to express low levels of integrin β6 mRNA (Patsenker et al., 2008), analogous to normal BDECs *in vivo*. Of importance, MMNK-1 cells expressed PAR-1 mRNA (data not shown) and PAR-1 protein on the cell surface (Fig. 4.7A). Stimulation of MMNK-1 cells with human α-thrombin or the specific PAR-1 agonist peptide TFLLRN (Blackhart et al., 1996) induced MCP-1 mRNA expression (Fig. 4.7B and data not shown), a positive control for PAR-1 activation. Thrombin stimulation also increased MCP-1 levels in the culture supernatant (Fig. 4.7C). Interestingly, hepatic MCP-1 mRNA induction was reduced by TF-deficiency and PAR-1-deficiency in mice fed the ANIT diet (Fig. 4.7D-E). The results suggest a PAR-1-dependent pathway of MCP-1 expression during chronic cholestatic liver injury. Furthermore, these data demonstrate that activation of PAR-1 on BDECs activates signaling pathways that lead to gene expression changes.

4.4.7 PAR-1 activation enhances TGF-β1 induction of integrin β6 mRNA expression. In contrast to thrombin stimulation of MMNK-1 cells *in vitro,* thrombin generated during cholestasis likely promotes fibrosis in synergy with other mediators. Accordingly, thrombin could modify the response of BDECs to other profibrogenic mediators that induce integrin β6 mRNA expression. Interestingly, we found that mice fed the ANIT diet and treated with mTGFβRII-Fc showed a significant inhibition of hepatic integrin β6 expression as compared to isotype control-treated mice (Fig. 4.8A). Consistent with this result, stimulation of MMNK-1 cells and primary rat BDECs with TGF-β1 increased integrin β6 mRNA levels

(Fig. 4.8B-C). Stimulation of MMNK-1 cells and primary rat BDECs with thrombin alone did not affect integrin β6 mRNA levels. In contrast, thrombin enhanced TGF-β1-mediated induction of integrin β6 mRNA expression in MMNK-1 cells and primary rat BDECs (Fig. 4.8B-C). We also evaluated the role of PAR-1 in this cell system by utilizing pharmacologic agonists of this receptor. The PAR-1 agonist peptides SFLLRN and TFLLRN, which are based on the N-terminal tethered-ligand sequence of PAR-1 (Blackhart et al., 1996), also enhanced TGF-β1-induced integrin β6 mRNA expression in MMNK-1 cells (Fig. 4.8D-E). In contrast, the peptide FSLLRN, which does not activate PAR-1, did not enhance TGF-β1-induced integrin β6 mRNA expression in MMNK-1 cells (Fig. 4.8F).The data indicate that activation of PAR-1 on BDECs enhances TGF-β1 induction of integrin β6 mRNA expression.

4.4.8 TF and PAR-1 mRNAs are increased in livers of mice fed the ANIT diet and in patients with primary biliary cirrhosis and sclerosing cholangitis. It is unlikely that patients with cholestatic liver disease are uniformly procoagulant to an extent considered pathologic (i.e., thrombosis), especially insofar as prothrombin time can be prolonged in these patients. However, a few studies have shown modest thrombin generation and increased circulating tissue factor levels in patients with PBC (Segal et al., 1997; Biagini et al., 2006). Although such changes may be insufficient to dramatically affect systemic hemostasis, low levels of hepatic thrombin generation could be sufficient to trigger intracellular signaling in the liver. Of importance, we found that similar to mice fed the ANIT diet (Fig. 4.9A-B), levels of both TF mRNA and PAR-1 mRNA were increased in liver samples from patients with fibrosis associated with chronic cholestatic liver disease (PBC [n=5] and PSC [n=3]) compared to control liver samples without evidence of inflammation or fibrosis (Fig. 4.9C-D).

4.5 Discussion

It is increasingly clear that BDECs are not simply passive targets of injury in models of cholestatic liver disease. Rather, these cells actively participate in liver fibrosis by producing a wide array of mediators (Glaser et al., 2009). One of these is the heterodimeric integrin αVβ6, which has diverse functions including activation of latent-TGF-β to its mature, active form (Munger et al., 1999). Elegant

studies using pharmacologic and genetic interventions demonstrated a critical role for the αVβ6 integrin in liver fibrosis induced by MDR2-deficiency or BDL in rodents (Wang et al., 2007a; Patsenker et al., 2008). We found that administration of a function blocking anti-αVβ6 integrin antibody also reduced liver fibrosis in the ANIT diet model of cholestasis, indicating the effectiveness of αVβ6 blockade across multiple models of cholestasis, and further supporting the case for taking therapeutics forward. Moreover, administration of a murine recombinant TGF-β receptor type II-Fc fusion protein significantly reduced liver fibrosis in mice fed the ANIT diet. Taken together, the results implicate the αVβ6 integrin and TGF-β in the pathogenesis of liver fibrosis induced by the ANIT diet.

The TGF-β isoforms are expressed as part of an inactive complex by both normal and diseased tissues (Nishimura, 2009). In liver, TGF-β is expressed by several cell types including myofibroblasts, hepatocytes, and Kupffer cells (Gressner and Weiskirchen, 2006). Our findings in the ANIT diet model and previous studies (Wang et al., 2007a; Patsenker et al., 2008) indicate that the αVβ6 integrin is required for activation of TGF-β to its profibrogenic form during cholestasis, and that the αVβ6 integrin expression is primarily localized to the BDEC. One potential cellular source of latent TGF-β complex relevant to cholestatic liver disease is the periportal myofibroblast (Dranoff and Wells, 2010). Liver myofibroblasts have been shown to express the latent TGF-β complex (Mangasser-Stephan et al., 2001), and the proximity of these cells to BDECs may deliver latent TGF-β to αVβ6 integrin on BDECs for activation. Another intriguing possibility is that BDECs themselves express the requisite latent TGF-β. Increased expression of TGF-β1 by BDECs after BDL has been described previously, although BDEC expression levels were low compared to the adjacent fibroblasts (Sedlaczek et al., 2001). Of importance, the expression of αVβ6 integrin appears to be the critical, rate-limiting step for the activation of latent TGF-β during cholestasis.

Expression of the αVβ6 integrin is negligible in normal liver (Wang et al., 2007a). However, after biliary injury, hepatic integrin β6 mRNA levels increase and expression of the αVβ6 integrin

increases on BDECs (Wang et al., 2007a; Patsenker et al., 2008). Similar to extrahepatic, obstructive cholestasis (e.g., BDL), we found that chronic xenobiotic-induced intrahepatic BDEC injury markedly increased integrin β6 mRNA levels in liver and expression of the integrin β6 protein selectively on BDECs. Of importance, the mechanism whereby αVβ6 integrin expression increases during cholestatic liver injury has not been identified. Potential inducers of αVβ6 include direct cellular injury and a number of profibrogenic mediators produced in response to chronic cholestatic liver injury. Analogous to previous studies in other extrahepatic cell types (Copple et al., 2003; Levy and Hill, 2005), we found that TGF-β1 stimulation of BDECs induced integrin β6 mRNA expression, suggesting the presence of a feed-forward pathway whereby TGF-β1 amplifies activation of additional latent-TGF-β via induction of integrin β6 mRNA (Fig. 4.10). In agreement with our findings *in vitro*, administration of a soluble TGF-β receptor type II attenuated the induction of integrin β6 mRNA expression in livers of mice fed the ANIT diet. Interestingly, administration of the anti-αVβ6 integrin antibody did not impact induction of integrin β6 mRNA in mice fed the ANIT diet, suggesting that the αVβ6 integrin is not the only activator of TGF-β in this model, or that low levels of αVβ6 are sufficient for localized activation of TGF-β and subsequent integrin β6 mRNA induction. Overall, the data indicate that TGF-β contributes to integrin β6 mRNA induction during cholestasis. However, TGF-β stimulates various cell types concurrently with other pathways activated by liver damage and interaction between these pathways may increase profibrogenic stimuli.

One pathway activated by chronic liver damage is the coagulation cascade. Pharmacologic inhibition of thrombin or its receptor PAR-1 reduced hepatic collagen deposition after bile duct ligation (BDL) (Fiorucci et al., 2004; Abdel-Salam et al., 2005). Despite this and other evidence supporting a role for thrombin and PAR-1 in liver fibrosis, the mechanism of coagulation activation and the distal mechanism whereby PAR-1 activation contributes to liver fibrosis has not been identified. Our results indicate that pathologic coagulation cascade activation during chronic cholestasis in mice fed the ANIT diet is TF-dependent, and that the thrombin generated contributes to liver fibrosis by activating PAR-1.

Of interest, TF-deficiency and PAR-1-deficiency attenuated αVβ6 integrin expression and TGF-β activation in livers of mice fed the ANIT diet. These results reveal a novel mechanism whereby coagulation protease signaling contributes to liver fibrosis during cholestasis (Fig. 4.10). Of importance, the mechanism whereby thrombin contributes to liver fibrosis may be model dependent.

Previous studies suggested that the expression of PAR-1 in the liver is restricted to non-parenchymal cells (Copple et al., 2003). We found that PAR-1 is expressed on the surface of transformed human BDECs (i.e., MMNK-1 cells) and that these cells respond to thrombin and PAR-1 agonist peptide stimulation by producing MCP-1. Of importance, PAR-1-deficiency also reduced MCP-1 expression in mice fed the ANIT diet. Insofar as MCP-1 contributes to liver fibrosis after BDL (Seki et al., 2009), this suggests another mechanism whereby PAR-1 could contribute to liver fibrosis in this model. Although treatment of MMNK-1 cells or primary rat BDECs with thrombin had no effect on integrin β6 mRNA levels *in vitro,* thrombin enhanced TGF-β1-induced integrin β6 mRNA expression in both cell types. Similar experiments using agonist peptides mimicking the PAR-1 N-terminal tethered-ligand support the hypothesis that this effect is PAR-1-dependent. These experiments reveal a novel mechanism whereby thrombin and TGF-β synergistically promote profibrogenic gene expression and provide an important *in vitro* correlate for our observation that both PAR-1 and TGF-β contribute to αVβ6 expression *in vivo*. Interestingly, another study showed that stimulation of pulmonary epithelial cells with thrombin or PAR-1 agonist peptide increased αVβ6 integrin-dependent activation of latent TGF-β (Jenkins et al., 2006). In the latter study, *de novo* synthesis of integrin β6 mRNA was not required. Taken together, the results suggest that the coagulation cascade fine tunes, via PAR-1, the TGF-β-dependent induction of integrin β6 expression and the fibrogenic activity of αVβ6 in models of fibrosis (Fig. 4.10).

Despite prolonged prothrombin time in patients with liver disease (Segal et al., 1997), moderate thrombin generation occurs, as indicated by elevated plasma TAT levels (Segal et al., 1997; Biagini et al., 2006). This low level of thrombin generation could be sufficient to elicit signaling through PAR-1 that contributes to disease progression. We found that TF and PAR-1 mRNA levels, as well as integrin β6

mRNA levels (not shown) were increased in patients with cholestatic liver disease. Another study also found elevated PAR-1 expression in patients with PBC (Shackel et al., 2001). Moreover, we have shown previously that normal murine BDECs express TF *in vitro* and *in vivo* (Luyendyk et al., 2009). The intricate association and apparent cellular co-localization of TF, PAR-1 and αVβ6 in liver is intriguing, as it suggests a paradigm where critical profibrogenic processes can respond rapidly to BDEC injury. That is, BDEC injury could result in membrane disruption that exposes TF or TF-positive microparticles to the blood, generating locally high thrombin concentrations. Subsequent activation of PAR-1 on BDECs could promote αVβ6 expression and peribiliary fibrosis.

In summary, the results indicate that TF and PAR-1 contribute to liver fibrosis in a model of chronic xenobiotic-induced cholestatic liver injury by enhancing TGF-β-dependent αVβ6 expression by BDECs. Continued investigation of the mechanism whereby coagulation protease signaling contributes to liver fibrosis may lead to novel approaches to limit TGF-β activation and fibrosis in patients.

4.6 Figures

Figure 4.1

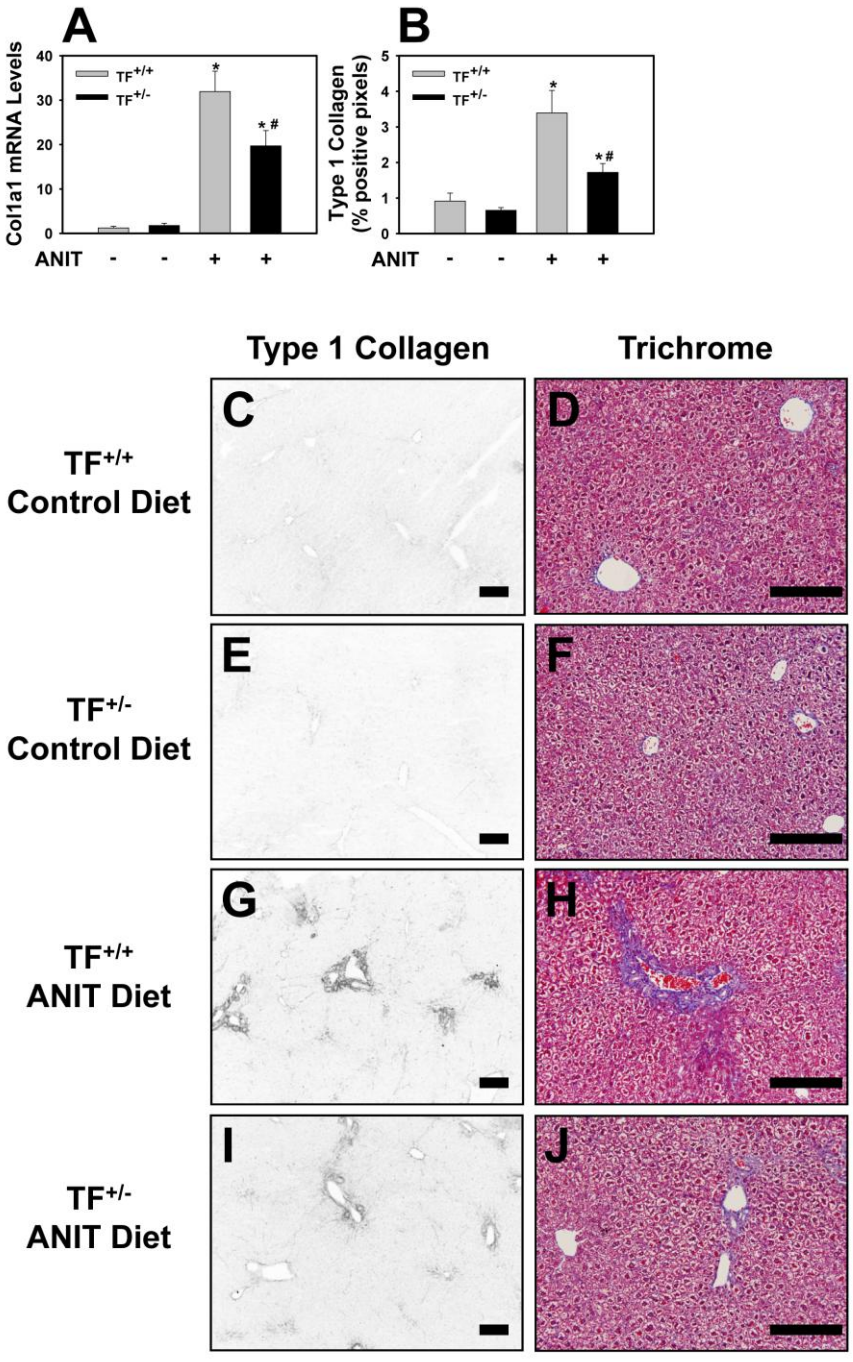

Figure 4.1: Reduced liver fibrosis in livers of TF-deficient mice fed the ANIT diet.

Mice wild type for TF ($TF^{+/+}$) and mice heterozygous for TF ($TF^{+/-}$) were fed either control diet (CD) or identical diet containing 0.025% ANIT (AD) for 14 days. (A) Levels of Col1a1 mRNA were determined in liver. (B) Quantification of Type 1 collagen staining (see below) as described in Methods. n=4-8 mice per group. Data are expressed as mean ± SEM. *Significantly different from the same mice fed control diet. $^{\#}$Significantly different from $TF^{+/+}$ mice fed the ANIT diet. (C-J) Representative photomicrographs showing immunofluorescent Type 1 collagen staining and Trichrome staining (bar = 20 microns) of liver sections from $TF^{+/+}$ mice (C-D, G-H) or $TF^{+/-}$ mice (E-F, I-J) fed control diet (C-F) or ANIT diet (G-J). For Type 1 collagen staining, the images were converted to grayscale and inverted such that positive staining is dark.

Figure 4.2

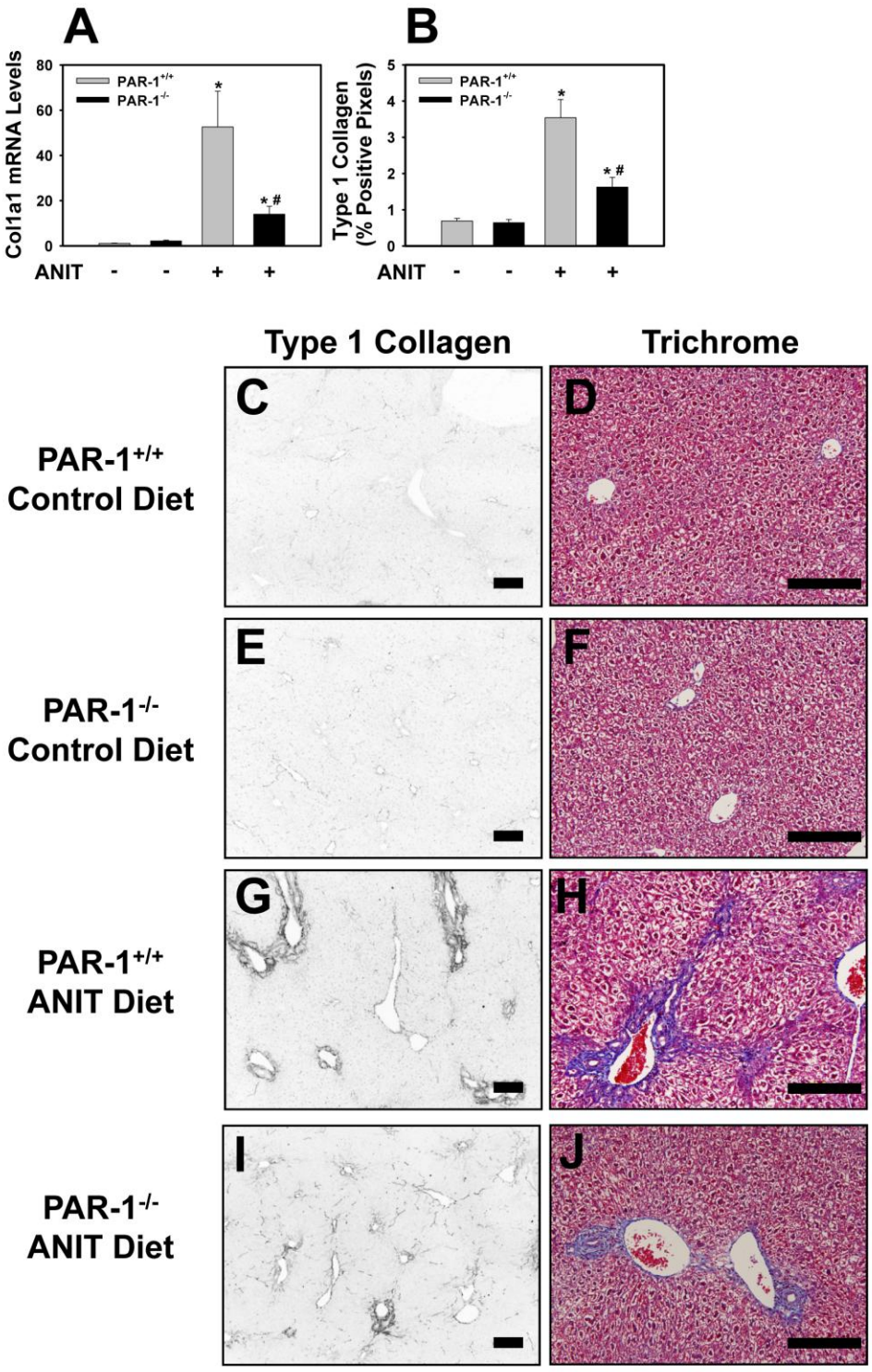
A
B
Col1a1 mRNA Levels
Type 1 Collagen (% Positive Pixels)
PAR-1+/+
PAR-1-/-
ANIT
Type 1 Collagen
Trichrome
PAR-1+/+ Control Diet
PAR-1-/- Control Diet
PAR-1+/+ ANIT Diet
PAR-1-/- ANIT Diet
C
D
E
F
G
H
I
J

Figure 4.2: Reduced liver fibrosis in livers of PAR-1$^{-/-}$ mice fed the ANIT diet.

PAR-1$^{+/+}$ mice and PAR-1$^{-/-}$ mice were fed either control diet (CD) or identical diet containing 0.025% ANIT (AD) for 14 days. (A) Levels of Col1a1 mRNA were determined in liver. (B) Quantification of Type 1 collagen staining (see below) as described in Methods. n=4-12 mice per group. Data are expressed as mean ± SEM. *Significantly different from the same mice fed control diet. $^{\#}$Significantly different from PAR-1$^{+/+}$ mice fed the ANIT diet. (C-J) Representative photomicrographs showing immunofluorescent Type 1 collagen staining and Trichrome staining (bar = 20 microns) of liver sections from PAR-1$^{+/+}$ mice (C-D, G-H) or PAR-1$^{-/-}$ mice (E-F, I-J) fed control diet (C-F) or ANIT diet (G-J). For Type 1 collagen staining, the images were converted to grayscale and inverted such that positive staining is dark.

Figure 4.3

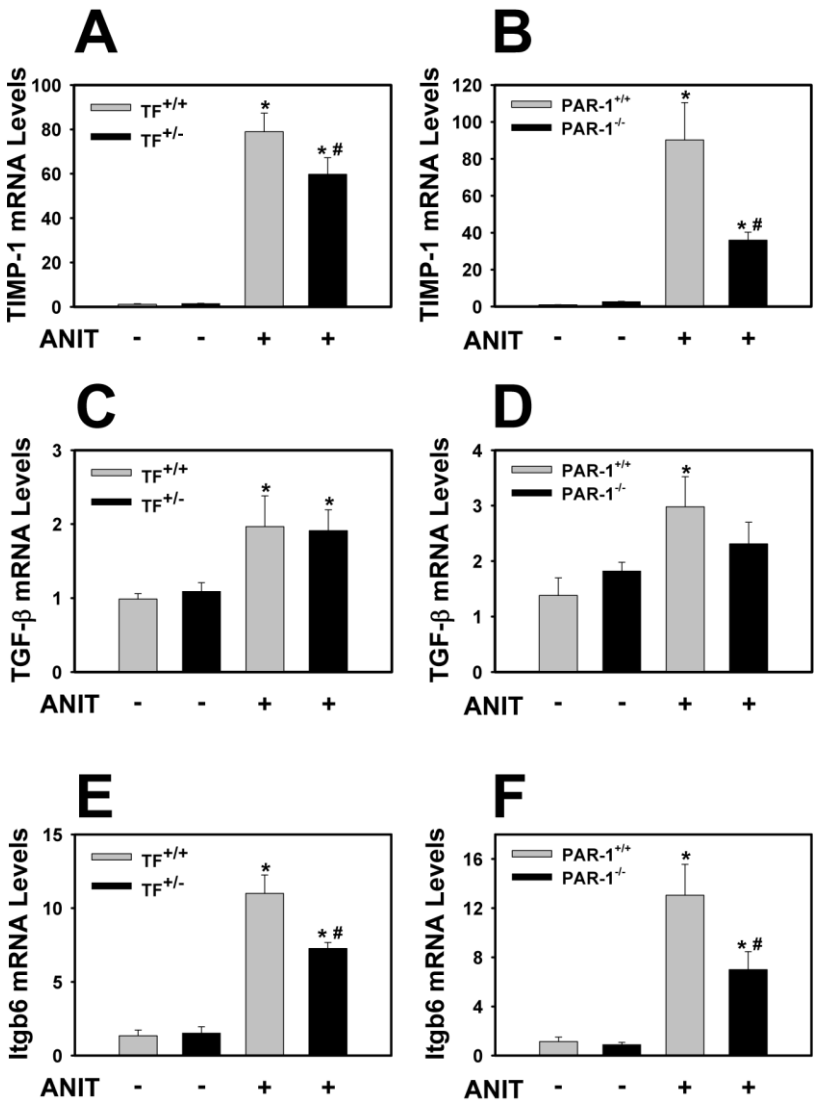

Figure 4.3: Effect of TF-deficiency and PAR-1-deficiency on the expression of fibrogenic genes in livers of mice fed the ANIT diet.

Mice wild type for TF ($TF^{+/+}$) and mice heterozygous for TF ($TF^{+/-}$), and PAR-$1^{+/+}$ mice and PAR-$1^{-/-}$ mice were fed either control diet or identical diet containing 0.025% ANIT for 14 days. Levels of (A,B) TIMP-1, (C,D) TGF-β, and (E,F) integrin β6 (Itgb6) mRNA in liver were determined as described in Methods. n=4-12 mice per group. Data are expressed as mean ± SEM. *Significantly different from the

same mice fed control diet. [#]Significantly different from control mice ($TF^{+/+}$ mice or PAR-$1^{+/+}$ mice) fed the ANIT diet.

Figure 4.4

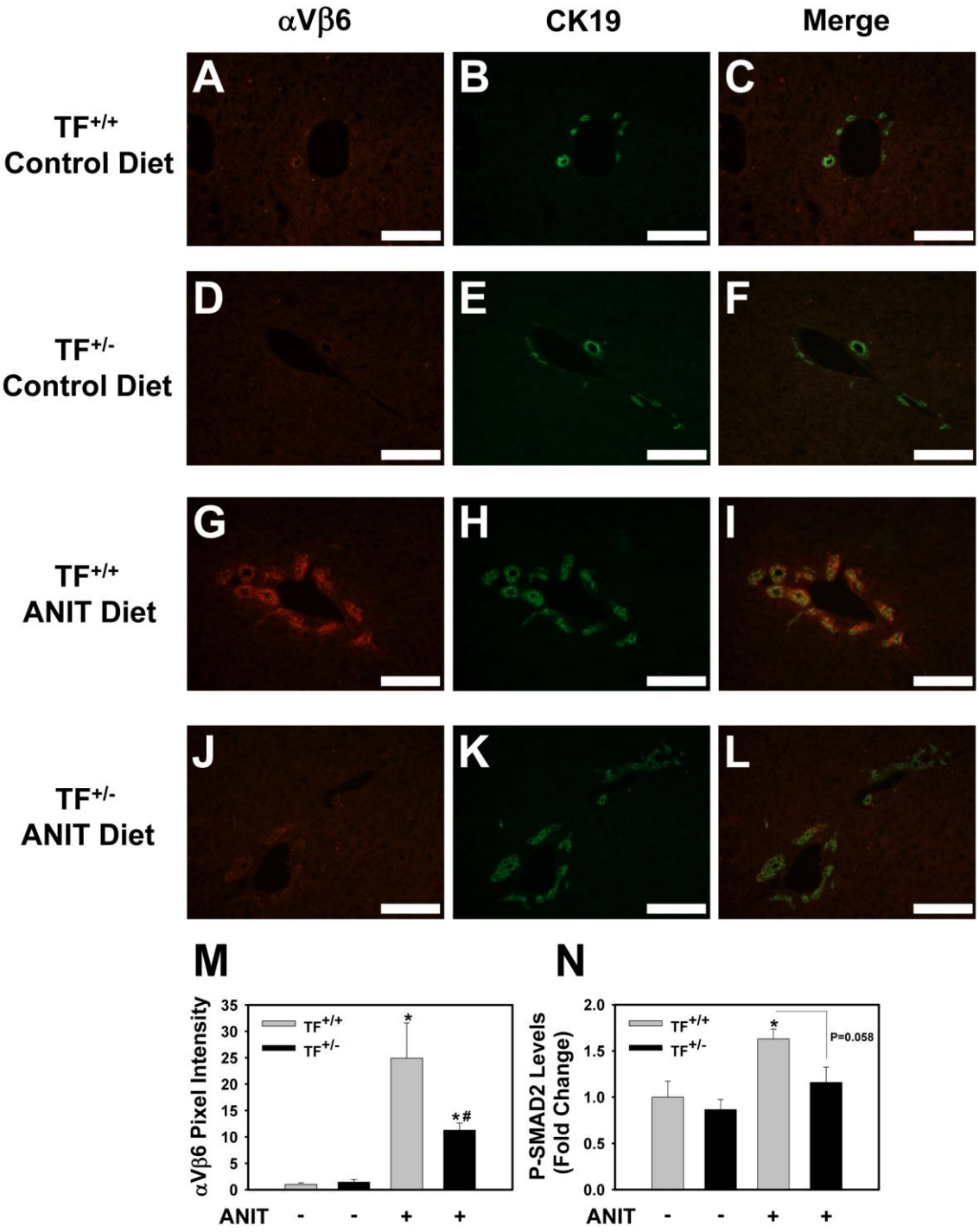
αVβ6
CK19
Merge
A
B
C
TF+/+
Control Diet
D
E
F
TF+/-
Control Diet
G
H
I
TF+/+
ANIT Diet
J
K
L
TF+/-
ANIT Diet
M
αVβ6 Pixel Intensity
35
30
25
20
15
10
5
0
TF+/+
TF+/-
*
*#
ANIT - - + +
N
P-SMAD2 Levels (Fold Change)
2.0
1.5
1.0
0.5
0.0
TF+/+
TF+/-
*
P=0.058
ANIT - - + +

Figure 4.4: Effect of TF-deficiency on αVβ6 integrin expression by BDECs in mice fed the ANIT diet.

Mice wild type for TF ($TF^{+/+}$) (A-C, G-I) and mice heterozygous for TF ($TF^{+/-}$) (D-F, J-L) were fed either control diet (CD) (A-F) or identical diet containing 0.025% ANIT (AD) (G-L) for 14 days. Representative photomicrographs showing immunofluorescent staining for αVβ6 integrin (red), cytokeratin 19 (CK19, green) and the digital merge (yellow) were captured from liver sections. Bar = 10 microns. (M) αVβ6 integrin staining intensity adjusted for CK19 area was determined as described in Methods. n=3-6 mice per group. (N) Levels of phosphorylated (Ser465/467) SMAD2 were determined in liver homogenate by ELISA as described in Methods. Data are expressed as mean ± SEM. *Significantly different from the same mice fed control diet. $^{\#}$Significantly different from $TF^{+/+}$ mice fed the ANIT diet.

Figure 4.5

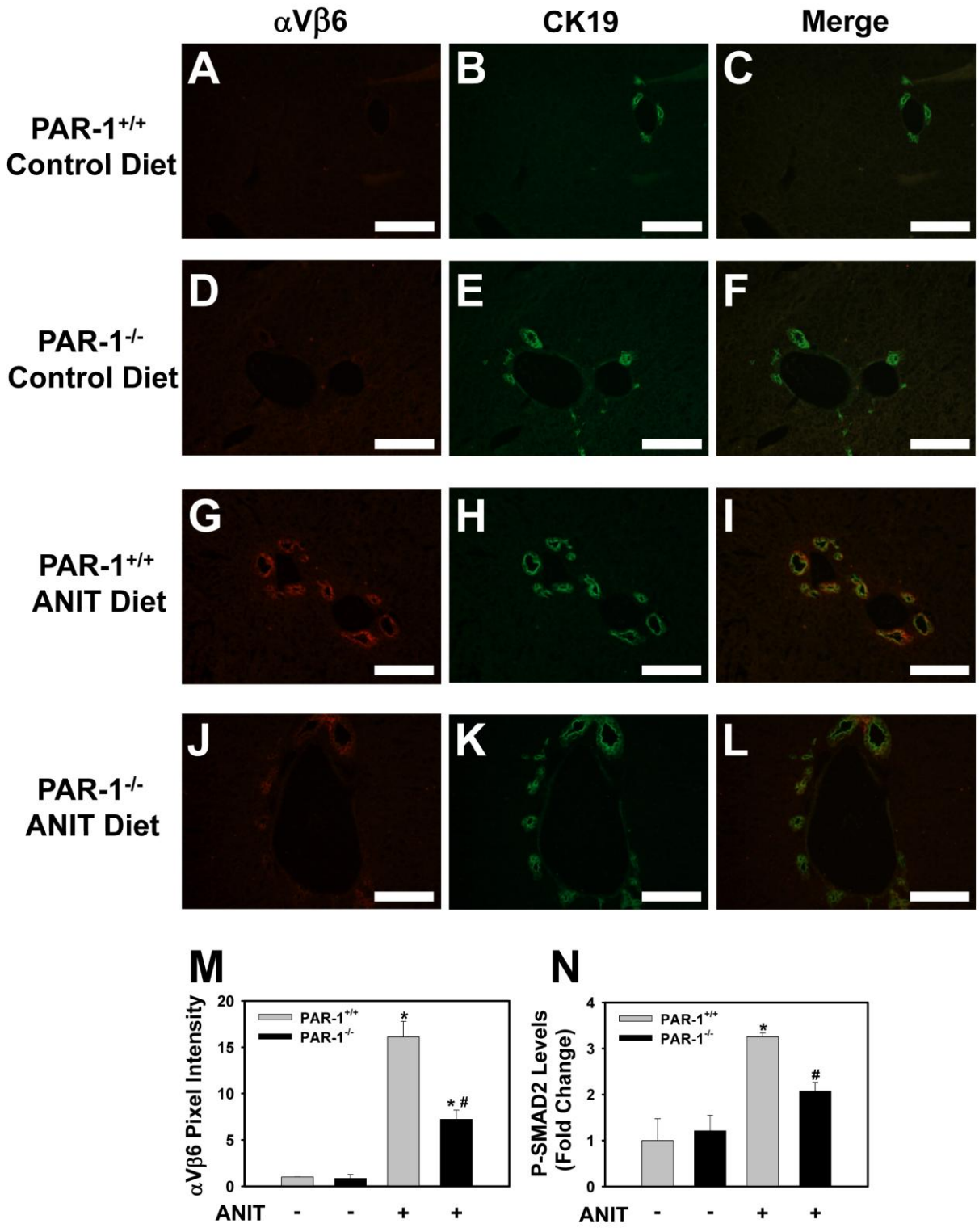
αVβ6
CK19
Merge
A
B
C
PAR-1+/+
Control Diet
D
E
F
PAR-1-/-
Control Diet
G
H
I
PAR-1+/+
ANIT Diet
J
K
L
PAR-1-/-
ANIT Diet
M
αVβ6 Pixel Intensity
20
15
10
5
0
PAR-1+/+
PAR-1-/-
*
*#
ANIT - - + +
N
P-SMAD2 Levels
(Fold Change)
4
3
2
1
0
PAR-1+/+
PAR-1-/-
*
#
ANIT - - + +

Figure 4.5: Effect of PAR-1-deficiency on αVβ6 integrin expression by BDECs in mice fed the ANIT diet.

PAR-$1^{+/+}$ mice (A-C, G-I) and PAR-$1^{-/-}$ mice (D-F, J-L) were fed either control diet (CD) or identical diet containing 0.025% ANIT (AD) for 14 days. Representative photomicrographs showing immunofluorescent staining for αVβ6 integrin (red), cytokeratin 19 (CK19, green) and the digital merge (yellow) were captured from liver sections. Bar = 10 microns. (M) αVβ6 integrin staining intensity adjusted for CK19 area was determined as described in Methods. n=3-7 mice per group. (N) Levels of phosphorylated (Ser465/467) SMAD2 were determined in liver homogenate by ELISA as described in Methods. n=4-7 mice per group. Data are expressed as mean ± SEM. *Significantly different from the same mice fed control diet. #Significantly different from PAR-$1^{+/+}$ mice fed the ANIT diet.

Figure 4.6

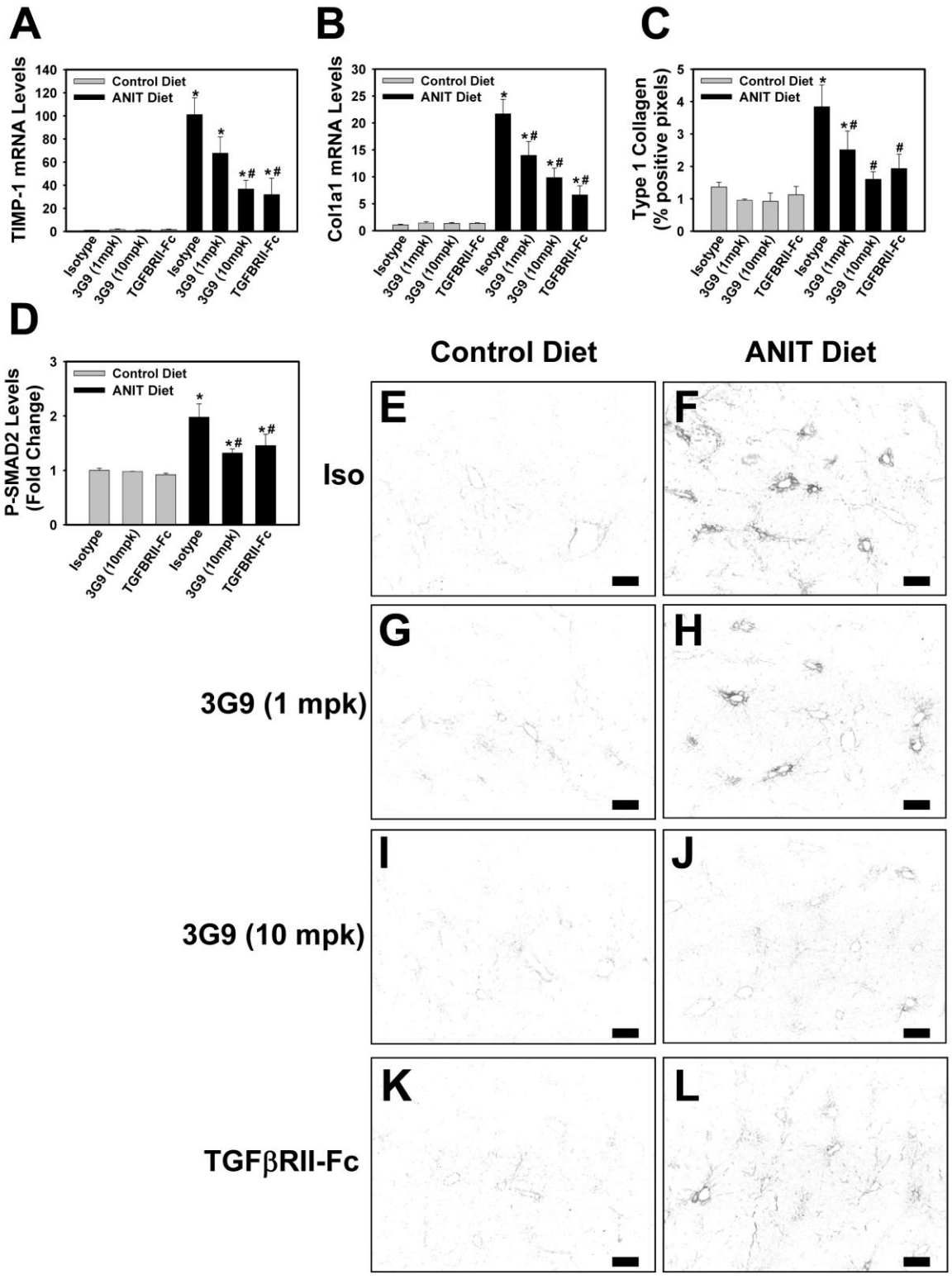
A
TIMP-1 mRNA Levels
Control Diet
ANIT Diet
Isotype
3G9 (1mpk)
3G9 (10mpk)
TGFBRII-Fc
B
Col1a1 mRNA Levels
C
Type 1 Collagen (% positive pixels)
D
P-SMAD2 Levels (Fold Change)
Control Diet
ANIT Diet
Iso
3G9 (1 mpk)
3G9 (10 mpk)
TGFβRII-Fc
E
F
G
H
I
J
K
L

Figure 4.6: Effect of inhibitory anti-αVβ6 integrin antibody and soluble TGF-β receptor treatment on liver fibrosis in mice fed the ANIT diet.

Wild type C57Bl/6J mice were fed either control diet or identical diet containing 0.025% ANIT for 14 days. Mice were given intraperitoneal injections of isotype control antibody (1E6, 10 mg/kg), recombinant TGF-β receptor type II-Fc fusion protein (TGFBRII-Fc, 5 mg/kg), or inhibitory anti-αVβ6 antibody (6.3G9, 1 or 10 mg/kg) on experiment days 1 and 7. Levels of (A) TIMP-1 and (B) Col1a1 mRNA in liver were determined as described in Methods. n=10 mice per group. (C) Quantification of Type 1 collagen staining (see panel E-L) as described in Methods. n=5 mice per group (D) Levels of phosphorylated (Ser465/467) SMAD2 were determined in liver homogenate by ELISA as described in Methods. n=10 mice per group. Data are expressed as mean ± SEM. *Significantly different from the same mice fed control diet. #Significantly different from isotype control-treated mice fed the ANIT diet. (E-L) Representative photomicrographs showing immunofluorescent Type 1 collagen staining of liver sections. (bar = 20 microns) . The images were converted to grayscale and inverted such that positive staining is dark.

Figure 4.7

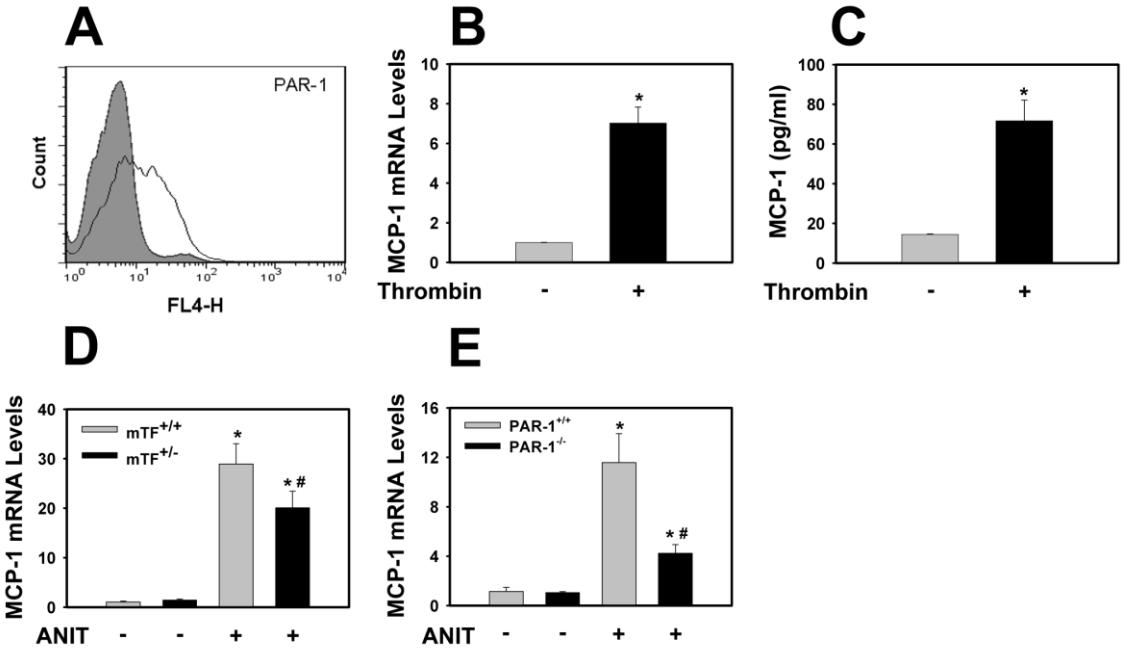

Figure 4.7: Thrombin stimulation of transformed human BDECs.

(A) Flow cytometric detection of PAR-1 expression on the surface of MMNK-1 cells (isotype control, gray; white, anti-PAR-1). For B-C, MMNK-1 cells were stimulated with human α-thrombin (10 U/ml) for 4 hours and (B) MCP-1 mRNA and (C) supernatant MCP-1 levels were determined. Data are expressed as mean ± SEM from at least 3 independent experiments. *Significantly different from vehicle-treated cells. For D-E, mice wild type for TF ($TF^{+/+}$) and mice heterozygous for TF ($TF^{+/-}$), and $PAR\text{-}1^{+/+}$ mice and $PAR\text{-}1^{-/-}$ mice were fed either control diet or identical diet containing 0.025% ANIT for 14 days. Levels of MCP-1 mRNA in liver were determined as described in Methods. n=4-12 mice per group. Data are expressed as mean ± SEM. *Significantly different from the same mice fed control diet. #Significantly different from control mice ($TF^{+/+}$ mice or $PAR\text{-}1^{+/+}$ mice) fed the ANIT diet.

Figure 4.8

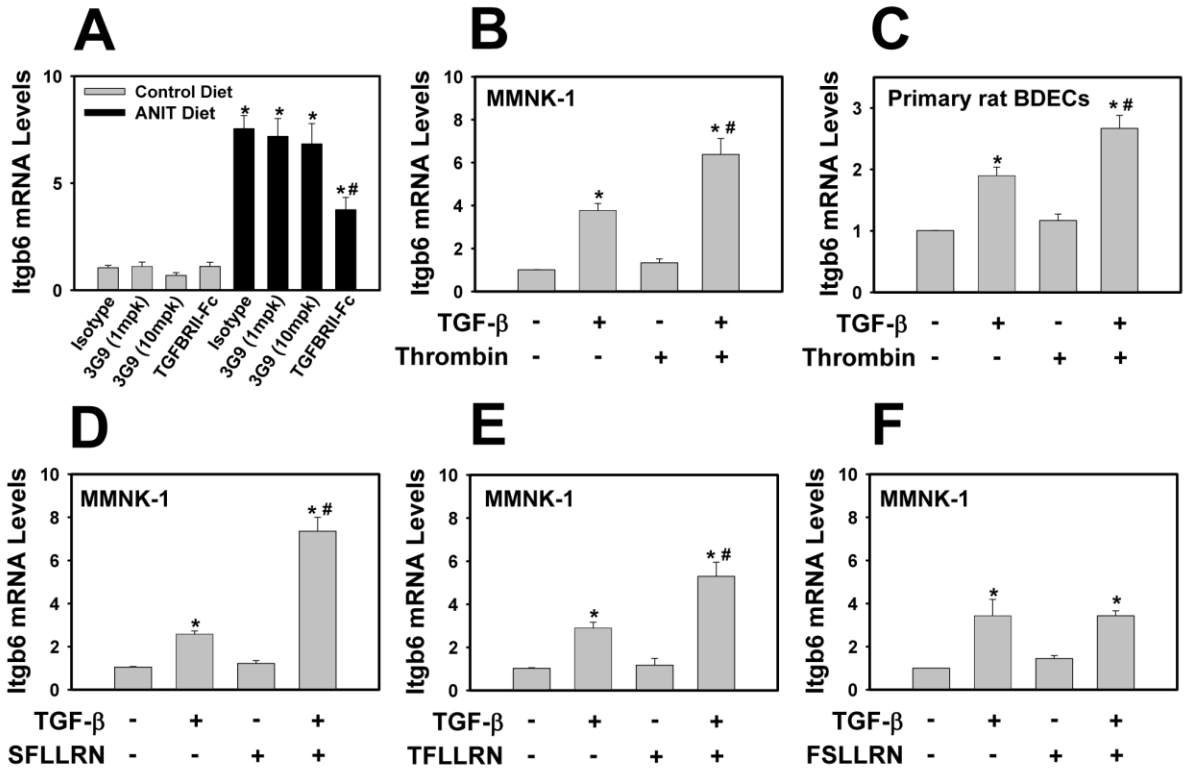

Figure 4.8: PAR-1 activation enhances TGF-β-induced integrin β6 mRNA expression.

(A) Wild type C57Bl/6J mice were fed either control diet or identical diet containing 0.025% ANIT for 14 days. Mice were given intraperitoneal injections of isotype control antibody (1E6, 10 mg/kg), recombinant TGF-β receptor type II-Fc fusion protein (TGFBRII-Fc, 5 mg/kg), or inhibitory anti-αVβ6 antibody (3G9, 1 or 10 mg/kg) on experiment days 1 and 7. Levels of integrin β6 (Itgb6) mRNA in liver were determined as described in Methods. n=10 mice per group. Data are expressed as mean ± SEM. *Significantly different from the same mice fed control diet. #Significantly different from isotype control-treated mice fed the ANIT diet. (B) MMNK-1 cells or (C) primary rat BDECs were stimulated with TGF-β1 (5 ng/ml) or vehicle in the presence or absence of human α-thrombin (10 U/ml), for 4 hours and Itgb6 mRNA levels determined. For D-F, MMNK-1 cells were stimulated with TGF-β1 (5 ng/ml) or vehicle in the presence or absence of (D) 100 μM SFLLRN, (E) 10 μM TFLLRN, or (F) 100 μM FSLLRN. Data are expressed as mean ± SEM from at least 4 independent experiments. *Significantly different from respective treatment group in the absence of TGF-β1. #Significantly different from cells treated with TGF-β1 alone.

Figure 4.9

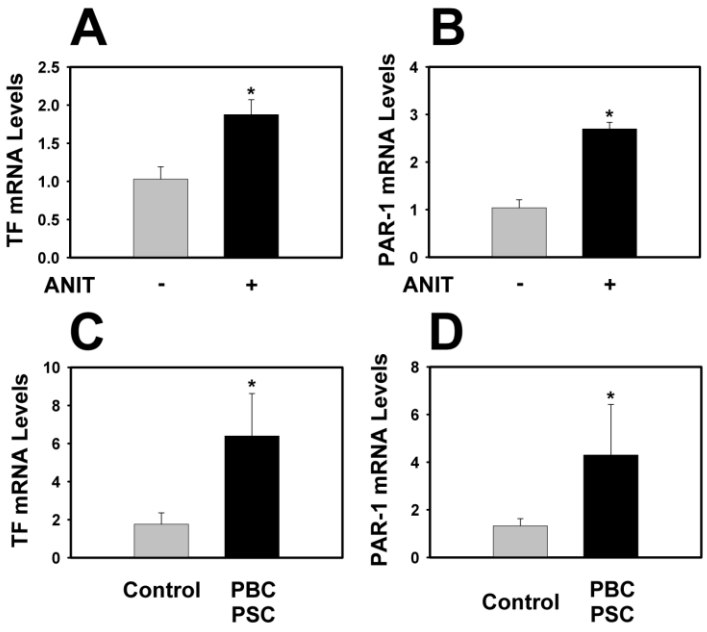

Figure 4.9: Increased expression of TF and PAR-1 mRNA in mice fed the ANIT diet and in patients with cholestatic liver disease.

(A-B) TF and PAR-1 mRNA levels were determined in livers from wild type C57Bl/6J mice fed either control diet or identical diet containing 0.025% ANIT for 14 days. Data are expressed as mean ± SEM. n=5-13 mice per group. *Significantly different from mice fed the control diet. (C-D) TF and PAR-1 mRNA levels were determined in livers from patients with PBC (n=5) and PSC (n=3) and from control livers (n=10) as described in methods. Data are expressed as mean ± SEM. *Significantly different from the control livers.

Figure 4.10

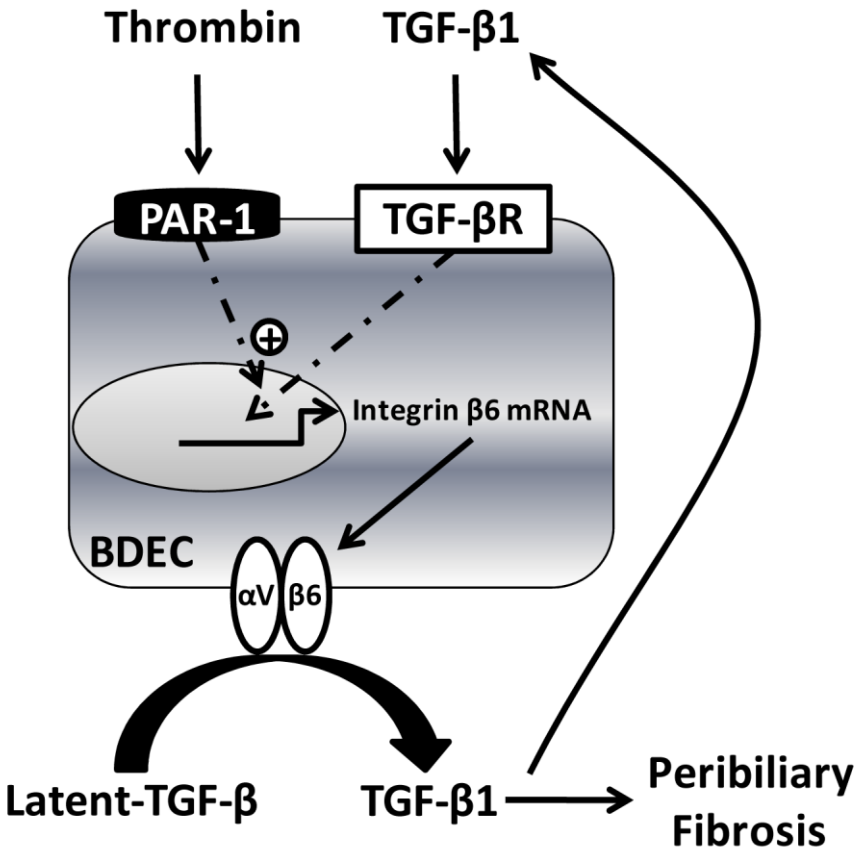

Figure 4.10: Proposed mechanism of amplified β6 integrin expression by thrombin and TGF-β1 in bile duct epithelial cells.

TGF-β1 generated during chronic cholestasis induces β6 integrin expression in bile duct epithelial cells (BDECs), which is expressed on the cell surface as an αVβ6 integrin heterodimer. The αVβ6 integrin contributes to activation of additional TGF-β1 that stimulates peribiliary fibroblasts to produce collagen, leading to peribiliary fibrosis. In a feed-forward amplification loop, TGF-β1 also stimulates additional β6 integrin expression by BDECs. Chronic cellular injury elicits tissue factor-dependent coagulation cascade activation and thrombin generation. Thrombin activation of PAR-1 on BDECs contributes to peribiliary fibrosis by enhancing TGF-β1-induced β6 integrin expression.

4.7 Supplemental Figures

Supplemental Figure 4.1

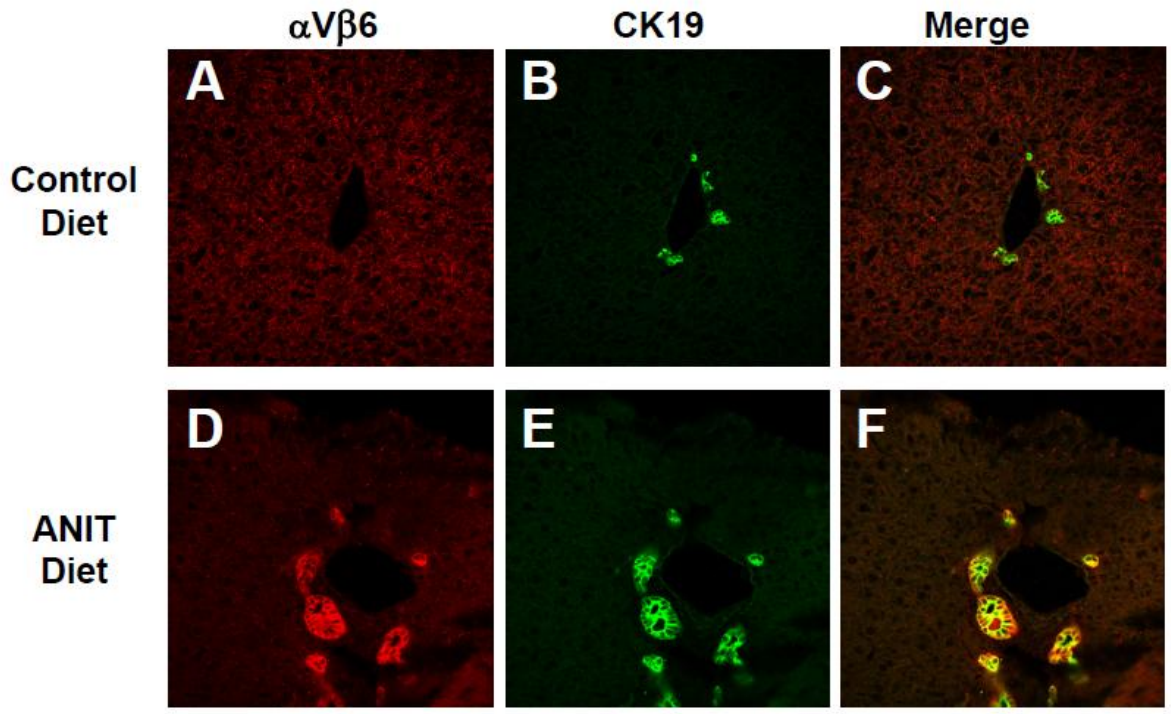

Supplemental Figure 4.1: Assessment of αVβ6 and CK19 co-staining in liver sections from mice fed the ANIT diet by confocal microscopy.

Wild type C57Bl/6J mice were fed either control diet or identical diet containing 0.025% ANIT for 14 days. Shown in A-F are representative photomicrographs obtained using confocal microscopy (see Methods) showing immunofluorescent staining for αVβ6 integrin (red), cytokeratin 19 (CK19, green) and the digital merge (yellow) in liver sections from mice fed control diet (A-C) or ANIT diet (D-F). Images were captured at 400X using an oil immersion objective.

Chapter 5

Regulation of TGF-β1-dependent integrin β6 expression by p38 MAPK in bile duct epithelial cells.

Bradley P. Sullivan, Karen M. Kassel, Sharon Manley, Alyson K. Baker and James P. Luyendyk

Department of Pharmacology, Toxicology and Therapeutics, University of Kansas Medical Center, Kansas City, KS.

This article was published in The Journal of Pharmacology and Experimental Therapeutics, May 2011 337:471-478.

5.1 Abstract

Bile duct epithelial cells (BDECs) contribute to liver fibrosis by expressing αVβ6 integrin, a critical activator of latent transforming growth factor β (TGF-β). β6 integrin (Itgβ6) mRNA induction and αVβ6 integrin expression in BDECs are partially TGF-β-dependent. However, the signaling pathways required for TGF-β-dependent Itgβ6 mRNA induction in BDECs are not known. We tested the hypothesis that the p38 MAPK signaling pathway contributes to TGF-β1 induction of Itgβ6 mRNA by activating SMAD and AP-1 transcription factors. Pretreatment of transformed human BDECs (MMNK-1 cells) with two different p38 MAPK inhibitors, but not a control compound, inhibited TGF-β1 induction of Itgβ6 mRNA. Inhibition of p38 also reduced TGF-β1 activation of a SMAD-dependent reporter construct. Expression of a dominant negative SMAD3 (SMAD3ΔC) significantly reduced TGF-β1-induced Itgβ6 mRNA expression. Expression of JunB mRNA, but not other AP-1 proteins, increased in TGF-β1-treated MMNK-1 cells and induction of JunB expression was p38-dependent. Consistent with a requirement for *de novo* induction of JunB protein, cycloheximide pretreatment inhibited TGF-β1 induction of Itgβ6 mRNA. Expression of a dominant negative AP-1 mutant (TAM67) also inhibited TGF-β1 induction of Itgβ6 mRNA. Overall, the results suggest that p38 contributes to TGF-β1-induced Itgβ6 mRNA expression in MMNK-1 cells by regulating activation of both SMAD and AP-1 transcription factors.

5.2 Introduction

Bile duct epithelial cells (BDECs) are injured chronically in cholestatic liver diseases such as primary sclerosing cholangitis and primary biliary cirrhosis. In addition to being targets of disease processes, it is increasingly clear that BDECs actively participate in the pathogenesis of cholestatic liver disease by producing proinflammatory and profibrogenic mediators such as transforming growth factor beta 1 (TGF-β1) and the αVβ6 integrin (Sedlaczek et al., 2001; Hahm et al., 2007; Sullivan et al., 2010b). These mediators stimulate other cell types including portal fibroblasts to produce collagen, leading to liver fibrosis (Bataller and Brenner, 2005).

The αVβ6 integrin is selectively expressed by epithelial cells in multiple tissues and plays a role in physiological processes such as fetal development and wound healing (Breuss et al., 1995), as well as pathological processes including tumor cell invasion and fibrosis (Marsh et al., 2008; Patsenker et al., 2008). Most notably, the αVβ6 integrin binds to and facilitates the activation of latent transforming growth factor beta 1 (TGF-β1) (Munger et al., 1999), a cytokine and important profibrogenic mediator (Bataller and Brenner, 2005). Several recent studies utilizing mice deficient in the β6 integrin subunit have demonstrated a crucial role for this integrin in the activation of TGF-β1 during fibrosis induced by chronic tissue injury. For example, in rodent models of lung and liver fibrosis, integrin β6 (Itgβ6) deficiency reduced the deposition of extracellular matrix in these tissues (Jenkins et al., 2006; Hahm et al., 2007).

The Itgβ6 gene, which encodes the limiting subunit of the αVβ6 integrin, is expressed at low levels in normal liver. However, in rodent models of cholestasis, both hepatic Itgβ6 mRNA and αVβ6 protein are increased (Hahm et al., 2007; Patsenker et al., 2008; Popov et al., 2008; Sullivan et al., 2010b), and αVβ6 protein expression co-localizes with BDECs (Hahm et al., 2007; Patsenker et al., 2008; Sullivan et al., 2010b). Various genetic and pharmacologic interventions targeting the αVβ6 integrin have been shown to reduce the activation of TGF-β1 and fibrosis in mice and rats during cholestasis (Jenkins et al., 2006; Patsenker et al., 2008; Sullivan et al., 2010b). Taken together, these studies suggest that the induction of Itgβ6 expression is a critical step in the fibrogenic response associated with chronic cholestasis. However, the mechanism of Itgβ6 mRNA induction in BDECs is not known.

We have shown previously that neutralizing TGF-β reduces Itgβ6 mRNA expression during cholestasis (Sullivan *et al*., 2010), suggesting the presence of a feed-forward amplification loop of TGF-β activation. Of importance, the mechanism whereby TGF-β regulates Itgβ6 in bile duct epithelial cells is not completely understood. Mature TGF-β1 binds its type II receptor, which is expressed by BDECs (Lu et al., 2003). This binding event initiates downstream canonical signaling involving activation of TGF-β type I receptor, C-terminal phosphorylation of the regulatory (R-)SMAD transcription factors (SMAD 2

and SMAD3), the heterodimerization of these proteins with SMAD4, and translocation to the nucleus where this complex regulates transcription (Derynck and Zhang, 2003). The importance of SMAD-dependent transcription in fibrosis has been demonstrated previously (Schnabl et al., 2001; Zhao et al., 2002). Of importance, TGF-β-induced Itgβ6 mRNA in keratinocytes is SMAD4-dependent (Levy and Hill, 2005). TGF-β1 also activates non-canonical signaling pathways such as the p38 mitogen activated protein kinase (MAPK), which can regulate gene expression through activation of downstream transcription factors such as activator protein 1 (AP-1). Non-canonical signaling pathways have been shown to be involved in profibrogenic gene induction (Shaulian and Karin, 2001; Derynck and Zhang, 2003; Javelaud and Mauviel, 2005). However, the involvement of the p38 MAPK pathway in the regulation of Itgβ6 gene induction has not been determined.

This study aimed to investigate the signaling mechanisms of TGF-β1-dependent expression of the profibrogenic β6 integrin in BDECs. We utilized transformed human BDECs (MMNK-1 cells) to test the hypothesis that TGF-β1 activation of the SMAD and p38 MAPK signaling pathways coordinate the induction of the β6 integrin mRNA.

5.3 Materials and Methods

5.3.1 Antibodies and Reagents: TGF-β1 (Peprotech, Rocky Hill, NJ), SB203580 (LC Laboratories, Woburn, MA), SB202190 and SB202474 (EMD Chemicals, Gibbstown, NJ), cycloheximide (Sigma-Aldrich, Saint Louis, MO) and dimethyl sulfoxide (DMSO; Research Organics, Cleveland, OH) were used to treat cultured cells. SMAD (SBE4, SABiosciences, Fredrick, MD) and AP-1 (pAP-1-Luc, Stratagene, Santa Clara, CA) responsive luciferase reporter constructs mixed 40:1 with renilla transfection control vector (pRL-CMV, Promega, Madison, WI), Fugene 6 transfection reagent (Roche, Indianapolis, IN), and Dual-glo luciferase assay kit (Promega) were used for luciferase activity experiments. Dominant negative SMAD2 (SMAD2ΔC) and SMAD3 (SMAD3ΔC) mutant as well as a control (pRK7) plasmid were obtained from addgene (Cambridge, MA), donated by Dr. Rik Derynck (Zhang et al., 1996). A dominant negative AP-1 (TAM67) mutant and control (pCMV) plasmids were a

gift from Dr. Michael J. Soares (University of Kansas Medical Center, Kansas City, KS) (Brown et al., 1993). A TriFecta RNAi kit (IDT, Coralville, IA) containing ATF-2 siRNA, control siRNA, and triFECTin^{TM} transfection reagent were used for siRNA knockdown of ATF-2. TRI reagent (Molecular Research Center, Inc., Cincinnati, OH), High Capacity cDNA Reverse Transcription kit (Applied Biosystems, Foster City, CA) and a MyCycler thermal cycler (Bio-Rad, Hercules, CA) were used for the isolation of RNA and synthesis of cDNA. TaqMan gene expression assays, TaqMan master mix and a StepOnePlus sequence detection analyzer (Applied Biosystems) were used for quantitative PCR. Primary antibodies including rabbit anti-human p38, phospho-p38 (Thr180/Tyr182) (12F8) Rabbit mAb), SMAD2, and phospho-SMAD2 (Ser465/Ser467), SMAD3, phospho-SMAD3 (Ser423/425), ATF-2, phospho-ATF2 (Thr71), JunB, and Histone H3 (Cell Signaling Technology, Inc., Danvers, MA) were used for western blotting and immunoprecipitation. HRP conjugated anti-rabbit secondary (Pierce, Rockford, IL) antibody was used for western blotting and ChIP-grade protein G conjugated magnetic beads were used for immunoprecipitation (Cell Signaling Technology).

5.3.2 Cell Culture and treatments: MMNK-1 cells were kindly provided by Dr. Melissa Runge-Morris (Wayne State University, Detroit, MI), on behalf of Dr. Naoya Kobayashi (Okayama University, Okayama, Japan). MMNK-1 cells were maintained at 37^{o} C at 5% CO_2 in DMEM (Sigma) supplemented with 10% fetal bovine serum (FBS [Sigma]), 10 U/ml Penicillin and 10 µg/ml Streptomycin (Sigma) in 75 cm^2 flasks (ISC BioExpress, Kaysville, UT) and were routinely passaged with 0.5% trypsin (Sigma) after cells reached 95% confluency. Prior to treatment, MMNK-1 cells were grown to 70% confluency and were serum-starved for 1 hour prior to stimulation with 5 ng/ml TGF-β1 or its vehicle (0.1% BSA [Fisher] in endotoxin free PBS [Sigma]). For inhibitor studies, MMNK-1 cells were serum starved for 30 minutes, and then pre-treated with, 10 µM SB203580, SB202190, SB202474 (LC Laboratories), 10 µg/ml cycloheximide (Sigma), or DMSO vehicle (final concentration, 0.1%) for an additional 30 minutes prior to treatment with 5 ng/ml TGF-β1 or vehicle. For dominant negative mutant studies, cells were grown to 50% confluency and transfected with 1 µg of plasmid using Fugene6 transfection reagent and allowed to

incubate for 24 hours to reach 70% confluency and were treated as described above. For ATF-2 siRNA studies, cells were grown to 30% confluency, transfected with 10 nM control siRNA or ATF-2 siRNA (IDT) using triFECTin^{TM} transfection reagent (IDT) according to the manufacturer's protocol, and allowed to incubate for 48 hours to reach 70% confluency prior to treatment.

5.3.3 RNA isolation, cDNA synthesis, and real-time PCR: RNA was isolated from adherent cells using TRI Reagent according to the manufacturer's protocol. One microgram of total RNA was utilized for the synthesis of cDNA using a High Capacity cDNA Reverse Transcription kit on a MyCycler thermal cycler. Levels of Itgβ6, GAPDH, ATF-2, and JunB mRNAs were determined using TaqMan gene expression assays and TaqMan gene expression master mix on a StepOnePlus sequence detection system. The relative expression levels of Itgβ6, ATF-2, and JunB mRNAs were determined using the comparative Ct method utilizing GAPDH mRNA as the endogenous control.

5.3.4 Cytosolic and nuclear sample preparation, immunoprecipitation, western blotting and densitometry: Cells were harvested by scraping into ice cold PBS and pelleted by centrifugation at 3,500g at 4^{o}C for 5 minutes. The cell pellet was then resuspended in lysis buffer (10 mM HEPES, 10 mM KCl, 300 mM sucrose, 1.5 mM $MgCl_2$, 0.5 mM DTT, 0.5 mM PMSF, 0.1% NP40) containing protease and phosphatase inhibitors (Roche) and incubated for 10 minutes on ice. Nuclei were pelleted from lysate by centrifugation at 3,500g for 10 minutes at 4^{o} C, and supernatant saved as the cytosolic fraction. Nuclei were then resuspended in nuclear lysis buffer (20 mM HEPES, 100 mM KCl, 100 mM NaCl, 0.5 mM DTT, 0.5 mM PMSF in 20% glycerol) for 30 minutes on ice. Nuclear debris was cleared by centrifugation at 20,000g for 2 minutes and supernatant saved as the nuclear fraction. Protein concentration was determined using a commercially available kit (D_C protein assay, Bio-Rad) according to manufacturer's protocol. For immunoprecipitation, 100 µg of total nuclear protein was incubated with SMAD3 antibody 1:100 (Cell Signaling) overnight with mild rotation at 4^{o}C. 5 µg of protein was diluted into 2X NuPage LDS buffer containing 2.5% 2-Mercaptoethanol (2X LDS, Invitrogen), and saved as the input fraction. Magnetic protein G conjugated beads were then added to the remaining sample and

incubated at 4°C for 2 hours. The magnetic beads were separated and immobilized using a magnetic tube rack, and the samples were then washed 5X in 1ml of nuclear lysis buffer. The magnetic beads were separated and resuspended into 2X LDS and samples were eluted at 95° C for 5 minutes prior to western blotting. All western blotting samples were denatured and reduced in 2X LDS for 5 minutes at 95° C, separated by SDS-PAGE using Criterion XT pre-cast 4-12% Bis-Tris gels and XT MOPS running buffer (Bio-Rad), and transferred onto PVDF membranes (Millipore, Billerica, MA). Membranes were blocked for 60 minutes with 3% BSA in TBST (50 mM Tris, 150 mM NaCl, 0.1% Tween-20, pH 7.4). Membranes were then incubated overnight with primary antibodies diluted 1:1000 for p38, phospho-p38 (Thr183/Tyr185), phospho-SMAD2 (Ser465/Ser467), SMAD2, phospho-SMAD3 (Ser423/425), SMAD3, ATF-2, phospho-ATF2 (Thr71), JunB, or Histone H3 (Cell Signaling Technology) in 1% BSA in TBST at 4° C. Membranes were washed 6 times in TBST for 5 minutes and then incubated with HRP conjugated goat anti-rabbit secondary antibody diluted 1:1000 in 1% BSA in TBST for 1 hour at room temperature. Membranes were washed 6 additional times, then incubated with Super Signal West Pico Chemiluminescence Substrate Solution (Pierce) and exposed to blue autoradiography film (ISC BioExpress). Developed films were scanned using an Epson Expression 1680 scanner and images were analyzed using Gel-Pro Analyzer 32 (Media Cybernetics, Inc, Bethesda, MD). For densitometry, a ratio of phosphorylated p38 or ATF-2 to the respective band(s) indicating total p38 or ATF-2 protein was generated.

5.3.5 Luciferase assays: MMNK-1 cells grown to 50% confluency were transfected overnight using Fugene 6 transfection reagent with 1 µg of SMAD-responsive (SBE4) or AP-1-responsive (pAP-1-Luc) luciferase reporter constructs, each mixed 40:1 with control renilla construct. After 16 hours of transfection, cells were treated with 5 ng/ml TGF-β1 as described above. Luciferase and renilla activities were determined using a Dual-Glo luciferase kit (Promega) per manufacturer's protocol and read by an Infinite M200 plate reader (Tecan, Durham, NC). For each sample, luciferase relative light units (RLU) were adjusted based on renilla activity as an estimation of transfection efficiency.

5.3.6 Statistics: Comparison of the effect of interventions with dominant negative proteins on TGF-β-induced Itgb6 mRNA and luciferase reporter expression was made using a paired t-test. For these experiments, at least 3 independent experiments were performed. Each individual experiment utilized a separate passage (i.e,. split) of MMNK-1 cells. For each experimental replicate, MMNK-1 cells derived from the same flask (i.e., a single split) were distributed identically into wells of 6-well culture plates and 'control' and 'experimental' treatments were performed in parallel from a single cell passage. By design, comparing 'control' and 'experimental' groups using the paired t-test is appropriate (Motulsky, 1995). Comparison of 3 or more groups was performed using an analysis of variance and Student-Neuman-Keuls post-hoc test. The criterion for statistical significance was $P<0.05$.

5.4 Results

5.4.1 TGF-β1 induction of Itgβ6 mRNA in MMNK-1 cells is SMAD-dependent. TGF-β1 increased Itgβ6 mRNA in human transformed bile duct epithelial cells (MMNK-1) (Fig. 5.1A). The cellular response to TGF-β is elicited in part through the canonical signaling pathway via the R-SMAD transcription factors, SMAD2 and SMAD3 (Derynck and Zhang, 2003). Stimulation of MMNK-1 cells with TGF-β1 also increased nuclear levels of C-terminal phosphorylated SMAD2 and SMAD3 (Fig. 5.1B). TGF-β1 treatment of MMNK-1 cells increased activation of a SMAD-dependent reporter construct (Fig. 5.1C). To test the hypothesis that TGF-β1-dependent Itgβ6 mRNA induction is SMAD-dependent, we utilized dominant negative SMAD2 (SMAD2ΔC) and SMAD3 (SMAD3ΔC) mutants (Zhang et al., 1996). MMNK-1 cells transfected with SMAD3ΔC significantly reduced (~25%) TGF-β1-dependent induction of Itgβ6 mRNA (Fig. 5.1D). However, the inhibition (~15%) of TGF-β1-induced Itgβ6 mRNA by expression of SMAD2ΔC did not achieve statistical significance (Fig. 5.1E, $P=0.108$). The data suggest SMAD3 is involved in TGF-β-induced Itgβ6 mRNA expression in MMNK-1 cells.

5.4.2 Activation of p38 MAPK contributes to TGF-β1-dependent induction of Itgβ6 mRNA in MMNK-1 cells. TGF-β can also signal through SMAD-independent, non-canonical signaling pathways leading to activation of the p38 MAPK (Derynck and Zhang, 2003). Treatment of MMNK-1 cells with

TGF-β1 increased levels of phosphorylated p38 MAPK (Fig. 5.2A- B), an indicator of p38 MAPK activation. To determine the role of p38 MAPK signaling pathway in TGF-β1-dependent induction of Itgβ6 mRNA, we utilized two selective pharmacologic inhibitors of p38 (SB203580 and SB202190). Pretreatment of MMNK-1 cells with SB203580 significantly reduced Itgβ6 mRNA expression in MMNK-1 cells treated with TGF-β1 by 40% (Fig. 5.2C). Similarly, pretreatment with a more potent p38 MAPK inhibitor, SB202190, significantly reduced Itgβ6 mRNA expression in MMNK-1 cells treated with TGF-β1 by 70% (Fig. 5.2D). In contrast, pretreatment with a structurally related negative control compound for these two inhibitors (SB202474) had no effect (Fig. 5.2E). The results indicate that p38 is involved in TGF-β1-dependent induction of Itgβ6 mRNA in MMNK-1 cells.

5.4.3 Activation of AP-1 contributes to TGF-β1 induction of Itgβ6 mRNA in MMNK-1 cells. Activation of p38 MAPK directs transcriptional regulation in part through activation of AP-1 transcription factor family members, including FosB, ATF-2, JunB, and c-Jun (Kumar et al., 1997; Shaulian and Karin, 2001; Humar et al., 2007). Indeed, in MMNK-1 cells stimulated with TGF-β1, AP-1-dependent luciferase activity was increased (Fig. 5.3A). Of importance, MMNK-1 cells expressing a dominant negative AP-1 mutant (TAM67), which inhibits all AP-1 family members (Brown et al., 1994), attenuated (~20%) the TGF-β1-dependent induction of Itgβ6 mRNA (Fig. 5.3B). The data indicate that AP-1 contributes to Itgβ6 mRNA induction in MMNK-1 cells.

5.4.4 ATF-2 does not contribute to TGF-β1-induction of Itgβ6 mRNA in MMNK-1 cells. ATF-2 is an AP-1 family member subject to phosphorylation and activation by p38 MAPK. TGF-β-dependent activation of p38 MAPK and subsequent phosphorylation of ATF-2 is reduced after treatment with SB203580 (Edlund et al., 2003). Interestingly, ATF-2 has been shown to bind SMAD3 and increase SMAD-dependent transcriptional activity (Kumar et al., 1997; Yamamura et al., 2000; Ionescu et al., 2003). TGF-β1 treatment increased the levels of phosphorylated ATF-2 in MMNK-1 cells (Fig. 5.4A-B), but did not increase ATF-2 mRNA levels (Fig. 5.4E). Pretreatment with SB203580 reduced the levels of phosphorylated ATF-2 in two independent experiments (data not shown). Co-immunoprecipitation experiments revealed an increased association of SMAD3 and ATF-2 in the nucleus of MMNK-1 cells

treated with TGF-β1 (Fig. 5.4C). Interestingly, SB203580 pretreatment reduced TGF-β1-dependent SMAD luciferase activity by approximately 40% (Fig. 5.4D). To determine whether ATF-2 contributes to Itgβ6 mRNA induction, an siRNA approach was used. ATF-2 mRNA (Fig. 5.4E) and protein (Fig. 5.4F) levels were reduced in MMNK-1 cells transfected with ATF-2 siRNA compared to a length-matched control siRNA that has no complimentary human sequence. Of importance, ATF-2 knockdown did not affect TGF-β1-dependent induction of Itgβ6 mRNA in MMNK-1 cells (Fig. 5.4G). Although ATF-2 interacts with SMAD3 after TGF-β1 treatment, the data suggest that ATF-2 is not required for TGF-β1-induced Itgβ6 mRNA expression in MMNK-1 cells.

5.4.5 TGF-β1 increases JunB expression in MMNK-1 cells in a p38-dependent manner. In a transcription factor binding ELISA screen (TransAM, Active Motif, Carlsbad, CA) to identify other AP-1 family members that could contribute to TGF-β-induced Itgβ6 mRNA expression, we found that TGF-β1 treatment increased the nuclear levels of JunB, but not FosB, c-Fos, Fra-1, c-Jun-P(S73), or JunD (data not shown). Validating this result, we found that JunB mRNA and protein increased in TGF-β1-treated MMNK-1 cells at 30 minutes (Fig. 5.5A) and 120 minutes, respectively (Fig. 5.5B). Of importance, pretreatment of MMNK-1 cells with SB203580 prevented the induction of JunB mRNA (Fig. 5.5C) and the accumulation of nuclear JunB protein (Fig. 5.5D). These results suggest that p38-dependent JunB induction could be a mechanism whereby TGF-β1 contributes to Itgβ6 mRNA expression. Interestingly, pretreatment with the protein synthesis inhibitor cycloheximide (CHX) reduced the TGF-β1-dependent induction of Itgβ6 mRNA in MMNK-1 cells by approximately 30% (Fig. 5.5E). The data suggest that p38 MAPK contributes to TGF-β1-induced JunB mRNA and increased nuclear protein levels. Furthermore, full TGF-β1-dependent Itgβ6 mRNA induction requires *de novo* protein synthesis in MMNK-1 cells.

5.5 Discussion

The αVβ6 integrin has been shown to facilitate activation of latent TGF-β1 (Munger et al., 1999), which contributes to fibrosis in multiple models (Hahm et al., 2007; Popov et al., 2008; Sullivan et al.,

2010b). Cholestatic liver injury is associated with increased expression of Itgβ6 mRNA in liver and expression of αVβ6 by bile duct epithelial cells (BDECs). Induction of mRNA encoding the β6 subunit is likely a critical limiting factor for the surface expression of the αVβ6 integrin (Breuss et al., 1995). To this end, identifying the mediators and pathways required for the expression of this gene in BDECs could reveal novel targets for the treatment of liver fibrosis.

In agreement with our previous study (Sullivan et al., 2010b), we found that treatment of MMNK-1 cells with TGF-β1 increased Itgβ6 mRNA expression. It is initially counterintuitive to consider active TGF-β1 as a key player in the induction of a gene essential for activation of its own latent form. However, it should be noted that there are multiple mechanisms whereby TGF-β1 can become activated. For instance, other factors such as thrombospondin-1 may play a role in the initial activation of latent-TGF-β1 (Crawford et al., 1998). Moreover, there may be low basal levels of surface αVβ6 integrin expression in normal liver. Finally, it is highly likely that more than one mediator contributes to Itgβ6 mRNA expression during cholestasis. Of importance, the induction of the limiting β6 subunit mRNA by active TGF-β1 may form the basis of an amplification loop whereby TGF-β1 drives the further activation of latent TGF-β1 and ultimately liver fibrosis. Supporting this hypothesis are data from a previous study suggesting that inhibition of TGF-β signaling *in vivo* reduces Itgβ6 mRNA and αVβ6 expression in BDECs (Sullivan et al., 2010b). Also, pharmacologic inhibition of αVβ6 integrin reduces fibrosis in several rodent models of cholestasis (Wang et al., 2007a; Patsenker et al., 2008; Sullivan et al., 2010b). These studies further suggest that αVβ6 integrin is a key player in the development of fibrosis and enhance the argument for developing therapies targeting the αVβ6 integrin for the treatment of cholestasis-induced liver fibrosis.

TGF-β1-induced intracellular signaling elicits SMAD-dependent gene induction in multiple cell types (Derynck and Zhang, 2003), including BDECs (Luo et al., 2005). Of importance, the pathogenesis of liver fibrosis in rodent models has been shown to involve SMAD-dependent induction of various profibrogenic genes including PAI-I and CTGF (Holmes et al., 2001; Schnabl et al., 2001; Levy and Hill,

2005; Wang et al., 2007b). A recent study demonstrated that SMAD4 deficiency reduced TGF-β1-dependent induction of Itgβ6 expression in keratinocytes (Levy and Hill, 2005). Similarly, we found that inhibition of SMAD3 reduced the TGF-β1-dependent mRNA induction of Itgβ6. Interestingly, various genes have shown differential dependency on SMAD2 and SMAD3 for their induction. For example, TGF-β-dependent induction of MMP-2 has been shown to be SMAD2-dependent, while CTGF is SMAD3-dependent, and α-SMA relies on both SMAD2 and SMAD3 for induction (Holmes et al., 2001; Phanish et al., 2006). Although the use of a dominant negative SMAD2 showed the same inhibitory trend on TGF-β1-dependent Itgβ6 mRNA induction, this did not meet the level of significance. Further studies are needed to clarify the individual roles of SMAD2 and SMAD3 in the induction of Itgβ6 by TGF-β1 in BDECs.

It is increasingly clear that in addition to activation of the SMAD transcription factors, TGF-β1 activates other signaling pathways, including p38 MAPK (Derynck and Zhang, 2003; Ohshima and Shimotohno, 2003). Indeed, TGF-β1 stimulation of MMNK-1 cells activated the p38 MAPK signaling pathway, and pretreatment of MMNK-1 cells with inhibitors of the p38 MAPK significantly reduced both TGF-β1-dependent Itgβ6 mRNA expression and SMAD-luciferase reporter activation. The finding that two independent pharmacologic inhibitors of p38, but not a structurally related negative control compound, reduced TGF-β1-dependent Itgβ6 mRNA expression constitutes strong evidence of p38 involvement in Itgβ6 induction in MMNK-1 cells. However, we cannot exclude the possibility that "off target" effects of these inhibitors (Bain et al., 2007; Shanware et al., 2009) contributes to their activity in MMNK-1 cells.

Of importance, TGF-β1 activation of the p38 MAPK has been shown to modify gene expression changes via cooperative enhancement of SMAD activity through multiple mechanisms. For example, TGF-β1-dependent p38 MAPK activation stimulates sumoylation of SMAD4, promoting SMAD4 stabilization and sustained transcriptional activity (Ohshima and Shimotohno, 2003). Alternatively, p38 can regulate AP-1 transcription factor components such as ATF-2, which have been shown to modify

SMAD transcriptional activity by directly binding SMAD3 and SMAD4 (Kumar et al., 1997; Yamamura et al., 2000; Ionescu et al., 2003). Although we observed an association of ATF-2 with SMAD3 in TGF-β1-treated MMNK-1 cells, knockdown of ATF-2 did not affect TGF-β1-dependent Itgβ6 mRNA induction.

Other AP-1 family members such as Fos and Jun can alter transcriptional activation of TGF-β target genes (Liboi et al., 1988; Laiho et al., 1991). Of importance, inhibition of AP-1 by the expression of a dominant negative AP-1 mutant (TAM67), which inhibits all AP-1 family members, reduced TGF-β1-dependent Itgβ6 mRNA expression. The relatively modest inhibition of Itgβ6 mRNA expression by the dominant negative AP-1 suggests that AP-1 activation by p38 is one of several pathways that contribute to Itgβ6 mRNA induction. Indeed, p38 activation of the SMAD3 transcription factor may be a parallel pathway regulating Itgβ6 mRNA induction, as the dominant negative SMAD3 protein also reduced Itgβ6 mRNA induction.

In a screen to identify AP-1 family members that could be TGF-β1 sensitive, only nuclear levels of JunB were increased in TGF-β1 treated MMNK-1 cells. Interestingly, JunB has been shown to be induced in response to TGF-β1 stimulation (Coussens et al., 1994; Shaulian and Karin, 2001) JunB can also bind to SMAD3, and its expression is essential for TGF-β-dependent induction of select genes (Verrecchia et al., 2001; Selvamurugan et al., 2004). Indeed, TGF-β1 stimulation of MMNK-1 cells increased JunB mRNA and nuclear protein levels in a p38 dependent manner. It is important to note that the induction of JunB mRNA and nuclear protein accumulation occurred prior to the induction of Itgβ6 mRNA, suggesting a requirement for JunB induction. Similarly, inhibition of protein synthesis reduced Itgβ6 mRNA expression, further suggesting that a key step in Itgβ6 mRNA induction is the *de novo* synthesis of this key regulatory protein. However, further studies are required to elucidate the mechanism whereby individual AP-1 family members participate in TGF-β1-induced Itgβ6 mRNA expression.

In summary, TGF-β1 increased the expression of Itgβ6 mRNAs in transformed human BDECs. Itgβ6 induction required activation of the p38 MAPK signaling pathway and was also dependent upon

AP-1 and SMAD3 transcription factors. Overall, the data suggest that both the SMAD and p38 MAPK pathways contribute to Itgβ6 mRNA expression in BDECs.

5.6 Figures

Figure 5.1

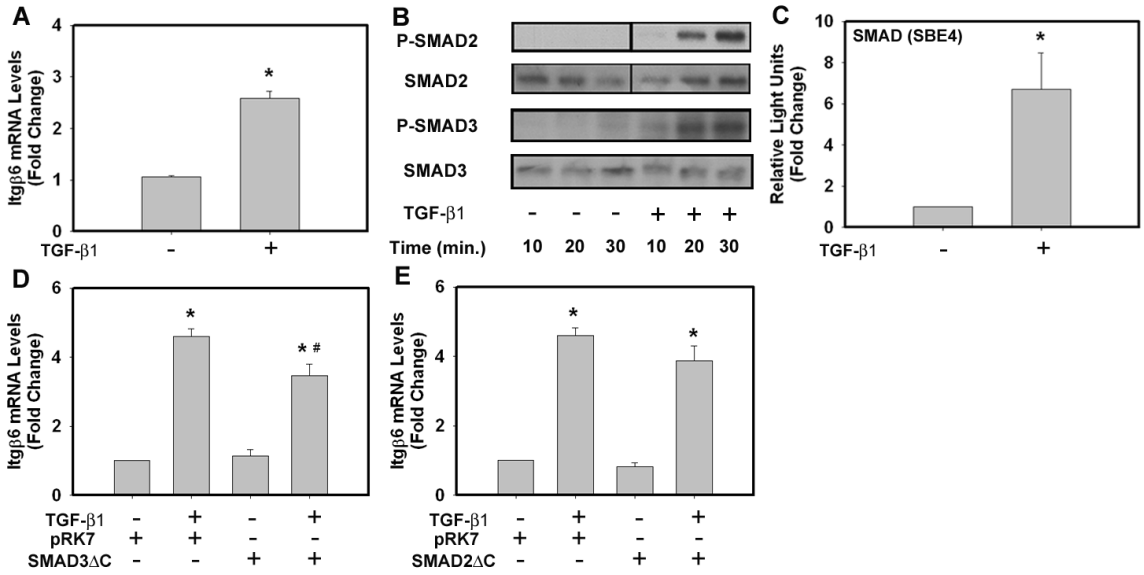

Figure 5.1: Role of SMAD 3 in TGF-β1-induced Itgβ6 mRNA expression in MMNK-1 cells.

(A) MMNK-1 cells were stimulated with 5 ng/ml TGF-β1 or vehicle (0.1% BSA in PBS) for 4 hours. Itgβ6 mRNA levels were determined by qPCR. (B) MMNK-1 cells were treated with 5 ng/ml TGF-β1 or vehicle for various times. Levels of C-terminally phosphorylated SMAD2 and SMAD3, total SMAD2, and total SMAD3 levels were determined in nuclear extracts by western blotting. A representative western blot is shown. (C) MMNK-1 cells transiently transfected with a SMAD-responsive luciferase reporter construct (SBE4) were stimulated with 5 ng/ml TGF-β1 or vehicle for 4 hours, lysed, and luciferase activity was determined. Data are expressed as fold change + SEM compared to vehicle treated MMNK-1 cells. MMNK-1 cells transiently transfected with (D) SMAD3ΔC or (E) SMAD2ΔC mutants were treated with 5 ng/ml TGF-β1 or vehicle for 4 hours and Itgβ6 mRNA levels were determined by qPCR. Data are expressed as mean + SEM relative to vehicle-treated cells transfected with an empty

control plasmid (pRK7) from at least three independent experiments. *Significantly different from 0.1% BSA vehicle-treated group P<0.05. #Significantly different from cells transfected with control plasmid P<0.05.

Figure 5.2

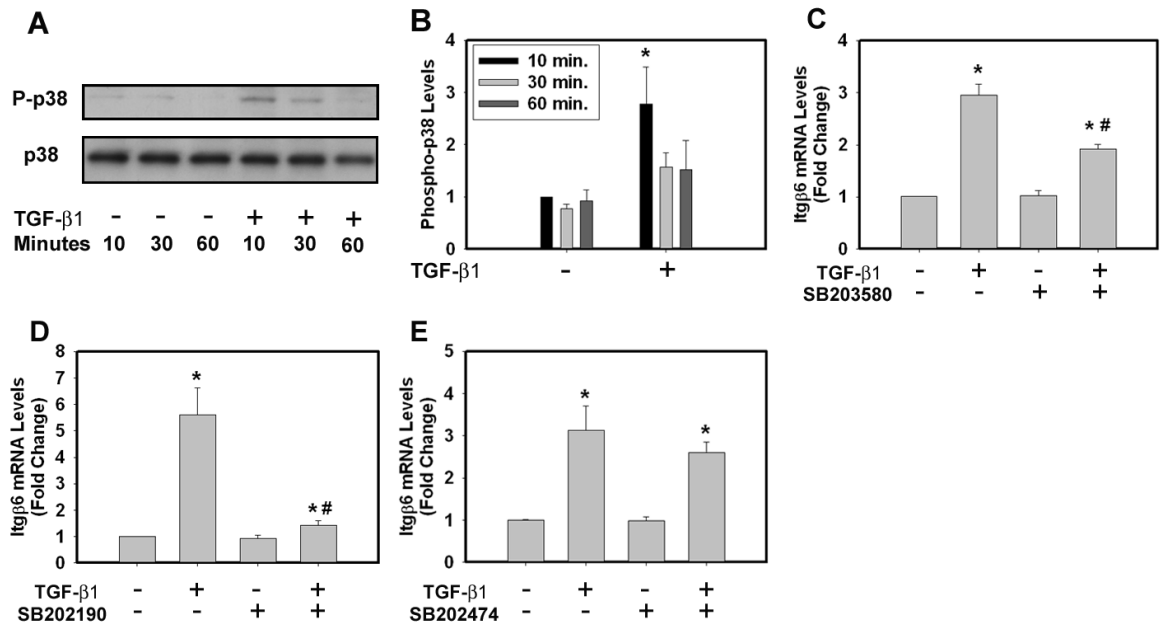

Figure 5.2: Role of p38 MAPK in TGF-β1-induced Itgβ6 mRNA expression in MMNK-1 cells.

MMNK-1 cells were treated with 5 ng/ml TGF-β1 or vehicle for 10, 30 or 60 minutes. (A) Representative western blot showing phosphorylated p38 and total p38 levels. (B) Densitometry was performed on western blots from 3 independent experiments. Data is expressed as a ratio of phosphorylated p38 to total p38 relative to vehicle treated cells at 10 minutes. For panels C-E, MMNK-1 cells were pre-treated with (C) 10 μM SB203580, (D) 10 μM SB202190, (E) 10 μM SB202474 or (C-E) DMSO vehicle (0.1% final concentration) for 30 minutes and then treated with 5 ng/ml TGF-β1 or vehicle for 4 hours. Itgβ6 mRNA levels were determined by qPCR. *Significantly different from 0.1% BSA vehicle-treated cells P<0.05. #Significantly different from cells pretreated with DMSO P<0.05. Data are expressed as mean ± SEM from at least 3 independent experiments.

Figure 5.3

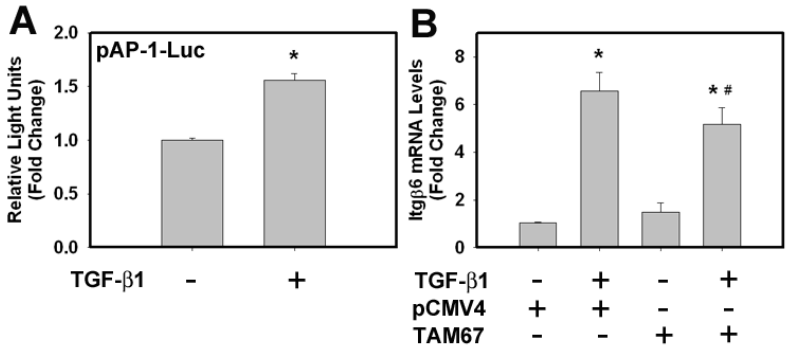

Figure 5.3: Role of AP-1 in TGF-β1-dependent Itgβ6 mRNA induction in MMNK-1 cells.

(A) MMNK-1 cells transfected with an AP-1 luciferase reporter construct (pAP-1-Luc) were treated with 5 ng/ml TGF-β1 or vehicle for 4 hours, lysed, and luciferase activity was determined. (B) MMNK-1 cells were transfected with a plasmid containing a dominant negative AP-1 (TAM67) mutant for 24 hours and then treated with 5 ng/ml TGF-β1 or vehicle for 4 hours. Itgβ6 mRNA levels were determined by qPCR. *Significantly different from 0.1% BSA vehicle-treated cells $P<0.05$. $^{\#}$Significantly different from cells transfected with a control plasmid (pCMV4) $P<0.05$. Data are expressed as mean $\pm$ SEM relative to vehicle-treated cells from 3 independent experiments.

Figure 5.4

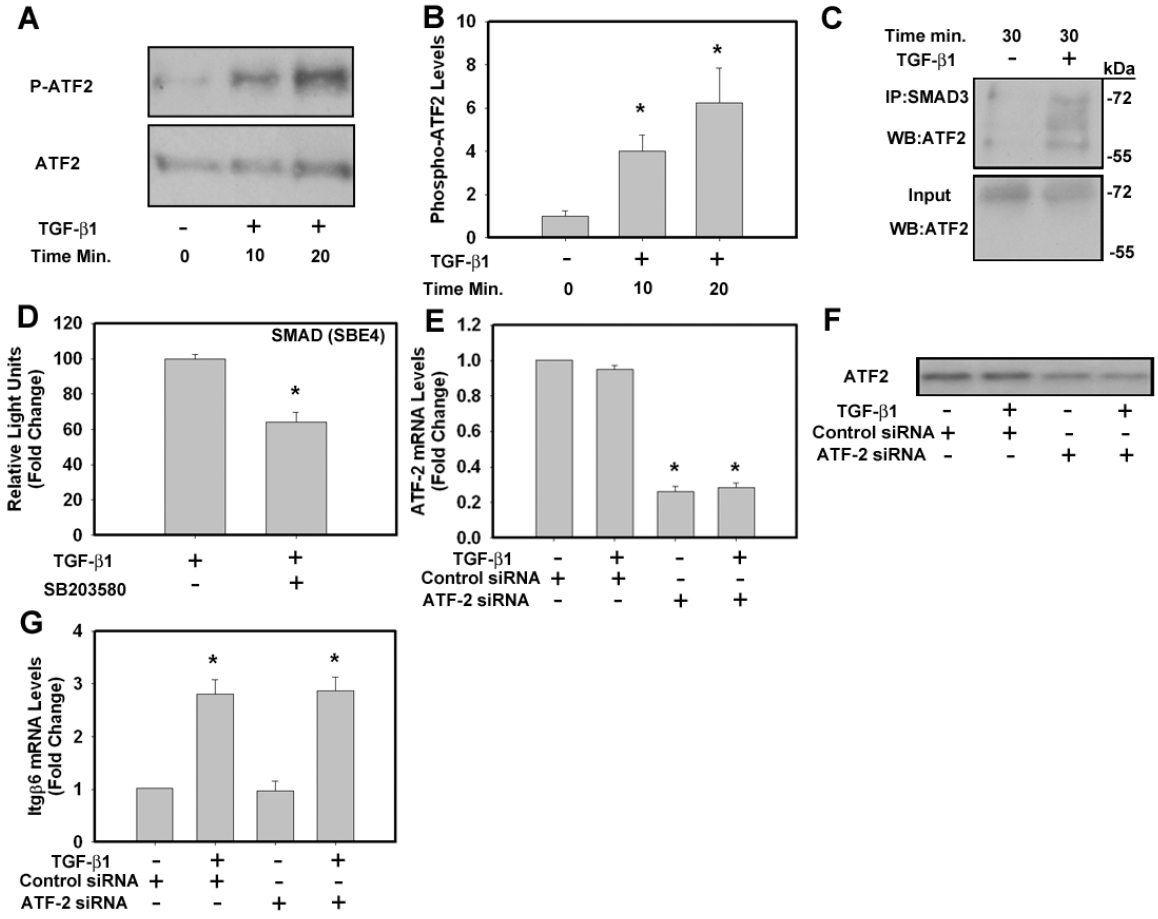

Figure 5.4: Role of activating transcription factor 2 in TGF-β1-dependent Itgβ6 mRNA induction in MMNK-1 cells.

(A) MMNK-1 cells were treated with 5 ng/ml TGF-β1 or vehicle (0.1% BSA in PBS) for 10 or 20 minutes. A representative western blot indicating levels of phosphorylated ATF-2 and total ATF-2 is shown. (B) Densitometry was performed on western blots from 3 independent experiments. Data is expressed as a ratio of phosphorylated ATF-2 to total ATF-2 relative to vehicle treated cells. *Significantly different from 0.1% BSA vehicle treated cells $P<0.05$. (C) MMNK-1 cells were treated with 5 ng/ml TGF-β1 or vehicle for 30 minutes and nuclear proteins were collected. SMAD3 immunoprecipitation was performed and levels of co-immunoprecipitated ATF-2 were determined by

western blot. A representative western blot is shown. (D) MMNK-1 cells transfected with a SMAD-dependent reporter construct were pretreated with 10 μM SB203580 or vehicle (0.1% DMSO vehicle) for 30 minutes prior to treatment with 5 ng/ml TGF-β1 for 4 hours, lysed, and luciferase activity was determined. Data are expressed as fold change ± SEM compared to DMSO treated cells. *Significantly different from DMSO treated cells P<0.05. (E-G) MMNK-1 cells were transfected with an ATF-2 siRNA or control siRNA for 48 hours prior to treatment with 5 ng/ml TGF-β1 or vehicle for 4 hours. (E) ATF-2 mRNA, (F) ATF-2 protein, and (G) Itgβ6 mRNA levels were determined. Representative western blots are shown. Data are expressed as mean ± SEM relative to vehicle-treated cells from 3 independent experiments. For E, *Significantly different from the same group treated with control siRNA P<0.05. For G, *Significantly different from the same group treated with 0.1% BSA vehicle P<0.05.

Figure 5.5

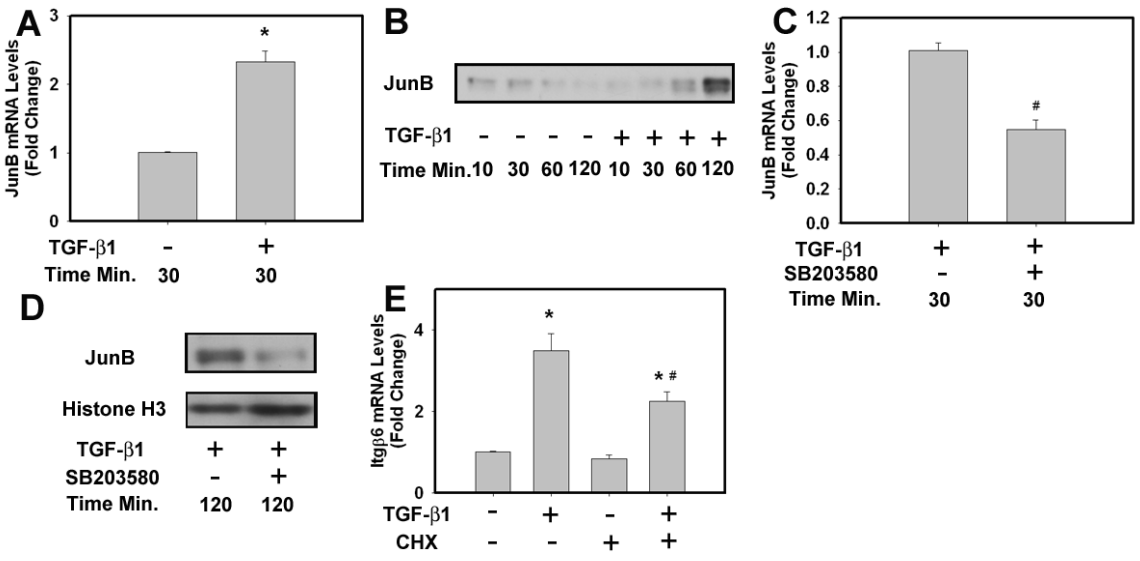

Figure 5: TGF-β1-dependent Itgβ6 mRNA induction requires protein synthesis in MMNK-1 cells.

MMNK-1 cells were treated with 5 ng/ml TGF- β 1 or vehicle for various times. (A) JunB mRNA and (B) nuclear protein levels were determined. (C-D) MMNK-1 cells were pretreated with 10 μM SB203580 or vehicle (0.1% DMSO) for 30 minutes prior to treatment with 5 ng/ml TGF-β1 for (C) 30 minutes or (D) 2 hours and (C) mRNA and (D) nuclear protein levels were determined. (E) MMNK-1

cells were pretreated with 10 µg/ml cycloheximide (CHX) or vehicle (0.1% DMSO) for 30 minutes prior to treatment with 5 ng/ml TGF-β1 or vehicle for 4 hours and Itgβ6 mRNA levels were determined by qPCR. Data are expressed as mean ± SEM from 3 independent experiments. *Significantly different from 0.1% BSA vehicle-treated cells $P<0.05$. #Significantly different from cells pretreated with DMSO $P<0.05$.

Chapter 6

Fibrin(ogen)-Independent Role of Plasminogen Activators in Acetaminophen-Induced Liver Injury.

Bradley P. Sullivan, Karen M. Kassel, Alice Jone[†], Matthew J. Flick[†], and James P. Luyendyk

Department of Pharmacology, Toxicology and Therapeutics, University of Kansas Medical Center, 3901 Rainbow Blvd, Kansas City, KS

[†]Department of Pediatrics, Cincinnati Children's Hospital Medical Center, 3333 Burnet Ave, Cincinnati, OH

This article was published in American Journal of Pathology. 2012 April 13 Jun;180(6):2321-9

6.1 Abstract

Hepatic fibrin(ogen) (Fbg) deposition has been noted to occur following acetaminophen (APAP)-induced liver injury in mice. Deficiency in plasminogen activator inhibitor-1 (PAI-1), the endogenous inhibitor of fibrinolysis (i.e., fibrin breakdown), has been shown to increase APAP-induced liver injury in mice. However, the role of Fbg and fibrinolysis in APAP-induced liver injury is not known. We tested the hypothesis that hepatic Fbg deposition reduces severity of APAP-induced liver injury. APAP (300 mg/kg)-induced liver injury in mice was accompanied by thrombin generation, consumption of plasma Fbg, and deposition of hepatic fibrin. Neither Fbg depletion with ancrod nor complete Fbg deficiency ($Fbg^{-/-}$) affected APAP-induced liver injury. PAI-1 deficiency ($PAI\text{-}1^{-/-}$) increased APAP-induced liver injury and hepatic fibrin deposition 6 hours after APAP administration, which was followed by marked hemorrhage at 24 hours. Mirroring $PAI\text{-}1^{-/-}$ mice, administration of recombinant tissue plasminogen activator (tenecteplase, 5 mg/kg) worsened APAP-induced liver injury and hemorrhage in wild type mice. In contrast, APAP-induced liver injury was reduced in both plasminogen-deficient mice and in wild type mice treated with tranexamic acid, an inhibitor of plasminogen activation. Of interest, activation of matrix metalloproteinase 9 (MMP-9) paralleled injury, but MMP-9 deficiency did not affect APAP-induced liver injury. The results indicate that Fbg does not contribute to development of APAP-induced liver injury. Rather, the results suggest that plasminogen activation contributes to APAP-induced liver injury.

6.2 Introduction

Acetaminophen (APAP) overdose is a leading cause of drug-induced liver failure in the United States (Chun et al., 2009). APAP bioactivation by hepatocytes to the highly reactive *N*-acetyl-*p*-benzoquinone imine (NAPQI) metabolite results in intracellular macromolecule modification and mitochondrial dysfunction, key initiating events of the subsequent hepatocellular necrosis (Chun et al., 2009). The progression of APAP-induced liver injury is associated with numerous events, including activation of the blood coagulation cascade. Thrombin generation is evident in patients suffering from acute APAP overdose and in mouse models of acute APAP-induced liver injury (Gazzard et al., 1975; Ganey et al., 2007). In mice given a hepatotoxic dose of APAP, tissue factor-dependent thrombin

generation is associated with consumption of circulating fibrinogen and deposition of insoluble fibrin clots in the liver (Ganey et al., 2007). However, the role of fibrin(ogen) in APAP-induced liver injury is not known.

Fibrin deposition is determined by a balance of procoagulant (i.e., thrombin) and fibrinolytic pathways. Tissue plasminogen activator (tPA) and urokinase plasminogen activator (uPA) convert plasminogen to the fibrinolytic enzyme plasmin, which degrades fibrin clots (Mackman, 2005). The primary physiological inhibitor of uPA and tPA is plasminogen activator inhibitor-1 (PAI-1) (Schaller and Gerber, 2011). Hepatic PAI-1 mRNA expression and plasma PAI-1 protein levels increase dramatically after APAP administration (Reilly et al., 2001; Ganey et al., 2007; Bajt et al., 2008). Interestingly, a recent study reported that APAP-induced liver injury is increased in PAI-1-deficient mice, suggesting a protective role of PAI-1 in APAP hepatotoxicity (Bajt et al., 2008). Bajt *et al*. proposed the intriguing hypothesis that accelerated fibrin degradation in livers of PAI-$1^{-/-}$ mice precipitates APAP-induced hemorrhage and increased parenchymal cell injury (Bajt et al., 2008), although the effect of PAI-1 deficiency on hepatic fibrin deposition is not known. Moreover, the exact role of fibrin and fibrinolytic enzymes has not been determined in APAP-induced liver injury.

Although exaggerated fibrinolysis and a reduction in hepatic fibrin composition is one mechanism whereby PAI-1 deficiency could increase APAP-induced liver injury, fibrin-independent mechanisms cannot be excluded. For example, plasmin can directly activate pro-matrix metalloproteinase-2 (MMP-2) and pro-MMP-9. (Mazzieri et al., 1997; Legrand et al., 2001; Monea et al., 2002; Takano et al., 2005; Gong et al., 2008). Interestingly, expression and activity of MMP-2 and MMP-9 were shown to be increased in livers of mice treated with APAP, and an inhibitor of these gelatinases significantly reduced APAP-induced liver injury (Ito et al., 2005). Accordingly, one potential fibrin-independent mechanism whereby increased plasmin could contribute to APAP-induced liver injury is by activation of the MMPs. However, it is not currently known if the fibrinolytic system contributes to MMP activation after APAP overdose in mice.

In this study, we characterized the time course of coagulation and hepatic fibrin deposition in a mouse model of APAP overdose, and utilized two strategies to determine the role of fibrin(ogen) in APAP-induced liver injury. Moreover, using a combination of gene-targeted mice and specific pharmacological tools, we explored the role of plasminogen activation on MMP activity and on the progression of APAP hepatotoxicity by using pharmacologic and genetic approaches to modulate the plasminogen activators.

6.3 Methods

6.3.1 Mice: All studies were carried out with male mice of 8 to 16 weeks of age. Wild-type C57Bl/6J mice were purchased from The Jackson Laboratory (Bar Harbor, ME). PAI-$1^{-/-}$ mice (B6.129S2-Serpine1tm1Mlg/J mice), MMP-$9^{-/-}$ mice (B6.FVB(Cg)-Mmp9tm1Tvu/J) and age-matched wild type C57Bl/6J mice were purchased from The Jackson Laboratory. Fbgα-deficient mice ($Fbg^{-/-}$) and heterozygous control mice ($Fbg^{+/-}$) mice back-crossed six generations onto a C57Bl/6J background [kindly provided by Dr. Jay Degen (Cincinnati Children's Hospital Medical Center, Cincinnati, OH)] were maintained in an Association for Assessment and Accreditation of Laboratory Animal Care International–accredited facility at the University of Kansas Medical Center. Mice were housed at an ambient temperature of 22°C with alternating 14/10-hour light/dark cycles and provided water and rodent chow *ad libitum* (Teklad 8604; Harlan, Indianapolis, IN). Plg-deficient mice ($Plg^{-/-}$) or wild type control mice ($Plg^{+/+}$) backcrossed 8 generations on a C57Bl/6J background were maintained at Cincinnati Children's Hospital Medical Center. All animal procedures were approved by the University of Kansas Medical Center or Cincinnati Children's Hospital Medical Center Institutional Animal Care and Use Committee(s).

6.3.2 APAP model and pharmacological interventions: Mice fasted for approximately 15 hours were given 300 mg/kg APAP (at 30 µl/gram body weight) or vehicle (sterile saline) via intraperitoneal (i.p.) injection and food was returned. To deplete fibrinogen, mice were given 1.5 U ancrod (The National Institute for Biological Standards and Control, Hertfordshire, U.K.) or its vehicle (300 µl phosphate-

buffered saline) i.p. 2 hours prior to APAP treatment. Tenecteplase (TNK; 5 mg/kg at 10 µl/gram body weight), a kind gift from Genentech (San Francisco, CA) or its vehicle (sterile saline) was given 2 hours after APAP administration by retrorbital injection under isoflurane anesthesia. Tranexamic acid (TA; 600 mg/kg at 30 µl/gram body weight, Spectrum, New Brunswick, NJ) or its vehicle (sterile saline) was given i.p. 2 hours after APAP treatment. Various times after APAP administration, mice were anesthetized using isoflurane, and blood was collected from the caudal vena cava into sodium citrate (final, 0.38%) or an empty syringe for the collection of plasma and serum, respectively. The liver was removed, washed in saline, and the intact gall bladder removed. The left medial lobe of the liver was affixed to a cork with O.C.T. and frozen for 3 minutes in liquid nitrogen-chilled isopentane. Sections of the left lateral lobe were fixed in neutral-buffered formalin for 48 hours before routine processing. The remaining liver was cut into 100-mg pieces and frozen in liquid nitrogen.

6.3.3 Histopathology and fibrin staining: Formalin-fixed livers were sectioned at 5 µm, stained with hematoxylin and eosin (H&E), and evaluated by light microscopy. Three sections of liver from the left lateral lobe were evaluated from each animal. The area of hepatocellular necrosis in several low magnification (40X) images encompassing the total area of the three sections was determined by J.P.L as described previously using Scion Image software (Luyendyk et al., 2011b) and was performed in a masked fashion. To determine percent necrotic area, the area of liver occupied by necrosis was compared with the total area of liver in each image. Immunofluorescent staining for insoluble hepatic fibrin(ogen) was performed as described previously (Luyendyk et al., 2009) using a rabbit anti-human fibrinogen antibody (Dako, Carpinteria, CA, A0080). The primary antibody was detected by the addition of goat anti-rabbit IgG conjugated to Alexa 488 (Invitrogen, Carlsbad, CA, A11008) and evaluated by fluorescent microscopy.

6.3.4 Clinical chemistry: The serum activity of alanine aminotransferase (ALT) was determined using a commercially available reagent (Thermo Fisher, Waltham, MA). Plasma thrombin-antithrombin (TAT) levels were determined using a commercial enzyme-linked immunosorbent assay kit (Siemens Health

care Diagnostics, Deerfield, IL). For each assay, data was acquired utilizing an Infinite M200 plate reader (Tecan, Durham, NC).

6.3.5 Zymography: Gelatinase (MMP-2 and MMP-9) activity was determined using gelatin zymography. Approximately 100 mg frozen liver tissue was homogenized in ice cold 50 mM Tris-HCl buffer (pH 7.4) containing 150 mM NaCl, 5 mM $CaCl_2$, and 1% Triton X-100. The homogenate was subjected to centrifugation at 9000 × g for 30 min at 4°C, supernatant was collected, and protein concentration determined using a commercial BCA protein assay kit (D_c, Bio-rad Laboratories, Hercules, CA). Supernatant containing 50 µg total protein was mixed with an equal volume of 2X Laemmli sample buffer lacking β-mercaptoethanol (Bio-rad) and subjected to electrophoresis in Ready Gel Zymogram Gels with gelatin (Bio-rad). After electrophoresis, SDS was removed from the gels by three 20 minute washes with zymogram renaturation buffer (2.5% Triton X-100; Bio-rad). The gels were then incubated in zymogram development buffer (50 mM Tris-HCl, pH 7.5, 200 mM NaCl, 5 mM CaCl2; Bio-rad) at 37°C without shaking for 48 hours. Gels were stained with Coomassie stain (Invitrogen) and MMPs were identified by their ability to digest gelatin (clear bands) and by their apparent molecular weights. Gel images were captured by a VersaDoc imaging system (Bio-rad) and converted to grayscale. Densitometry was performed using Quantity One Software (Bio-rad).

6.3.6 Statistics: Comparison of two groups was performed using Student's *t*-test. Comparison of 3 or more groups was performed using one- or two-way analysis of variance, as appropriate, and the Student-Newman-Keuls post hoc test. Data not conforming to a normal distribution were Log_{10} transformed prior to statistical evaluation. Statistical outliers identified by Grubb's Test outliers ($p<0.05$) were excluded from further statistical analysis. The criterion for statistical significance was $p<0.05$.

6.4 Results

6.4.1 Time course of coagulation cascade activation and hepatotoxicity in APAP-treated mice.

Administration of APAP (300 mg/kg) caused liver injury evident by increased serum ALT activity, with peak activity evident after 24 hours (Fig. 6.1A). Increased serum ALT activity was accompanied by

centrilobular hepatocellular necrosis (not shown). Plasma TAT levels, an indicator of thrombin generation, increased dramatically after APAP administration, indicating marked and rapid activation of the coagulation cascade (Fig. 6.1B). In agreement with a previous study (Ganey et al., 2007), increased TAT levels were accompanied by a decrease in plasma fibrinogen levels (Fig. 6.1C) and an increase in hepatic fibrin deposition within areas of hepatocellular necrosis as early as 2 hours (Fig. 6.1D-H). Taken together, the results indicate that APAP hepatotoxicity in mice is associated with coagulation cascade activation, fibrinogen consumption, and hepatic fibrin deposition.

6.4.2 Fibrin(ogen) does not contribute to acute APAP-induced liver injury. To determine the role of fibrin(ogen) in APAP-induced liver injury, we utilized two independent approaches. First, circulating fibrinogen was depleted prior to APAP treatment by administering ancrod, a component of snake venom that enzymatically cleaves circulating fibrinogen (Ewart et al., 1969). Compared to vehicle (PBS)-pretreated mice, pretreatment of mice with ancrod reduced hepatic fibrin deposition after APAP administration at 24 hours (Fig. 6.2B-C). However, ancrod pretreatment had no effect on serum ALT activity at this time in APAP-treated mice (Fig. 6.2A). Next, we utilized mice lacking the Fbgα gene ($Fbg^{-/-}$ mice), which completely lack circulating fibrinogen (Suh et al., 1995). As expected, hepatic fibrin deposition was not detected in $Fbg^{-/-}$ mice after APAP administration (Fig. 6.2E-F), confirming the absence of fibrinogen protein and the specificity of the immunofluorescent staining. In agreement with our fibrinogen depletion studies, complete fibrinogen deficiency did not affect APAP-induced liver injury, as indicated by serum ALT activity (Fig. 6.2D). Overall, these studies suggest that fibrin(ogen) is not a critical mediator of APAP-induced liver injury in mice.

6.4.3 PAI-1 deficiency enhances liver injury, hemorrhage and fibrin deposition in APAP-treated mice. A previous study found that APAP-induced liver injury was increased in PAI-1-deficient ($PAI\text{-}1^{-/-}$) mice (Bajt et al., 2008). In agreement, we found that APAP-induced liver injury, as indicated by increased serum ALT activity and centrilobular necrosis, was significantly increased at 6 hours after APAP administration in $PAI\text{-}1^{-/-}$ mice (Fig. 6.3A and not shown). In association with increased necrosis, hepatic fibrin deposition was increased in $PAI\text{-}1^{-/-}$ mice at this time (Fig. 6.3B-C). Serum ALT activity also

trended higher in APAP-treated PAI-$1^{-/-}$ mice relative to wild type control mice at 24 hours (Fig. 6.3D). In agreement with previous studies, marked hemorrhage was evident in livers of PAI-$1^{-/-}$ mice by 24 hours (see Supplemental Fig. 6.1). Interestingly, fibrin was evident in areas of necrosis in both wild-type and PAI-$1^{-/-}$ mice at 24 hours (Fig. 6.3E-F). The results indicate that increased liver injury in APAP-treated PAI-$1^{-/-}$ mice is not a consequence of reduced hepatic fibrin deposition.

6.4.4 Recombinant human tPA (tenecteplase) administration enhances APAP-induced liver injury in mice. Enhanced APAP-induced liver injury in PAI-$1^{-/-}$ mice suggests that increased plasminogen activator activity could worsen APAP-induced liver injury. To test this hypothesis, we utilized tenecteplase (TNK), a recombinant human tPA (Verstraete, 2000). Administration of TNK (5 mg/kg) alone to wild type mice had no effect on serum ALT levels (Fig. 6.4A) or liver histopathology (not shown). To minimize potential effects of TNK on metabolism of APAP, we administered TNK 2 hours after APAP injection. TNK administration did not affect serum ALT activity 6 hours after APAP administration (Fig. 6.4A). However, increased hemorrhage was evident in areas of necrosis at 6 hours in APAP-treated mice given TNK (Fig. 6.4B-C). Serum ALT activity was significantly increased at 24 hours in mice treated with APAP and TNK compared to mice treated with APAP alone (Fig. 6.4A). The increase in serum ALT activity at 24 hours in TNK-treated mice was accompanied by a dramatic increase in hemorrhage (Fig. 6.4D-E), which closely resembled livers of PAI-1-deficient mice treated with APAP for 24 hours (Supplemental Fig. 6.1 and (Bajt et al., 2008)). The data suggest that exaggerated activation of the plasminogen activators increases APAP-induced liver injury and hemorrhage.

6.4.5 Pharmacologic inhibition of plasminogen activation and genetic plasminogen deficiency reduces APAP-induced liver injury. One mechanism whereby the PAs could contribute to APAP-induced liver injury is through conversion of plasminogen to plasmin (Legrand et al., 2001; Gong et al., 2008). To identify whether plasmin participates in APAP-induced liver injury, we utilized tranexamic acid (TA), which binds plasminogen and inhibits its activation by the PAs (Iwamoto, 1975). Administration of TA alone did not alter serum ALT levels or liver histopathology (Fig. 6.5A-B). To minimize potential effects of TA on metabolism of APAP, TA was administered 2 hours after APAP

injection. Compared with vehicle (saline)-treated mice, TA administration reduced serum ALT activity at 6 and 24 hours after APAP administration (Fig. 6.5A), although this difference did not achieve statistical significance at 6 hours (p=0.058). Of importance, TA treatment significantly reduced the area of centrilobular necrosis in APAP-treated mice at 24 hours (Fig. 6.5B-D). Similar to pharmacologic inhibition of plasminogen activation by TA, complete plasminogen deficiency significantly reduced APAP-dependent liver injury at 24 hours, as indicated by a reduction in serum ALT activity (Fig. 6.5E) and area of centrilobular necrosis (Fig. 6.5F-H). The results suggest that plasminogen contributes to APAP-induced liver injury.

6.4.6 Role of the plasminogen activators in MMP-9 activation in APAP-treated mice. One mechanism whereby plasmin could contribute to APAP-induced liver injury is by activating pro-MMP-2 and pro-MMP-9, enzymes implicated previously in the progression of APAP-induced liver injury (Legrand et al., 2001; Ito et al., 2005; Gong et al., 2008). Accordingly, we determined the time course of gelatinase (MMP-2/9) activation in APAP-treated mice and the effect of genetic and pharmacologic modulation of the PAs on MMP-2/9 activity. As indicated by gelatin zymography, MMP-9 activity was increased in livers of APAP-treated mice as early as 6 hours and remained elevated at 48 hours (Fig. 6.6A-B). However, we found no detectable increase in MMP-2 activity in mice treated with APAP (not shown). Of interest, MMP-9 activity in livers of APAP-treated mice at 6 hours was increased by PAI-1 deficiency (Fig. 6.6C-D) and by TNK treatment (Fig. 6.6E-F), suggesting that enhanced activation of the PAs increases MMP-9 activation in APAP-treated mice. TA administration significantly reduced hepatic MMP-9 activity in APAP-treated mice at 6 hours (Fig. 6.6G-H). The data indicate that MMP-9 is activated after APAP-induced liver injury.

6.4.7 MMP-9 deficiency does not protect against APAP-induced liver injury. A previous study showed that APAP-induced liver injury was reduced in mice given a MMP-2/9 inhibitor (2-[(4-biphenylsulfonyl)amino]-3-phenyl-propionic acid) (Ito et al., 2005). Insofar as we identified an increase in MMP-9 activity in livers of APAP-treated mice, we further evaluated whether MMP-9 could contribute to APAP-induced liver injury. Hepatic MMP-9 activity was not detectable by gelatin zymography in

MMP-9$^{-/-}$ mice, confirming specificity of this assay (Fig. 6.7A). Of interest, APAP-induced liver injury was similar in MMP-9$^{-/-}$ mice compared to wild type control mice, as indicated by serum ALT activity (Fig. 6.7B). The results indicate that MMP-9 does not contribute to APAP-induced liver injury.

6.5 Discussion

The role of PAI-1 in liver injury is model dependent. For example, whereas PAI-1 deficiency reduces liver injury after bile duct ligation (Wang et al., 2007b), PAI-1$^{-/-}$ mice are more susceptible to carbon tetrachloride-induced liver injury (von Montfort et al., 2010). The expression of PAI-1 mRNA is increased rapidly in liver after APAP overdose in mice (Reilly et al., 2001; Bajt et al., 2008) and PAI-1 protein levels increase markedly in the plasma (Ganey et al., 2007). In support of work by *Bajt et al*. (Bajt et al., 2008), we found that APAP-induced liver injury was increased in PAI-1$^{-/-}$ mice, suggesting that PAI-1 is a protective factor in APAP hepatotoxicity. Of importance, generation of the toxic metabolite NAPQI was unaffected by PAI-1 deficiency (Bajt et al., 2008), indicating this genotype does not affect APAP metabolism. It was suggested previously that the presence of marked hemorrhage in livers of APAP-treated PAI-1$^{-/-}$ mice could occur as a consequence of reduced hepatic fibrin deposition and a failure to maintain normal hemostasis. Of importance, we found that hepatic fibrin levels actually increased in association with increased hepatocellular injury in PAI-1$^{-/-}$ mice at 6 hours, and fibrin remained present in livers of APAP-treated PAI-1$^{-/-}$ mice at 24 hours. This suggests that increased APAP hepatotoxicity in PAI-1$^{-/-}$ mice is not a consequence of reduced fibrin levels in liver.

Hepatic fibrin deposition occurs in numerous models of xenobiotic-induced liver injury (Fujiwara et al., 1988; Bailie et al., 1993; Neubauer et al., 1995; Copple et al., 2002a; Ganey et al., 2007; Luyendyk et al., 2009), but the mechanistic contribution of fibrin(ogen) has not been determined in most models. In this study, we used two independent approaches to evaluate the role of fibrin(ogen) in APAP hepatotoxicity: 1) depletion of fibrinogen with ancrod and 2) Fbg$^{-/-}$ mice, which completely lack circulating fibrinogen protein (Suh et al., 1995). We found that neither fibrinogen depletion nor complete fibrinogen deficiency affected APAP-induced liver injury at 24 hours, suggesting that fibrin(ogen) does

not contribute to acute APAP hepatotoxicity. This is in contrast to other models where fibrin(ogen) has been shown to be either damaging or hepatoprotective (Luyendyk et al., 2011a; Luyendyk et al., 2011b). Of importance, the finding that fibrinogen is not required for acute APAP hepatotoxicity supports the hypothesis that a change in hepatic fibrin clearance is not the primary mechanism of increased APAP hepatotoxicity in PAI-1-deficient mice.

To further delineate the effect of enhanced plasminogen activation on APAP-induced liver injury, we utilized a recombinant human tPA (i.e., TNK). We selected to administer TNK two hours after APAP treatment to avoid the possibility of interfering with APAP metabolism, NAPQI generation, and glutathione depletion, the vast majority of which occurs within 60 minutes of APAP administration (Knight et al., 2001; Jaeschke et al., 2011). Mirroring changes in livers of APAP-treated PAI-$1^{-/-}$ mice, hepatocellular injury and hemorrhage were increased by TNK administration, consistent with the hypothesis that APAP-induced liver injury is increased by exaggeration of PA activity. However, it cannot be concluded from these studies that endogenous tPA is the critical PA participating in APAP-induced liver injury. Both uPA and tPA can convert plasminogen to plasmin, but each PA generally serves different biological functions. tPA is an important regulator of fibrin degradation and vascular hemostasis, whereas uPA generally participates in tissue repair and extracellular matrix remodeling (Schaller and Gerber, 2011). Interestingly, tPA directly binds fibrin polymers and this enhances its enzymatic activity by several hundred-fold (Schaller and Gerber, 2011). Insofar as fibrin deficiency did not affect APAP-induced liver injury, this could suggest that uPA rather than tPA is the critical endogenous PA during APAP-induced liver injury. However, additional studies are required to determine the relative contribution of uPA and tPA in APAP-induced liver injury.

Studies in PAI-1-deficient mice indicate that PAI-1 limits APAP-induced liver injury, and our studies with TNK administration support the hypothesis that exaggerated plasminogen activation worsens APAP-induced liver injury. To determine whether administration of an inhibitor of plasminogen activation could confer additional protection against APAP-induced liver injury under conditions where PAI-1 was present, we utilized tranexamic acid, an antifibrinolytic drug that prevents the conversion of

plasminogen to plasmin (Iwamoto, 1975). Like our studies with TNK, tranexamic acid was given 2 hours after APAP to avoid any potential effect on APAP metabolism. Our results suggest that the activation of plasmin, even in wild type mice with sufficient levels of PAI-1, contributes to the progression of liver injury in APAP-treated mice. Of importance, we found that complete genetic plasminogen deficiency also reduced APAP-induced liver injury. However, these results do not identify the PA (tPA and/or uPA) that is responsible for activating plasminogen during APAP-induced liver injury. Additionally, these studies do not test the possibility that either tPA and/or uPA also contribute to the progression of APAP-induced liver injury in a plasminogen-independent manner. These studies are the subject of ongoing investigation in our laboratory.

Our studies indicate that fibrin(ogen) is not involved in the development of APAP-induced liver injury. However, the results suggest that plasmin, the primary endogenous fibrinolytic enzyme, contributes to APAP-induced liver injury. One fibrin-independent mechanism whereby plasmin might contribute to APAP toxicity is through activation of pro-MMP-2/9. Plasmin has been shown previously to contribute to activation of both pro-MMP-2 and pro-MMP-9 to their active forms (Mazzieri et al., 1997; Legrand et al., 2001; Monea et al., 2002; Takano et al., 2005; Gong et al., 2008). A previous study showed that hepatic MMP-2 and MMP-9 expression and activity are increased in livers of mice after APAP overdose (Ito et al., 2005). In agreement with that study, we found that MMP-9 activity increased in liver as early as 6 hours after APAP administration. In contrast, we were not able to detect an increase in MMP-2 activity after APAP administration (not shown). To this end, we focused on the possibility that plasmin-dependent MMP-9 activation could contribute to APAP hepatotoxicity. In contrast to a previous study demonstrating that a pharmacologic inhibitor of MMP-2/9 reduced APAP hepatotoxicity [10], MMP-9 deficiency did not affect APAP induced liver injury. Notable differences between our study utilizing MMP-9-deficient mice and a previous study utilizing a pharmacologic inhibitor of MMP-9 include the use of DMSO as the solvent for the MMP inhibitor, a compound which is known to affect APAP metabolism and glutathione depletion (Jaeschke et al., 2011). The fast prior to APAP administration was also extensive (24 hours), and the dose/route of APAP administration differed

between the two studies. Our studies with MMP-9$^{-/-}$ mice strongly suggest that the protection observed previously cannot be attributed to inhibition of MMP-9.

In the clinic, patients that present with APAP overdose arrive with varying degrees of liver injury and at various stages of injury progression. Our data suggest that a PA-plasmin pathway participates in the early progression of APAP-induced liver injury in a mouse model. Inhibition of this pathway could provide a therapeutic benefit to patients during the early progression phase of APAP-toxicity. However, the fibrinolytic system and MMPs have also been shown to participate in tissue regeneration and wound healing processes. Deficiency in plasminogen has been shown to derange the wound healing process, including chronic liver injury (Pohl et al., 2001). A previous study showed that impaired liver regeneration in plasminogen-deficient mice was not affected by a combined deficiency of fibrinogen, suggesting that plasminogen contributes to liver repair in a fibrinolysis-independent mechanism in that model (Bezerra et al., 1999). Although we found that fibrinogen deficiency does not affect acute APAP hepatotoxicity development, we cannot exclude a role for fibrinogen in the resolution of APAP-induced liver injury. Similarly, this raises questions about the potential for differential roles of PAs and MMPs during the development and recovery phases of APAP-induced liver injury. Accelerated injury resolution has been described in PAI-1$^{-/-}$ mice in a dermal injury model (Chan et al., 2001). Of importance, uPA is known to activate hepatocyte growth factor, a critical cytokine that promotes liver regeneration (Shimizu et al., 2001). Interestingly, a previous study showed that increased liver injury 24 hours after APAP administration in PAI-1$^{-/-}$ mice was accompanied by a decrease in hepatic PCNA protein expression, suggesting that these mice have delayed liver regeneration (Bajt et al., 2008). However, in that same study PAI-1$^{-/-}$ mice with dramatically increased liver injury recovered alongside wild type mice by 48 hours, suggesting those mice had enhanced liver regeneration in the recovery phase of APAP (Bajt et al., 2008). Further experiments are needed to determine the role(s) of fibrin(ogen) and fibrinolytic enzymes in the resolution and repair of APAP-induced liver injury.

In summary, we have shown through genetic and pharmacologic interventions that fibrinogen and fibrin are not involved in the development of APAP hepatotoxicity in mice. Furthermore, we found that

both genetic (PAI-$1^{-/-}$) and pharmacologic (TNK) interventions that increase PA activity also increase APAP-induced liver injury and hemorrhage. Of importance, inhibition of plasminogen activation with tranexamic acid and complete plasminogen deficiency reduced liver injury in APAP-treated mice. Taken together, our studies indicate that the plasminogen activators and plasmin contribute to APAP-induced liver injury development in a fibrin(ogen)-independent manner. Inhibition of the PA-Plasmin pathway may serve as a potential therapeutic target to limit acute liver injury development in patients presenting with APAP-overdose.

6.6 Figures

Figure 6.1

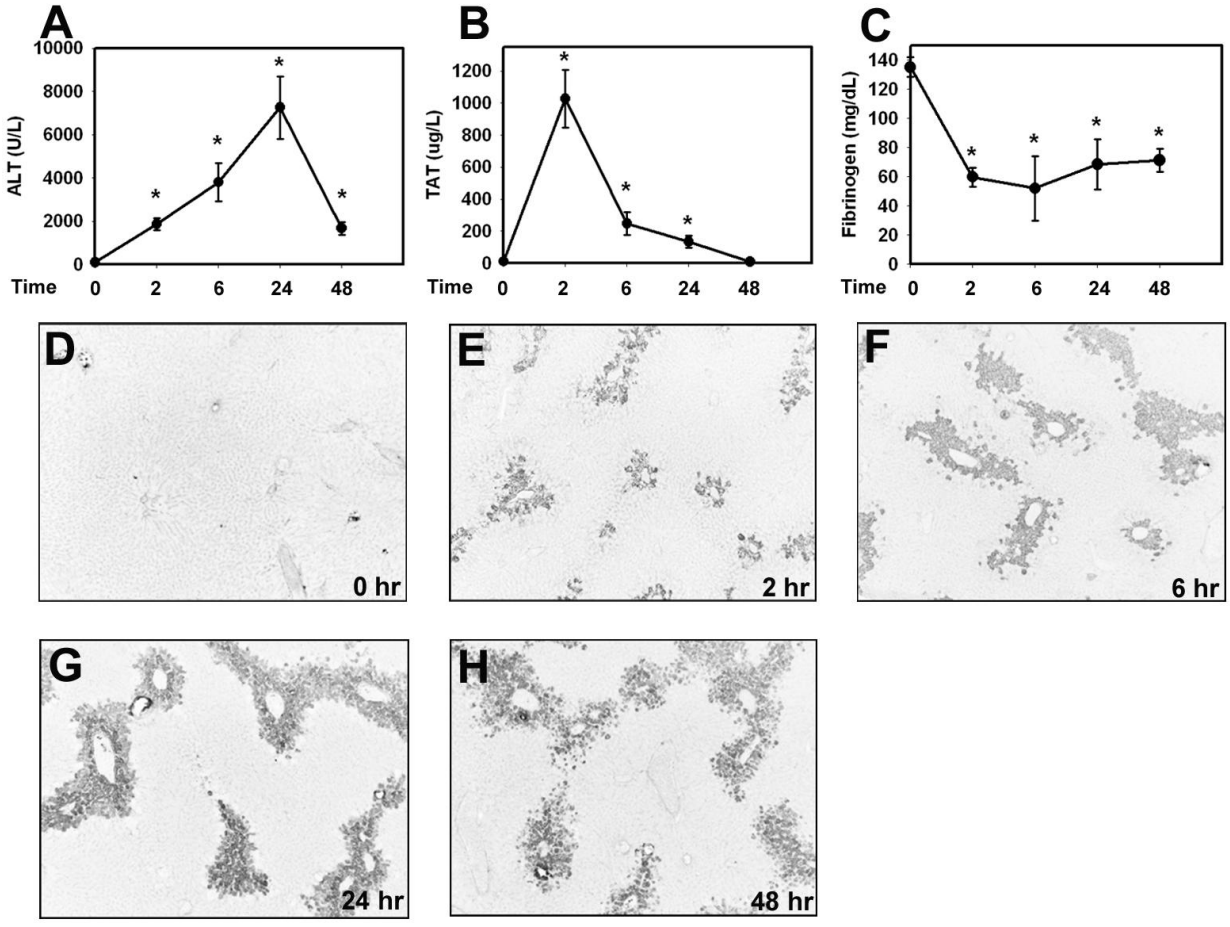

Figure 6.1: Time course of coagulation cascade activation and hepatotoxicity in APAP-treated mice.

Fasted wild type mice were given a toxic dose of APAP (300 mg/kg, i.p.) or vehicle (sterile saline, time 0) and samples were collected 2, 6, 24, and 48 hours later. Levels of (A) serum ALT activity, (B) plasma thrombin anti-thrombin (TAT), and (C) plasma fibrinogen levels were determined. Data are expressed as mean ± SEM. *Significantly different from saline-treated control mice ($p<0.05$). (D-H) Representative photomicrographs of hepatic fibrin (dark) staining at (D) 0, (E) 2, (F) 6, (G) 24, and (H) 48 hours after APAP treatment. n=5 mice per group.

Figure 6.2

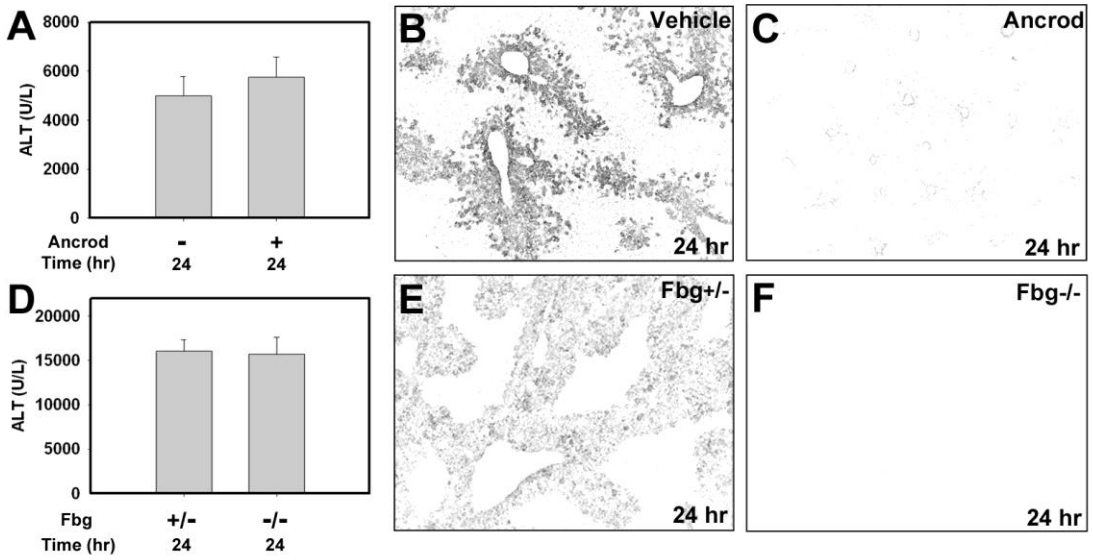

Figure 6.2: Fibrin(ogen) does not contribute to acute APAP-induced liver injury.

(A-C) Fasted wild type mice were treated with 1.5 U ancrod or vehicle (300 µl sterile PBS) two hours prior to treatment with APAP (300mg/kg) and then samples were collected 24 hours later. (D-F) Fasted $Fbg^{+/-}$ control mice and $Fbg^{-/-}$ were treated with APAP (300 mg/kg) for 24 hours. (A, D) Serum ALT activity was determined. Data is expressed as mean ± SEM. (B-C, E-F) Representative

photomicrographs of fibrin (dark) staining after APAP treatment in livers of wild type mice treated with (B) PBS or (C) ancrod and in (E) $Fbg^{+/-}$ or (F) $Fbg^{-/-}$ mice. n=7-12 mice per group.

Figure 6.3

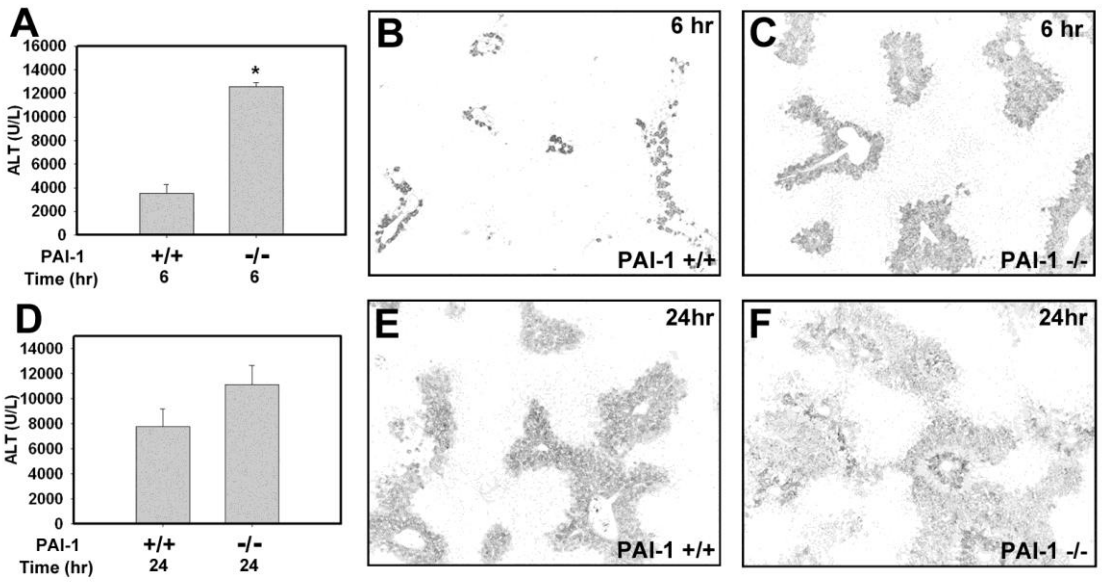

Figure 6.3: PAI-1-deficiency enhances liver injury and fibrin deposition in APAP-treated mice.

Fasted wild type or $PAI\text{-}1^{-/-}$ mice were treated with APAP (300 mg/kg) and samples were collected (A-C) 6 or (D-F) 24 hours later. (A, D) Levels of serum ALT activity were determined. Data is expressed as mean $\pm$ SEM. *Significantly different from wild type mice ($p<0.05$). (B-C, E-F) Representative photomicrographs of fibrin (dark) stained livers from APAP-treated (B, E) wild type and (C, F) $PAI\text{-}1^{-/-}$ mice. n=3-4 mice per group.

Figure 6.4

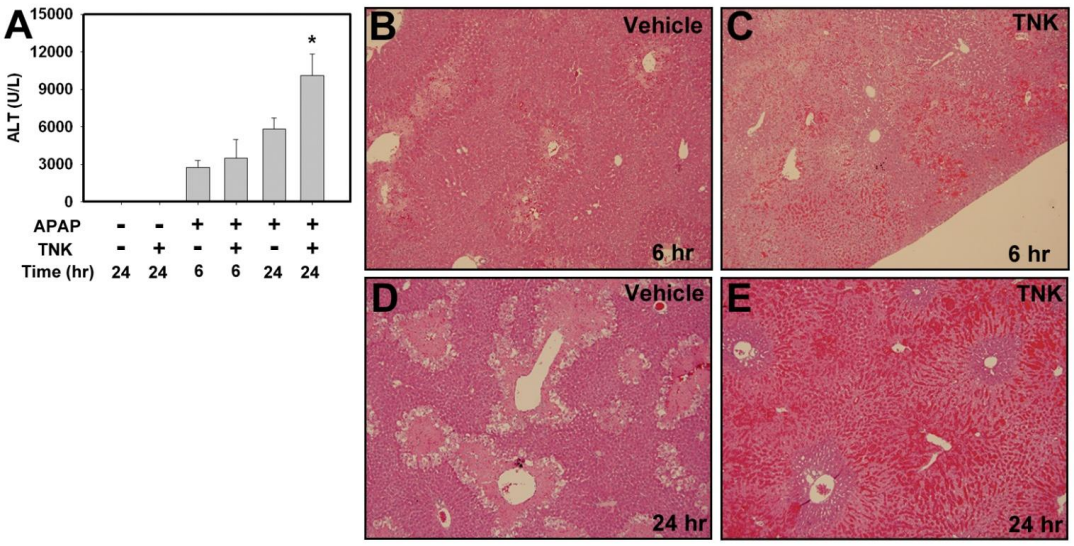

Figure 6.4: Recombinant human tPA (tenecteplase) administration enhances APAP-induced liver injury in mice.

Fasted wild type mice were treated with APAP (300 mg/kg) or vehicle (sterile saline) and 2 hours later mice were given tenecteplase (5 mg/kg, TNK, r.o.). (A) Serum levels of ALT activity were determined after 6 and 24 hours of APAP treatment. Data is expressed as mean $\pm$ SEM. *Significantly different from APAP-treated mice given saline vehicle at that time ($p<0.05$). (B-E) Representative photomicrographs of hematoxylin and eosin stained liver sections from mice given (B, D) vehicle or (C, E) TNK and treated with APAP for (B-C) 6 or (D-E) 24 hours. n=3-8 mice per group.

Figure 6.5

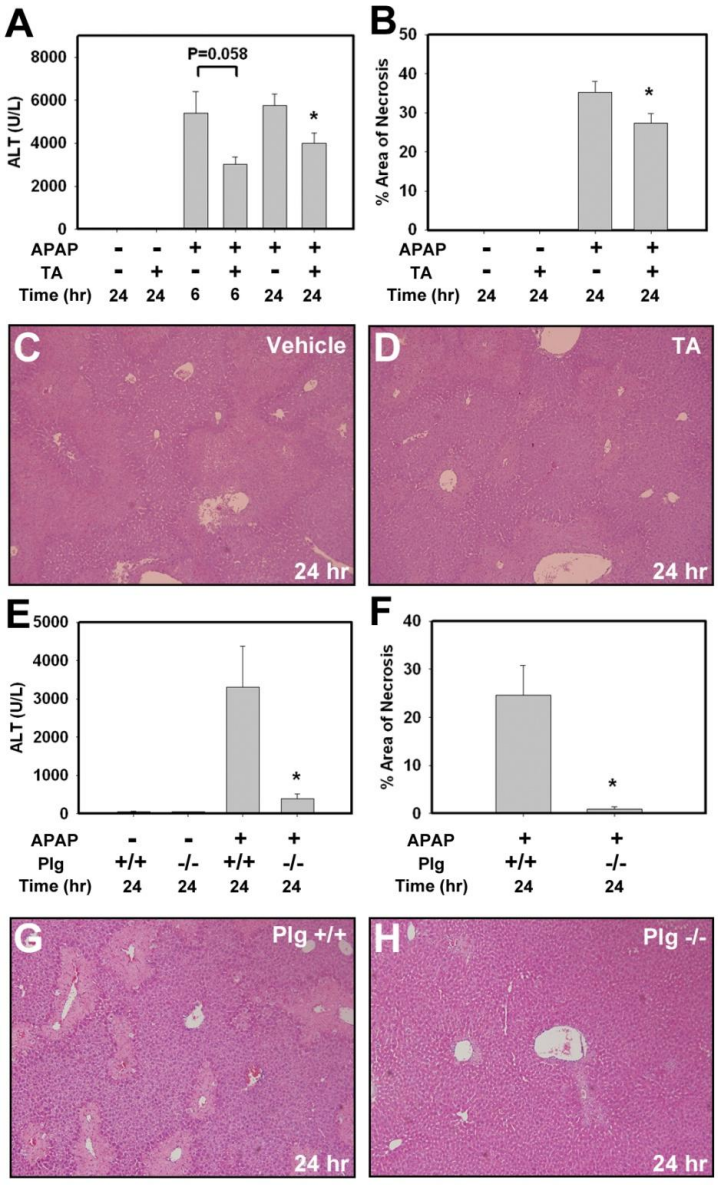

Figure 6.5: Inhibition of plasminogen activation and complete plasminogen deficiency reduces APAP-induced liver injury.

(A-D) Fasted wild type mice were treated with APAP (300 mg/kg) or vehicle (sterile saline). Two hours later mice were treated with tranexamic acid (600 mg/kg, TA, i.p.) or vehicle (sterile saline). (A) Serum ALT activity was determined 6 and 24 hours after APAP treatment and (B) area of necrosis (see methods) was determined 24 hours after APAP treatment. Data are expressed as mean ± SEM. *Significantly

different from APAP treated mice given saline vehicle at that time ($p<0.05$). (C-D) Representative photomicrographs of hematoxylin and eosin stained liver sections from mice treated with APAP for 24 hours and treated with (C) vehicle (saline) or (D) TA. (E-H) Fasted wild type ($Plg^{+/+}$) or plasminogen deficient ($Plg^{-/-}$) mice were treated with APAP (300 mg/kg) or vehicle (sterile saline) and samples were collected 24 hours later. (E) Serum ALT activity and (F) area of necrosis (see methods) were determined. Data are expressed as mean ±SEM. *Significantly different from APAP treated $Plg^{+/+}$ mice ($p<0.05$). (G-H) Representative photomicrographs of hematoxylin and eosin stained liver sections from APAP-treated (G) $Plg^{+/+}$ or (H) $Plg^{-/-}$ mice 24 hours after APAP treatment. n=3-10 mice per group.

Figure 6.6

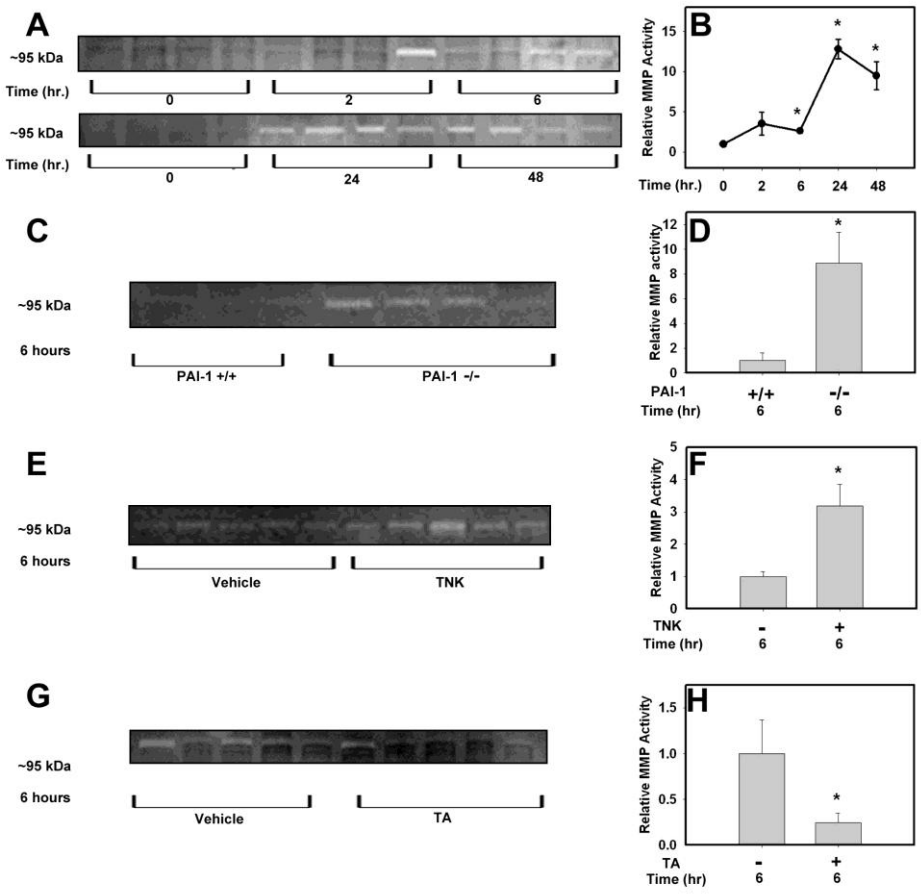

Figure 6.6: Role of the plasminogen activators in MMP-9 activation in APAP-treated mice.

(A, C, E, G) Represenative zymogram images (~95 kDa) and (B, D, F, H) respective zymogram quantification from liver homogenates of APAP-treated mice. (A-B) Gelatinase activity was determined from homogenates of APAP-treated wild type mice various times after APAP treatment. (C-H) Gelatinase activity was determined at 6 hours in liver homogenates from (C-D) PAI-$1^{+/+}$ and PAI-$1^{-/-}$ mice, (E-F) wild type mice treated with TNK or vehicle, and (G-H) wild type mice treated with TA or vehicle. Data is expressed as mean ± SEM. *Significantly different from respective control mice ($p<0.05$). n=3-5 mice per group.

Figure 6.7

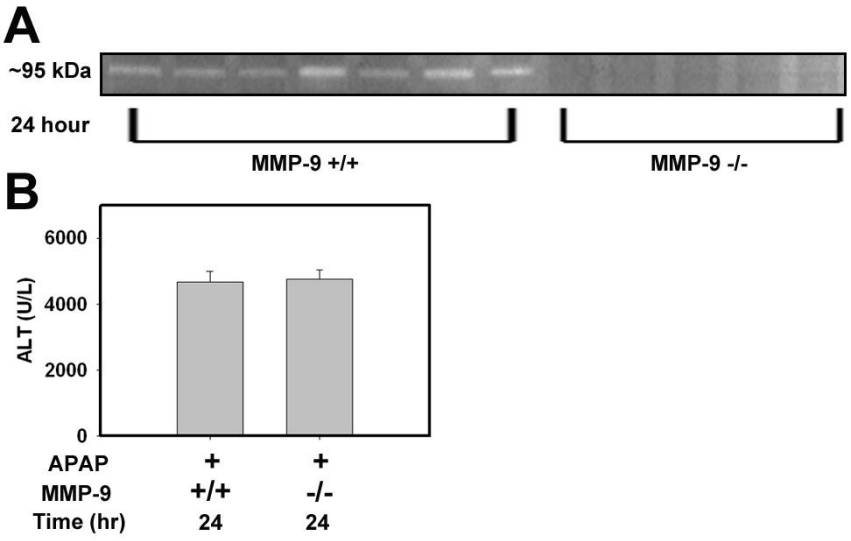

Figure 6.7: MMP-9 deficiency does not protect against APAP-induced liver injury.

Fasted wild type (MMP-$9^{+/+}$) and MMP-9-deficient (MMP-$9^{-/-}$) mice were treated with APAP (300 mg/kg) and samples were collected 24 hours later. (A) Representative gelatin zymogram (~95 kDa) from liver homogenates of APAP-treated MMP-$9^{+/+}$ or MMP-$9^{-/-}$ mice 24 hours after APAP treatment. (B) Serum ALT activity was determined 24 hours after APAP treatment. n=5-9 mice per group.

6.7 Supplemental Figures

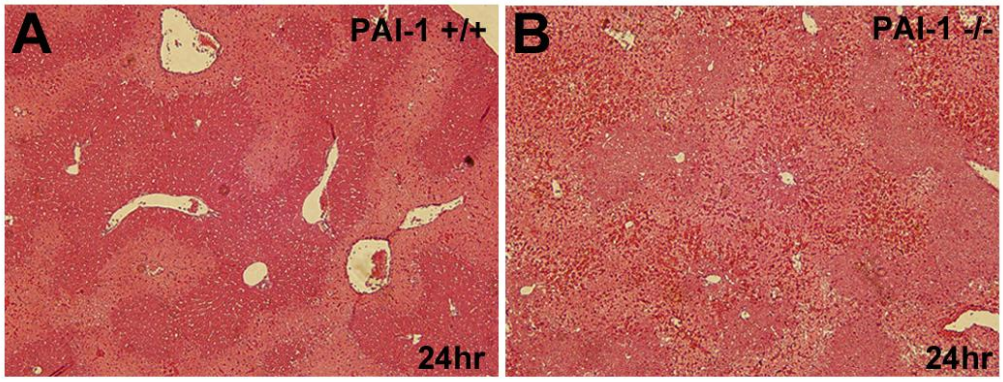

Supplemental Figure 6.1: PAI-1 deficiency enhances hepatic hemorrhage in APAP-treated mice.

Fasted wild type or PAI-$1^{-/-}$ mice were treated with APAP (300 mg/kg) and samples were collected 24 hours later. Representative photomicrographs of hematoxylin and eosin stained liver sections from (A) wild type and (B) PAI-$1^{-/-}$ mice.

Chapter 7

Conclusions and Discussion

Summary

In this dissertation several components of the blood coagulation cascade were evaluated in two different models of hepatotoxicity initiated in separate zones of the liver lobule. Insofar as fibrin is a classical downstream end product of coagulation cascade activation and is known to be present in liver injury induced by several models of acute liver injury, we explored the role of fibrionogen and fibrin in APAP- and ANIT-induced liver injuries. Furthermore, as thrombin is generated in ANIT-induced hepatotoxicity, we evaluated the role of the thrombin receptors PAR-1 and PAR-4 in the acute ANIT-induced liver injury model. Additionally, as fibrosis develops in response to chronic injury, we evaluated mechanisms of liver fibrosis induced by TF and PAR-1 in the chronic model of BDEC injury elicited by ANIT. Insofar as PAI-1 is protective in APAP-induced liver injury in mice we evaluated the role of several components of the fibrinolytic pathway in the development of liver injury.

Coagulation in ANIT-induced liver injury.

In the first set of studies we evaluated the role of platelets in acute ANIT-induced hepatotoxicity as platelets were shown to be protective in early BDL (12 hours) and ANIT-induced hepatotoxicity (24 hours) (Bailie et al., 1994; Laschke et al., 2008). This led us to test the hypothesis that inhibition of platelets could protect mice against acute ANIT-induced hepatotoxicity. In contrast to these previously published results, mice depleted of platelets had increased liver injury as assessed by serum ALT levels 24 hours after ANIT treatment and this was associated with marked pooling of blood in areas of necrosis (see Ch.2). Furthermore, limiting platelet activation at the thrombin receptor on platelets both by PAR-4-deficiency and by pretreating mice with a pharmacological inhibitor of PAR-4 increased liver injury and was associated with hepatic pooling of blood 24 hours after ANIT administration (see Ch. 3). These results strongly suggest that platelets provide essential hemostatic function and protection in mice against early ANIT-induced liver injury. This unique lesion was not reported in rats depleted of platelets and given ANIT, nor did rats have increased injury at the 24 hour time point (Bailie et al., 1994). As this pooling of blood is a rather rare pathological lesion, it would be interesting to identify the mechanisms between these two species during ANIT-induced liver injury and whether this lesion can occur in human

patients with cholestasis having certain genetic predispositions. Next, we further evaluated the role of platelets at a later time point in ANIT-induced liver injury. Surprisingly, in direct contrast to the early 24 hour time point, mice depleted of platelets actually had reduced liver injury 48 hours after ANIT administration compared to control injected animals, although pooling of blood was still evident at this time (see Ch. 2). Similarly, liver injury in PAR-4-deficient mice did not further progress after 24 hours, while liver injury in wild type mice continued to develop and surpassed their PAR-4-deficient counterparts by 48 hours after ANIT treatment (see Ch. 3). Additionally, mice treated with ANIT and then given a PAR-4 inhibitor 8 and 24 hours later had reduced liver injury at 48 hours, which was not associated with pooling of blood in the areas of necrosis (see Ch. 3). Finally, we found that mice given clopidogrel, an inhibitor of platelet activation, had reduced liver injury 48 hours after ANIT administration (see Ch. 2).

Taken together this series of experiments clearly identifies platelets having a biphasic role in cholestatic induced liver injury in mice. Further evidence supporting a biphasic role for platelets in cholestatic liver injury is the fact that platelet depletion is protective against early liver injury after BDL, but fibrosis is enhanced by this same treatment in response to chronic injury (Laschke et al., 2008; Kodama et al., 2010). Interestingly, protection afforded by platelet depletion in BDL (Laschke et al., 2008) and clopidogrel treatment in ANIT (see Ch. 2) was associated with a reduction in hepatic meloperoxidase levels, a marker of neutrophil activation. Of importance, as neutrophils promote chloestatic-induced liver injury, this suggests a mechanism whereby platelets may promote the progression of liver injury at later time points in cholestatic induced liver injury. If fibrosis is excessive in certain patient populations, stimulating platelet production or other types of platelet replacement therapy could protect these patients from liver fibrosis and maybe cirrhosis, although, the potential antifibrotic properties afforded by this type of therapy could be negated by increased liver injury as platelets seem to play a protective role in the acute phase of cholestatic liver injury.

It is interesting to note that TF-deficiency protected mice against ANIT-induced hepatotoxicity at both 24 and 48 hours, and was not associated with pooling of blood in the liver (Luyendyk et al., 2009).

Of importance, fibrinogen deficiency did not cause severe hepatic hemorrhage after ANIT-induced toxicity further suggesting a fibrin-independent mechanism for platelets preventing peliosis during ANIT-induced hepatotoxicity (see Ch. 3). As TF-deficiency did not precipitate the pooling of blood within the liver lesion of necrosis, this suggests that platelet activation at these times is not TF-dependent in this model. Of importance, several other activators of PAR-4 have been found including the fibrinolytic enzyme plasmin and cathepsin G, a protease found in neutrophils (Sambrano et al., 2000; Quinton et al., 2004). As, PAI-1-deficient mice have increase uPA and tPA activity and were protected from excess hepatic ECM deposition, this could suggest that increased plasmin activity generated by increased uPA and tPA activity could protect these mice from fibrosis through PAR-4 activation on platelets (Bergheim et al., 2006). Further experiments are needed to identify how platelets are activated during cholestasis and how they contribute to cholestatic-induced liver injury.

Another mechanism whereby TF could promote ANIT-induced liver injury is through the deposition of hepatic fibrin. In this dissertation we found that fibrinogen deficiency decreased acute liver injury as assessed by area of necrosis after ANIT treatment (see Ch. 3). This could suggest that the protection afforded by TF-deficiency in acute ANIT-induced liver injury was by limiting fibrin deposition within the injured liver. This is in complete contrast to what has been reported in the chronic model of ANIT-induced hepatotoxicity, where fibrinogen deficiency worsens liver injury and fibrosis (Luyendyk et al., 2011a). Interestingly, fibrinogen deficiency did not affect serum bile acid levels in the acute model (see Ch. 3), whereas bile acid levels were elevated in the chronic model suggesting that fibrinogen or fibrin might play a role in preventing cholestasis during chronic BDEC injury (Luyendyk et al., 2011a). Insofar as patients with end stage liver disease initiated by chronic cholestasis typically have a reduced capacity to produce fibrinogen, are generally considered to be at risk of bleeding, and also have enhanced fibrinolytic capacity (Mammen, 1992; Kerr, 2003; Bernal et al., 2010), this could suggest that recombinant fibrinogen or plasma replacement therapy could provide a beneficial response to patients with end stage liver disease to prevent cholestasis, fibrosis, and hemorrhage.

Another way that TF could contribute to ANIT-induced liver injury is through PAR-1 activation. Although PAR-1 contributes to liver injury in several models of liver injury (Rondeau et al., 2001; Fiorucci et al., 2004; Martinelli et al., 2008; Rullier et al., 2008; Luyendyk et al., 2010), PAR-1 deficiency did not affect the acute hepatotoxicity of ANIT (see Ch. 3). Insofar as previous studies have shown that PAR-1 contributes to the development of liver fibrosis in carbon tetrachloride-induced hepatotoxicity (Rullier et al., 2008), we tested the hypothesis that PAR-1 could promote biliary fibrosis in chronic ANIT-induced BDEC injury. Several studies have identified a role for PAR-1 on the activation of stellate cells, a major profibrotic cell type that contributes to liver fibrosis (Gaca et al., 2002; Fiorucci et al., 2004; Friedman, 2008). Additionally, PAR-1 activation has been suggested to contribute to fibrosis by regulating the αVβ6 integrin, a cellular receptor known to promote fibrosis by activating latent TGF-β, a potent profibrotic cytokine (Munger et al., 1999; Jenkins et al., 2006). In both biliary atresia and BDL models of cholestatic induced liver injury, induction of αVβ6 protein on BDECs is thought to contribute to the pathogenesis of liver injury by increasing the levels of local TGF-β signaling and promoting biliary fibrosis through ECM synthesis (Wang et al., 2007a; Nadler et al., 2009). In the studies of Chapter 4 we found that both TF- and PAR-1-deficiency reduced chronic ANIT-induced fibrosis. This led us to test the hypothesis that TF-dependent coagulation and subsequent PAR-1 activation contributed to liver BDEC injury and fibrosis by regulating the expression of the αVβ6 integrin. In these studies we found that hepatic induction of Itgb6 mRNA was dependent on both TF and PAR-1, which was essential for the expression of αVβ6 integrin on BDECs and the development of ANIT-induced biliary fibrosis. Further evaluation of the role of PAR-1 on BDECs *in vitro*, showed that PAR-1 stimulation alone could not alter Itgb6 mRNA expression in human transformed BDECs or primary rat BDECs. However, co-stimulation of BDECs with agonists of PAR-1 and TGF-β1, a known molecule that promotes Itgb6 expression, dramatically enhanced the expression of this gene. This suggests that while PAR-1 signaling does not regulate liver injury in acute BDEC injury, TF-dependent thrombin signaling can alter local profibrogenic signals, which contributes to disease progression. In line with this hypothesis, we found that PAR-1-

dependent signaling on BDECs also contributed to MCP-1 expression, an important proinflammatory cytokine that contributes to liver fibrosis in cholestatic liver injury (see Ch.4) (Harada et al., 2011; Baeck et al., 2012). Of importance, these studies are the first to identify that PAR-1 signaling on BDECs can contribute to the pathogenesis of liver disease by promoting fibrosis through induction of αVβ6 integrin expression. Furthermore, these studies identify that TF-dependent PAR-1 signaling can directly modify the local profibrotic response during chronic BDEC injury. Identifying ways to selectively inhibit PAR-1 and αVβ6 integrin on BDECs could help slow the development of liver fibrosis and prevent cirrhosis in patients with chronic cholestasis.

Coagulation in APAP-induced hepatotoxicity

Altered hemostasis is seen in patients presenting with APAP overdose and several of these coagulation factor changes are also represented in a mouse model of APAP-induced hepatotoxicity. Of importance, TF-dependent coagulation promotes liver injury in the mouse model of APAP hepatotoxicity, potentially through PAR-1 activation as both TF and PAR-1-deficient mice were protected against APAP-induced hepatotoxicity (Ganey et al., 2007). Hepatic fibrin deposition is also known to occur during APAP-induced hepatotoxicity (Ganey et al., 2007), while deficiency in PAI-1, the main inhibitor of fibrinolysis, makes liver injury and sinusoidal hemorrhage more severe, suggesting a protective effect for hepatic fibrin in this model (Bajt et al., 2008). This led us to test the hypothesis in Chapter 6 that hepatic fibrin deposition protects against APAP-induced liver injury. Using both genetic and pharmacologic strategies, we found that both fibrinogen and fibrin did not contribute to APAP-induced liver injury out to 24 hours, a time associated with peak injury in our model. However, we found that enhancing plasminogen activator activity by giving recombinant tPA (tenecteplase) recapitulated the liver injury and hemorrhage seen in PAI-1-deficient mice leading us to investigate fibrin-independent roles of plasmin in this model. In agreement with these studies, both complete genetic deficiency and pharmacologic inhibition of plasmin in wild type mice by tranexamic acid reduced APAP-induced liver injury.

Tranexamic acid is an inexpensive drug already on the market in the United States for several indications and could easily be repurposed to help limit liver injury in patients suffering from APAP-induced hepatotoxicity. Of importance, the time course of tranexamic acid administration in our mouse model is in a similar time frame of when a human patient might come into the clinic. Most admissions to the emergency room are after the onset of liver injury, but prior to the peak of liver injury. In this proof of principle study we gave mice tranexamic acid 2 hours after APAP by i.p. injection, a time at the onset of liver injury, but prior to peak injury. We did not explore the pharmacokinetics of tranexamic acid in this model, and in human patients the t_{max} could be accelerated by administering this drug by i.v. in combination with N-acetylcistein, the current gold standard therapy for APAP poisoning. Furthermore, as patients suffering from APAP overdose are also at risk of bleeding, tranexamic acid might help prevent lethal bleeding events by temporarily stabilizing blood clots in these patients until coagulation factor levels have recovered.

Additionally, the role of the plasmin system has also been shown to contribute to liver regeneration in several models of liver injury. We have not evaluated the role of the plasminogen activators or plasmin in the recovery phase of APAP-induced hepatotoxicity. However, increased plasminogen activator activity has been shown to promote recovery after acute carbon tetrachloride-induced liver injury (Shanmukhappa et al., 2006; Hsiao et al., 2008). As, liver recovery and regeneration is of key importance to patients suffering from APAP-toxicity, targeting these enzymes could lead to decreased hospitalization times by promoting liver regeneration. However, if the function of these enzymes mimic the resolution phase of carbon tetrachloride-induced liver injury and accelerate hepatic recovery, extreme caution would have to be applied when assessing therapeutic targets for APAP-hepatotoxicity as increased plasminogen activator activity promotes liver injury and hemorrhage in the development of early APAP-induced liver injury.

Take home message

In summary, the coagulation cascade is a highly dynamic and regulated pathway that contributes to liver injury through various mechanisms which seem to be model dependent. For example, PAR-1 protects against early APAP-induced liver injury whereas it does not affect acute ANIT-induced BDEC injury. On the contrary, fibrinogen protects against acute BDEC injury whereas this protein does not contribute to acute injury development in APAP-toxicity and worsens biliary fibrosis elicited by chronic ANIT-induced BDEC injury. Interestingly, PAI-1 seems to serve a protective role in APAP-induced liver injury whereas this protein promotes liver injury after BDL. The mechanisms whereby PAI-1 contributes to liver injury in these two models of liver injury are not known, but could involve plasmin and the plasminogen activators as these proteins have been shown to be involved in liver regeneration.

Similarly, dual roles for platelets via the thrombin receptor can also be drawn in ANIT-induced cholestatic liver injury. Our data suggest that in the acute ANIT model of BDEC injury platelets protect against early injury in mice, whereas they serve a protective role in the progression stage of acute liver injury. Interestingly, platelets also protect against BLD-induced liver fibrosis, suggesting a more complex and possibly biphasic role for thrombocytes in the development of cholestatic-induced liver injury. Interestingly, APAP hepatotoxicity is also associated with thrombocytopenia and several molecules known to inhibit platelets also inhibit injury in APAP-induced hepatotoxicity. However, a direct investigation on the role of platelets in APAP-induced hepatotoxicity has not been performed. Furthermore, as both patients suffering from APAP poisoning and end stage liver cirrhosis are at risk of bleeding, platelet therapy might reduce the risk of spontaneous bleeding events in these patients.

While several models have shown roles for one or more coagulation factors in liver injury, there is a lack of comprehensive understanding on the mechanisms whereby these factors participate in liver injury and disease. Additionally, several liver injury models have shown that components of the coagulation cascade contribute to liver injury in a model-dependent fashion. Furthermore, individual coagulation factors reviewed and tested within this dissertation seem to have differential and sometimes opposing effects within the same model at different phases of the injury process. A systematic approach

looking at the role of individual coagulation factors during these phases within each model could provide a more accurate and encompasing understanding of how these factors contribute to liver injury. Understanding how each of these factors contributes to the orchestra of liver injury and regeneration could help reveal new therapeutic targets to prevent liver injury and promote liver repair and regeneration in human patients.

References

Abdel-Salam OM, Baiuomy AR, Ameen A and Hassan NS (2005) A study of unfractionated and low molecular weight heparins in a model of cholestatic liver injury in the rat. *Pharmacol Res* **51**:59-67.

Abildgaard U (1969) Inhibition of the thrombin-fibrinogen reaction by alpha2-macroglobulin, studied by N-terminal analysis. *Thromb Diath Haemorrh* **21**:173-180.

Abildgaard U, Odegard OR, Kierulf P and Pepper DS (1974) Influence of platelet factor 4 on inhibited thrombin substrate reactions. *Thromb Res* **5**:185-196.

Anisfeld AM, Kast-Woelbern HR, Lee H, Zhang Y, Lee FY and Edwards PA (2005) Activation of the nuclear receptor FXR induces fibrinogen expression: a new role for bile acid signaling. *J Lipid Res* **46**:458-468.

Ansell J, Hirsh J, Hylek E, Jacobson A, Crowther M and Palareti G (2008) Pharmacology and management of the vitamin K antagonists: American College of Chest Physicians Evidence-Based Clinical Practice Guidelines (8th Edition). *Chest* **133**:160S-198S.

Anstee QM, Goldin RD, Wright M, Martinelli A, Cox R and Thursz MR (2008) Coagulation status modulates murine hepatic fibrogenesis: implications for the development of novel therapies. *J Thromb Haemost* **6**:1336-1343.

Bach RR (2006) Tissue factor encryption. *Arterioscler Thromb Vasc Biol* **26**:456-461.

Baeck C, Wehr A, Karlmark KR, Heymann F, Vucur M, Gassler N, Huss S, Klussmann S, Eulberg D, Luedde T, Trautwein C and Tacke F (2012) Pharmacological inhibition of the chemokine CCL2 (MCP-1) diminishes liver macrophage infiltration and steatohepatitis in chronic hepatic injury. *Gut* **61**:416-426.

Bagchus WM, Jeunink MF, Rozing J and Elema JD (1989) A monoclonal antibody against rat platelets. I. Tissue distribution in vitro and in vivo. *Clin Exp Immunol* **75**:317-323.

Bailie MB, Mullaney TP and Roth RA (1993) Characterization of acute 4,4'-methylene dianiline hepatotoxicity in the rat. *Environ Health Perspect* **101**:130-133.

Bailie MB, Pearson JM, Lappin PB, Killam AL and Roth RA (1994) Platelets and alpha-naphthylisothiocyanate-induced liver injury. *Toxicol Appl Pharmacol* **129**:207-213.

Bain J, Plater L, Elliott M, Shpiro N, Hastie CJ, McLauchlan H, Klevernic I, Arthur JS, Alessi DR and Cohen P (2007) The selectivity of protein kinase inhibitors: a further update. *Biochem J* **408**:297-315.

Bajt ML, Yan HM, Farhood A and Jaeschke H (2008) Plasminogen activator inhibitor-1 limits liver injury and facilitates regeneration after acetaminophen overdose. *Toxicol Sci* **104**:419-427.

Bari K and Garcia-Tsao G (2012) Treatment of portal hypertension. *World J Gastroenterol* **18**:1166-1175.

Bataller R and Brenner DA (2005) Liver fibrosis. *J Clin Invest* **115**:209-218.

Becker BA and Plaa GL (1965) The nature of alpha-naphthylisothiocyanate-induced cholestasis. *Toxicol Appl Pharmacol* **7**:680-685.

Belovejdov V, Staribratova D and Dikov D (2008) Microscopic peliosis of pancreatic islets associated with thrombotic thrombocytopenic purpura. *Pathol Oncol Res* **14**:205-208.

Bergheim I, Guo L, Davis MA, Duveau I and Arteel GE (2006) Critical role of plasminogen activator inhibitor-1 in cholestatic liver injury and fibrosis. *J Pharmacol Exp Ther* **316**:592-600.

Bernal W, Auzinger G, Dhawan A and Wendon J (2010) Acute liver failure. *Lancet* **376**:190-201.

Bezerra JA, Bugge TH, Melin-Aldana H, Sabla G, Kombrinck KW, Witte DP and Degen JL (1999) Plasminogen deficiency leads to impaired remodeling after a toxic injury to the liver. *Proc Natl Acad Sci U S A* **96**:15143-15148.

Bhandari BM, Bayat H and Rothstein KD (2011) Primary biliary cirrhosis. *Gastroenterol Clin North Am* **40**:373-386, viii.

Biagini MR, Tozzi A, Marcucci R, Paniccia R, Fedi S, Milani S, Galli A, Ceni E, Capanni M, Manta R, Abbate R and Surrenti C (2006) Hyperhomocysteinemia and hypercoagulability in primary biliary cirrhosis. *World J Gastroenterol* **12**:1607-1612.

Blackford MG, Felter T, Gothard MD and Reed MD (2011) Assessment of the clinical use of intravenous and oral N-acetylcysteine in the treatment of acute acetaminophen poisoning in children: a retrospective review. *Clin Ther* **33**:1322-1330.

Blackhart BD, Emilsson K, Nguyen D, Teng W, Martelli AJ, Nystedt S, Sundelin J and Scarborough RM (1996) Ligand cross-reactivity within the protease-activated receptor family. *J Biol Chem* **271**:16466-16471.

Bootle-Wilbraham CA, Tazzyman S, Thompson WD, Stirk CM and Lewis CE (2001) Fibrin fragment E stimulates the proliferation, migration and differentiation of human microvascular endothelial cells in vitro. *Angiogenesis* **4**:269-275.

Borensztajn K and Spek CA (2011) Blood coagulation factor Xa as an emerging drug target. *Expert Opin Ther Targets* **15**:341-349.

Bougie DW, Nayak D, Boylan B, Newman PJ and Aster RH (2010) Drug-dependent clearance of human platelets in the NOD/scid mouse by antibodies from patients with drug-induced immune thrombocytopenia. *Blood* **116**:3033-3038.

Braet F, De Zanger R, Baekeland M, Crabbe E, Van Der Smissen P and Wisse E (1995) Structure and dynamics of the fenestrae-associated cytoskeleton of rat liver sinusoidal endothelial cells. *Hepatology* **21**:180-189.

Breuss JM, Gallo J, DeLisser HM, Klimanskaya IV, Folkesson HG, Pittet JF, Nishimura SL, Aldape K, Landers DV, Carpenter W and et al. (1995) Expression of the beta 6 integrin subunit in development, neoplasia and tissue repair suggests a role in epithelial remodeling. *J Cell Sci* **108 (Pt 6)**:2241-2251.

Brown PH, Alani R, Preis LH, Szabo E and Birrer MJ (1993) Suppression of oncogene-induced transformation by a deletion mutant of c-jun. *Oncogene* **8**:877-886.

Brown PH, Chen TK and Birrer MJ (1994) Mechanism of action of a dominant-negative mutant of c-Jun. *Oncogene* **9**:791-799.

Carthew P and Smith AG (1994) Pathological mechanisms of hepatic tumour formation in rats exposed chronically to dietary hexachlorobenzene. *J Appl Toxicol* **14**:447-452.

Casarett LJ, Doull J and Klaassen CD (2008) *Casarett and Doull's toxicology : the basic science of poisons*. McGraw-Hill, New York.

Cavar I, Kelava T, Heinzel R and Culo F (2009) The role of prostacyclin in modifying acute hepatotoxicity of acetaminophen in mice. *Coll Antropol* **33 Suppl 2**:25-29.

Chan JC, Duszczyszyn DA, Castellino FJ and Ploplis VA (2001) Accelerated skin wound healing in plasminogen activator inhibitor-1-deficient mice. *Am J Pathol* **159**:1681-1688.

Chun LJ, Tong MJ, Busuttil RW and Hiatt JR (2009) Acetaminophen hepatotoxicity and acute liver failure. *J Clin Gastroenterol* **43**:342-349.

Copple BL, Banes A, Ganey PE and Roth RA (2002a) Endothelial cell injury and fibrin deposition in rat liver after monocrotaline exposure. *Toxicol Sci* **65**:309-318.

Copple BL, Moulin F, Hanumegowda UM, Ganey PE and Roth RA (2003) Thrombin and protease-activated receptor-1 agonists promote lipopolysaccharide-induced hepatocellular injury in perfused livers. *J Pharmacol Exp Ther* **305**:417-425.

Copple BL, Roth RA and Ganey PE (2006) Anticoagulation and inhibition of nitric oxide synthase influence hepatic hypoxia after monocrotaline exposure. *Toxicology* **225**:128-137.

Copple BL, Woolley B, Banes A, Ganey PE and Roth RA (2002b) Anticoagulants prevent monocrotaline-induced hepatic parenchymal cell injury but not endothelial cell injury in the rat. *Toxicol Appl Pharmacol* **180**:186-196.

Coughlin SR (1999) How the protease thrombin talks to cells. *Proc Natl Acad Sci U S A* **96**:11023-11027.

Coussens LM, Yokoyama K and Chiu R (1994) Transforming growth factor beta 1-mediated induction of junB is selectively inhibited by expression of Ad.12-E1A. *J Cell Physiol* **160**:435-444.

Covic L, Misra M, Badar J, Singh C and Kuliopulos A (2002) Pepducin-based intervention of thrombin-receptor signaling and systemic platelet activation. *Nat Med* **8**:1161-1165.

Crawford SE, Stellmach V, Murphy-Ullrich JE, Ribeiro SM, Lawler J, Hynes RO, Boivin GP and Bouck N (1998) Thrombospondin-1 is a major activator of TGF-beta1 in vivo. *Cell* **93**:1159-1170.

Dahm LJ, Schultze AE and Roth RA (1991) An antibody to neutrophils attenuates alpha-naphthylisothiocyanate-induced liver injury. *J Pharmacol Exp Ther* **256**:412-420.

DeLeve LD (2007) Hepatic microvasculature in liver injury. *Semin Liver Dis* **27**:390-400.

DeLeve LD, Wang X, Kaplowitz N, Shulman HM, Bart JA and van der Hoek A (1997) Sinusoidal endothelial cells as a target for acetaminophen toxicity. Direct action versus requirement for hepatocyte activation in different mouse strains. *Biochem Pharmacol* **53**:1339-1345.

Deng X, Luyendyk JP, Ganey PE and Roth RA (2009) Inflammatory stress and idiosyncratic hepatotoxicity: hints from animal models. *Pharmacol Rev* **61**:262-282.

Derynck R and Zhang YE (2003) Smad-dependent and Smad-independent pathways in TGF-beta family signalling. *Nature* **425**:577-584.

Dietrich CG, Ottenhoff R, de Waart DR and Oude Elferink RP (2001) Role of MRP2 and GSH in intrahepatic cycling of toxins. *Toxicology* **167**:73-81.

Divald A, Ujhelyi E, Jeney A, Lapis K and Institoris L (1985) Hepatoprotective effects of prostacyclins on CCl4-induced liver injury in rats. *Exp Mol Pathol* **42**:163-166.

Dorfleutner A, Hintermann E, Tarui T, Takada Y and Ruf W (2004) Cross-talk of integrin alpha3beta1 and tissue factor in cell migration. *Mol Biol Cell* **15**:4416-4425.

Drake TA, Morrissey JH and Edgington TS (1989) Selective cellular expression of tissue factor in human tissues. Implications for disorders of hemostasis and thrombosis. *Am J Pathol* **134**:1087-1097.

Dranoff JA and Wells RG (2010) Portal fibroblasts: Underappreciated mediators of biliary fibrosis. *Hepatology* **51**:1438-1444.

Edlund S, Bu S, Schuster N, Aspenstrom P, Heuchel R, Heldin NE, ten Dijke P, Heldin CH and Landstrom M (2003) Transforming growth factor-beta1 (TGF-beta)-induced apoptosis of prostate cancer cells involves Smad7-dependent activation of p38 by TGF-beta-activated kinase 1 and mitogen-activated protein kinase kinase 3. *Mol Biol Cell* **14**:529-544.

Eltzschig HK and Eckle T (2011) Ischemia and reperfusion--from mechanism to translation. *Nat Med* **17**:1391-1401.

Ewart MR, Hatton M, Basford JM and Dodgson KS (1969) The proteolytic action of arvin on human fibrinogen. *Biochem J* **115**:17P.

Fiorucci S, Antonelli E, Distrutti E, Severino B, Fiorentina R, Baldoni M, Caliendo G, Santagada V, Morelli A and Cirino G (2004) PAR1 antagonism protects against experimental liver fibrosis. Role of proteinase receptors in stellate cell activation. *Hepatology* **39**:365-375.

Fischereder M and Jaffe JP (1994) Thrombocytopenia following acute acetaminophen overdose. *Am J Hematol* **45**:258-259.

Flick MJ, Du X, Witte DP, Jirouskova M, Soloviev DA, Busuttil SJ, Plow EF and Degen JL (2004) Leukocyte engagement of fibrin(ogen) via the integrin receptor alphaMbeta2/Mac-1 is critical for host inflammatory response in vivo. *J Clin Invest* **113**:1596-1606.

Friedman SL (2008) Mechanisms of hepatic fibrogenesis. *Gastroenterology* **134**:1655-1669.

Fujiwara K, Ogata I, Ohta Y, Hirata K, Oka Y, Yamada S, Sato Y, Masaki N and Oka H (1988) Intravascular coagulation in acute liver failure in rats and its treatment with antithrombin III. *Gut* **29**:1103-1108.

Gaca MD, Zhou X and Benyon RC (2002) Regulation of hepatic stellate cell proliferation and collagen synthesis by proteinase-activated receptors. *J Hepatol* **36**:362-369.

Ganey PE, Luyendyk JP, Newport SW, Eagle TM, Maddox JF, Mackman N and Roth RA (2007) Role of the coagulation system in acetaminophen-induced hepatotoxicity in mice. *Hepatology* **46**:1177-1186.

Gazzard BG, Henderson JM and Williams R (1975) Early changes in coagulation following a paracetamol overdose and a controlled trial of fresh frozen plasma therapy. *Gut* **16**:617-620.

Gillibert-Duplantier J, Neaud V, Blanc JF, Bioulac-Sage P and Rosenbaum J (2007) Thrombin inhibits migration of human hepatic myofibroblasts. *Am J Physiol Gastrointest Liver Physiol* **293**:G128-136.

Giouleme O, Karabatsou S, Hytiroglou P, Xanthis A, Tsiaousi E, Katsaros M and Koliouskas D (2011) 4,4'-Methylenedianiline-induced hepatitis in an industrial worker: case report and review of the literature. *Hum Exp Toxicol* **30**:762-767.

Gismondi C, Dabove L, Dovi M, Picciotto A, Savarino V, Testa R and Mansi C (1980) [Hepatotoxicity of cyclophosphamide in the rat after prolonged treatment: a histomorphological study]. *Boll Soc Ital Biol Sper* **56**:2166-2172.

Glaser SS, Gaudio E, Miller T, Alvaro D and Alpini G (2009) Cholangiocyte proliferation and liver fibrosis. *Expert Rev Mol Med* **11**:e7.

Glaser SS, Onori P, Wise C, Yang F, Marzioni M, Alvaro D, Franchitto A, Mancinelli R, Alpini G, Munshi MK and Gaudio E (2010) Recent advances in the regulation of cholangiocyte proliferation and function during extrahepatic cholestasis. *Dig Liver Dis* **42**:245-252.

Gong Y, Hart E, Shchurin A and Hoover-Plow J (2008) Inflammatory macrophage migration requires MMP-9 activation by plasminogen in mice. *J Clin Invest* **118**:3012-3024.

Gressner AM and Weiskirchen R (2006) Modern pathogenetic concepts of liver fibrosis suggest stellate cells and TGF-beta as major players and therapeutic targets. *J Cell Mol Med* **10**:76-99.

Grypioti AD, Theocharis SE, Demopoulos CA, Papadopoulou-Daifoti Z, Basayiannis AC and Mykoniatis MG (2006) Effect of platelet-activating factor (PAF) receptor antagonist (BN52021) on acetaminophen-induced acute liver injury and regeneration in rats. *Liver Int* **26**:97-105.

Gujral JS, Farhood A, Bajt ML and Jaeschke H (2003) Neutrophils aggravate acute liver injury during obstructive cholestasis in bile duct-ligated mice. *Hepatology* **38**:355-363.

Gut I, Danielova V, Holubova J, Soucek P and Kluckova H (2000) Cytotoxicity of cyclophosphamide, paclitaxel, and docetaxel for tumor cell lines in vitro: effects of concentration, time and cytochrome P450-catalyzed metabolism. *Arch Toxicol* **74**:437-446.

Habeebu SS, Liu J and Klaassen CD (1998) Cadmium-induced apoptosis in mouse liver. *Toxicol Appl Pharmacol* **149**:203-209.

Hahm K, Lukashev ME, Luo Y, Yang WJ, Dolinski BM, Weinreb PH, Simon KJ, Chun Wang L, Leone DR, Lobb RR, McCrann DJ, Allaire NE, Horan GS, Fogo A, Kalluri R, Shield CF, 3rd, Sheppard D, Gardner HA and Violette SM (2007) Alphav beta6 integrin regulates renal fibrosis and inflammation in Alport mouse. *Am J Pathol* **170**:110-125.

Harada K, Chiba M, Okamura A, Hsu M, Sato Y, Igarashi S, Ren XS, Ikeda H, Ohta H, Kasashima S, Kawashima A and Nakanuma Y (2011) Monocyte chemoattractant protein-1 derived from biliary innate immunity contributes to hepatic fibrogenesis. *J Clin Pathol* **64**:660-665.

Hayward SR, Lucas CE and Ledgerwood AM (1991) Recurrent spontaneous intrahepatic hemorrhage from peliosis hepatis. *Arch Surg* **126**:782-783.

Hisakura K, Murata S, Fukunaga K, Myronovych A, Tadano S, Kawasaki T, Kohno K, Ikeda O, Pak S, Ikeda N, Nakano Y, Matsuo R, Konno K, Kobayashi E, Saito T, Yasue H and Ohkohchi N (2010) Platelets prevent acute liver damage after extended hepatectomy in pigs. *J Hepatobiliary Pancreat Sci* **17**:855-864.

Holmes A, Abraham DJ, Sa S, Shiwen X, Black CM and Leask A (2001) CTGF and SMADs, maintenance of scleroderma phenotype is independent of SMAD signaling. *J Biol Chem* **276**:10594-10601.

Horan GS, Wood S, Ona V, Li DJ, Lukashev ME, Weinreb PH, Simon KJ, Hahm K, Allaire NE, Rinaldi NJ, Goyal J, Feghali-Bostwick CA, Matteson EL, O'Hara C, Lafyatis R, Davis GS, Huang X, Sheppard D and Violette SM (2008) Partial inhibition of integrin alpha(v)beta6 prevents pulmonary fibrosis without exacerbating inflammation. *Am J Respir Crit Care Med* **177**:56-65.

Hsiao Y, Zou T, Ling CC, Hu H, Tao XM and Song HY (2008) Disruption of tissue-type plasminogen activator gene in mice aggravated liver fibrosis. *J Gastroenterol Hepatol* **23**:e258-264.

Humar M, Loop T, Schmidt R, Hoetzel A, Roesslein M, Andriopoulos N, Pahl HL, Geiger KK and Pannen BH (2007) The mitogen-activated protein kinase p38 regulates activator protein 1 by direct phosphorylation of c-Jun. *Int J Biochem Cell Biol* **39**:2278-2288.

Hutzinger O (1980) The Handbook of environmental chemistry, in p v., Springer-Verlag, Berlin ; New York.

Imaeda AB, Watanabe A, Sohail MA, Mahmood S, Mohamadnejad M, Sutterwala FS, Flavell RA and Mehal WZ (2009) Acetaminophen-induced hepatotoxicity in mice is dependent on Tlr9 and the Nalp3 inflammasome. *J Clin Invest* **119**:305-314.

Ionescu AM, Schwarz EM, Zuscik MJ, Drissi H, Puzas JE, Rosier RN and O'Keefe RJ (2003) ATF-2 cooperates with Smad3 to mediate TGF-beta effects on chondrocyte maturation. *Exp Cell Res* **288**:198-207.

Ito Y, Abril ER, Bethea NW and McCuskey RS (2005) Inhibition of matrix metalloproteinases minimizes hepatic microvascular injury in response to acetaminophen in mice. *Toxicol Sci* **83**:190-196.

Iwamoto M (1975) Plasminogen-plasmin system IX. Specific binding of tranexamic acid to plasmin. *Thromb Diath Haemorrh* **33**:573-585.

Jacquot C (1978) [Bioavailability and "first pass" effect of a drug]. *Therapie* **33**:683-697.

Jaeschke H, McGill MR, Williams CD and Ramachandran A (2011) Current issues with acetaminophen hepatotoxicity--a clinically relevant model to test the efficacy of natural products. *Life Sci* **88**:737-745.

Javelaud D and Mauviel A (2005) Crosstalk mechanisms between the mitogen-activated protein kinase pathways and Smad signaling downstream of TGF-beta: implications for carcinogenesis. *Oncogene* **24**:5742-5750.

Jean PA, Bailie MB and Roth RA (1995) 1-naphthylisothiocyanate-induced elevation of biliary glutathione. *Biochem Pharmacol* **49**:197-202.

Jenkins RG, Su X, Su G, Scotton CJ, Camerer E, Laurent GJ, Davis GE, Chambers RC, Matthay MA and Sheppard D (2006) Ligation of protease-activated receptor 1 enhances alpha(v)beta6 integrin-dependent TGF-beta activation and promotes acute lung injury. *J Clin Invest* **116**:1606-1614.

Jesmin S, Gando S, Zaedi S and Sakuraya F (2006) Chronological expression of PAR isoforms in acute liver injury and its amelioration by PAR2 blockade in a rat model of sepsis. *Thromb Haemost* **96**:830-838.

Kahn ML, Zheng YW, Huang W, Bigornia V, Zeng D, Moff S, Farese RV, Jr., Tam C and Coughlin SR (1998) A dual thrombin receptor system for platelet activation. *Nature* **394**:690-694.

Keitel V, Reinehr R, Gatsios P, Rupprecht C, Gorg B, Selbach O, Haussinger D and Kubitz R (2007) The G-protein coupled bile salt receptor TGR5 is expressed in liver sinusoidal endothelial cells. *Hepatology* **45**:695-704.

Kerr R (2003) New insights into haemostasis in liver failure. *Blood Coagul Fibrinolysis* **14 Suppl 1**:S43-45.

Kerr R, Newsome P, Germain L, Thomson E, Dawson P, Stirling D and Ludlam CA (2003) Effects of acute liver injury on blood coagulation. *J Thromb Haemost* **1**:754-759.

Kim ND, Moon JO, Slitt AL and Copple BL (2006) Early growth response factor-1 is critical for cholestatic liver injury. *Toxicol Sci* **90**:586-595.

Knight TR, Kurtz A, Bajt ML, Hinson JA and Jaeschke H (2001) Vascular and hepatocellular peroxynitrite formation during acetaminophen toxicity: role of mitochondrial oxidant stress. *Toxicol Sci* **62**:212-220.

Kodali P, Wu P, Lahiji PA, Brown EJ and Maher JJ (2006) ANIT toxicity toward mouse hepatocytes in vivo is mediated primarily by neutrophils via CD18. *Am J Physiol Gastrointest Liver Physiol* **291**:G355-363.

Kodama T, Takehara T, Hikita H, Shimizu S, Li W, Miyagi T, Hosui A, Tatsumi T, Ishida H, Tadokoro S, Ido A, Tsubouchi H and Hayashi N (2010) Thrombocytopenia exacerbates cholestasis-induced liver fibrosis in mice. *Gastroenterology* **138**:2487-2498, 2498 e2481-2487.

Kolozsvari B, Szijgyarto Z, Bai P, Gergely P, Verin A, Garcia JG and Bako E (2009) Role of calcineurin in thrombin-mediated endothelial cell contraction. *Cytometry A* **75**:405-411.

Kopelman H, Robertson MH, Sanders PG and Ash I (1966) The Epping jaundice. *Br Med J* **1**:514-516.

Kubo M, Van de Water L, Plantefaber LC, Mosesson MW, Simon M, Tonnesen MG, Taichman L and Clark RA (2001) Fibrinogen and fibrin are anti-adhesive for keratinocytes: a mechanism for fibrin eschar slough during wound repair. *J Invest Dermatol* **117**:1369-1381.

Kumar S, McDonnell PC, Gum RJ, Hand AT, Lee JC and Young PR (1997) Novel homologues of CSBP/p38 MAP kinase: activation, substrate specificity and sensitivity to inhibition by pyridinyl imidazoles. *Biochem Biophys Res Commun* **235**:533-538.

Kuroda T and Shiohara E (1996) Leukocyte and platelet depletion protects the liver from damage induced by cholestasis and ischemia-reperfusion in the dog. *Scand J Gastroenterol* **31**:182-190.

Laiho M, Ronnstrand L, Heino J, Decaprio JA, Ludlow JW, Livingston DM and Massague J (1991) Control of junB and extracellular matrix protein expression by transforming growth factor-beta 1 is independent of simian virus 40 T antigen-sensitive growth-sensitive growth-inhibitory events. *Mol Cell Biol* **11**:972-978.

Lang PA, Contaldo C, Georgiev P, El-Badry AM, Recher M, Kurrer M, Cervantes-Barragan L, Ludewig B, Calzascia T, Bolinger B, Merkler D, Odermatt B, Bader M, Graf R, Clavien PA, Hegazy AN, Lohning M, Harris NL, Ohashi PS, Hengartner H, Zinkernagel RM and Lang KS (2008) Aggravation of viral hepatitis by platelet-derived serotonin. *Nat Med* **14**:756-761.

Laschke MW, Dold S, Menger MD, Jeppsson B and Thorlacius H (2008) Platelet-dependent accumulation of leukocytes in sinusoids mediates hepatocellular damage in bile duct ligation-induced cholestasis. *Br J Pharmacol* **153**:148-156.

Legrand C, Polette M, Tournier JM, de Bentzmann S, Huet E, Monteau M and Birembaut P (2001) uPA/plasmin system-mediated MMP-9 activation is implicated in bronchial epithelial cell migration. *Exp Cell Res* **264**:326-336.

Lesage G, Glaser S, Ueno Y, Alvaro D, Baiocchi L, Kanno N, Phinizy JL, Francis H and Alpini G (2001) Regression of cholangiocyte proliferation after cessation of ANIT feeding is coupled with increased apoptosis. *Am J Physiol Gastrointest Liver Physiol* **281**:G182-190.

Lesurtel M, Graf R, Aleil B, Walther DJ, Tian Y, Jochum W, Gachet C, Bader M and Clavien PA (2006) Platelet-derived serotonin mediates liver regeneration. *Science* **312**:104-107.

Levy L and Hill CS (2005) Smad4 dependency defines two classes of transforming growth factor {beta} (TGF-{beta}) target genes and distinguishes TGF-{beta}-induced epithelial-mesenchymal transition from its antiproliferative and migratory responses. *Mol Cell Biol* **25**:8108-8125.

Liboi E, Di Francesco P, Gallinari P, Testa U, Rossi GB and Peschle C (1988) TGF beta induces a sustained c-fos expression associated with stimulation or inhibition of cell growth in EL2 or NIH 3T3 fibroblasts. *Biochem Biophys Res Commun* **151**:298-305.

Lindor KD (2011) New treatment strategies for primary sclerosing cholangitis. *Dig Dis* **29**:113-116.

Lindros KO (1997) Zonation of cytochrome P450 expression, drug metabolism and toxicity in liver. *Gen Pharmacol* **28**:191-196.

Lu JP, Mao JQ, Li MS, Lu SL, Hu XQ, Zhu SN and Nomura S (2003) In situ detection of TGF betas, TGF beta receptor II mRNA and telomerase activity in rat cholangiocarcinogenesis. *World J Gastroenterol* **9**:590-594.

Luo B, Tang L, Wang Z, Zhang J, Ling Y, Feng W, Sun JZ, Stockard CR, Frost AR, Chen YF, Grizzle WE and Fallon MB (2005) Cholangiocyte endothelin 1 and transforming growth factor beta1 production in rat experimental hepatopulmonary syndrome. *Gastroenterology* **129**:682-695.

Lupu C, Westmuckett AD, Peer G, Ivanciu L, Zhu H, Taylor FB, Jr. and Lupu F (2005) Tissue factor-dependent coagulation is preferentially up-regulated within arterial branching areas in a baboon model of Escherichia coli sepsis. *Am J Pathol* **167**:1161-1172.

Luyendyk JP, Cantor GH, Kirchhofer D, Mackman N, Copple BL and Wang R (2009) Tissue factor-dependent coagulation contributes to alpha-naphthylisothiocyanate-induced cholestatic liver injury in mice. *Am J Physiol Gastrointest Liver Physiol* **296**:G840-849.

Luyendyk JP, Kassel KM, Allen K, Guo GL, Li G, Cantor GH and Copple BL (2011a) Fibrinogen deficiency increases liver injury and early growth response-1 (Egr-1) expression in a model of chronic xenobiotic-induced cholestasis. *Am J Pathol* **178**:1117-1125.

Luyendyk JP, Mackman N and Sullivan BP (2011b) Role of fibrinogen and protease-activated receptors in acute xenobiotic-induced cholestatic liver injury. *Toxicol Sci* **119**:233-243.

Luyendyk JP, Maddox JF, Green CD, Ganey PE and Roth RA (2004) Role of hepatic fibrin in idiosyncrasy-like liver injury from lipopolysaccharide-ranitidine coexposure in rats. *Hepatology* **40**:1342-1351.

Luyendyk JP, Sullivan BP, Guo GL and Wang R (2010) Tissue factor-deficiency and protease activated receptor-1-deficiency reduce inflammation elicited by diet-induced steatohepatitis in mice. *Am J Pathol* **176**:177-186.

Mackman N (2004) Role of tissue factor in hemostasis, thrombosis, and vascular development. *Arterioscler Thromb Vasc Biol* **24**:1015-1022.

Mackman N (2005) Tissue-specific hemostasis in mice. *Arterioscler Thromb Vasc Biol* **25**:2273-2281.

Mackman N (2009) The many faces of tissue factor. *J Thromb Haemost* **7 Suppl 1**:136-139.

Mammen EF (1992) Coagulation abnormalities in liver disease. *Hematol Oncol Clin North Am* **6**:1247-1257.

Mangasser-Stephan K, Gartung C, Lahme B and Gressner AM (2001) Expression of isoforms and splice variants of the latent transforming growth factor beta binding protein (LTBP) in cultured human liver myofibroblasts. *Liver* **21**:105-113.

Mars WM, Zarnegar R and Michalopoulos GK (1993) Activation of hepatocyte growth factor by the plasminogen activators uPA and tPA. *Am J Pathol* **143**:949-958.

Marsh D, Dickinson S, Neill GW, Marshall JF, Hart IR and Thomas GJ (2008) alpha vbeta 6 Integrin promotes the invasion of morphoeic basal cell carcinoma through stromal modulation. *Cancer Res* **68**:3295-3303.

Martinelli A, Knapp S, Anstee Q, Worku M, Tommasi A, Zucoloto S, Goldin R and Thursz M (2008) Effect of a thrombin receptor (protease-activated receptor 1, PAR-1) gene polymorphism in chronic hepatitis C liver fibrosis. *J Gastroenterol Hepatol* **23**:1403-1409.

Maruyama M, Kobayashi N, Westerman KA, Sakaguchi M, Allain JE, Totsugawa T, Okitsu T, Fukazawa T, Weber A, Stolz DB, Leboulch P and Tanaka N (2004) Establishment of a highly differentiated immortalized human cholangiocyte cell line with SV40T and hTERT. *Transplantation* **77**:446-451.

Massaguer A, Perez-Del-Pulgar S, Engel P, Serratosa J, Bosch J and Pizcueta P (2002) Concanavalin-A-induced liver injury is severely impaired in mice deficient in P-selectin. *J Leukoc Biol* **72**:262-270.

Mazzieri R, Masiero L, Zanetta L, Monea S, Onisto M, Garbisa S and Mignatti P (1997) Control of type IV collagenase activity by components of the urokinase-plasmin system: a regulatory mechanism with cell-bound reactants. *EMBO J* **16**:2319-2332.

McCuskey RS (2000) Morphological mechanisms for regulating blood flow through hepatic sinusoids. *Liver* **20**:3-7.

McNeil JJ, Grabsch EA and McDonald MM (1999) Postmarketing surveillance: strengths and limitations. The flucloxacillin-dicloxacillin story. *Med J Aust* **170**:270-273.

Miyazawa Y, Tsutsui H, Mizuhara H, Fujiwara H and Kaneda K (1998) Involvement of intrasinusoidal hemostasis in the development of concanavalin A-induced hepatic injury in mice. *Hepatology* **27**:497-506.

Monea S, Lehti K, Keski-Oja J and Mignatti P (2002) Plasmin activates pro-matrix metalloproteinase-2 with a membrane-type 1 matrix metalloproteinase-dependent mechanism. *J Cell Physiol* **192**:160-170.

Moritoki Y, Ueno Y, Kanno N, Yamagiwa Y, Fukushima K, Gershwin ME and Shimosegawa T (2006) Lack of evidence that bone marrow cells contribute to cholangiocyte repopulation during experimental cholestatic ductal hyperplasia. *Liver Int* **26**:457-466.

Morotti RA, Suchy FJ and Magid MS (2011) Progressive familial intrahepatic cholestasis (PFIC) type 1, 2, and 3: a review of the liver pathology findings. *Semin Liver Dis* **31**:3-10.

Mosesson MW (2003) Fibrinogen gamma chain functions. *J Thromb Haemost* **1**:231-238.

Motulsky H (1995) *Intuitive Biostatistics*. Oxford University Press, New York.

Munger JS, Huang X, Kawakatsu H, Griffiths MJ, Dalton SL, Wu J, Pittet JF, Kaminski N, Garat C, Matthay MA, Rifkin DB and Sheppard D (1999) The integrin alpha v beta 6 binds and activates latent TGF beta 1: a mechanism for regulating pulmonary inflammation and fibrosis. *Cell* **96**:319-328.

Nadler EP, Patterson D, Violette S, Weinreb P, Lewis M, Magid MS and Greco MA (2009) Integrin alphavbeta6 and mediators of extracellular matrix deposition are up-regulated in experimental biliary atresia. *J Surg Res* **154**:21-29.

Navarro VJ and Senior JR (2006) Drug-related hepatotoxicity. *N Engl J Med* **354**:731-739.

Neubauer K, Knittel T, Armbrust T and Ramadori G (1995) Accumulation and cellular localization of fibrinogen/fibrin during short-term and long-term rat liver injury. *Gastroenterology* **108**:1124-1135.

Ngo JC, Jiang L, Lin Z, Yuan C, Chen Z, Zhang X, Yu H, Wang J, Lin L and Huang M (2011) Structural basis for therapeutic intervention of uPA/uPAR system. *Curr Drug Targets* **12**:1729-1743.

Nieswandt B, Bergmeier W, Rackebrandt K, Gessner JE and Zirngibl H (2000) Identification of critical antigen-specific mechanisms in the development of immune thrombocytopenic purpura in mice. *Blood* **96**:2520-2527.

Nieswandt B, Echtenacher B, Wachs FP, Schroder J, Gessner JE, Schmidt RE, Grau GE and Mannel DN (1999) Acute systemic reaction and lung alterations induced by an antiplatelet integrin gpIIb/IIIa antibody in mice. *Blood* **94**:684-693.

Niittynen M, Tuomisto JT, Auriola S, Pohjanvirta R, Syrjala P, Simanainen U, Viluksela M and Tuomisto J (2003) 2,3,7,8-tetrachlorodibenzo-p-dioxin (TCDD)-induced accumulation of biliverdin and hepatic peliosis in rats. *Toxicol Sci* **71**:112-123.

Nishimura SL (2009) Integrin-mediated transforming growth factor-beta activation, a potential therapeutic target in fibrogenic disorders. *Am J Pathol* **175**:1362-1370.

Nocito A, Dahm F, Jochum W, Jang JH, Georgiev P, Bader M, Renner EL and Clavien PA (2007) Serotonin mediates oxidative stress and mitochondrial toxicity in a murine model of nonalcoholic steatohepatitis. *Gastroenterology* **133**:608-618.

O'Reilly MS, Holmgren L, Shing Y, Chen C, Rosenthal RA, Cao Y, Moses M, Lane WS, Sage EH and Folkman J (1994) Angiostatin: a circulating endothelial cell inhibitor that suppresses angiogenesis and tumor growth. *Cold Spring Harb Symp Quant Biol* **59**:471-482.

Ofosu FA (2002) The blood platelet as a model for regulating blood coagulation on cell surfaces and its consequences. *Biochemistry (Mosc)* **67**:47-55.

Ohshima T and Shimotohno K (2003) Transforming growth factor-beta-mediated signaling via the p38 MAP kinase pathway activates Smad-dependent transcription through SUMO-1 modification of Smad4. *J Biol Chem* **278**:50833-50842.

Padda MS, Sanchez M, Akhtar AJ and Boyer JL (2011) Drug-induced cholestasis. *Hepatology* **53**:1377-1387.

Patsenker E, Popov Y, Stickel F, Jonczyk A, Goodman SL and Schuppan D (2008) Inhibition of integrin alphavbeta6 on cholangiocytes blocks transforming growth factor-beta activation and retards biliary fibrosis progression. *Gastroenterology* **135**:660-670.

Pearson JM, Schultze AE, Jean PA and Roth RA (1995) Platelet participation in liver injury from gram-negative bacterial lipopolysaccharide in the rat. *Shock* **4**:178-186.

Pearson JM, Schultze AE, Schwartz KA, Scott MA, Davis JM and Roth RA (1996) The thrombin inhibitor, hirudin, attenuates lipopolysaccharide-induced liver injury in the rat. *J Pharmacol Exp Ther* **278**:378-383.

Perez MJ and Briz O (2009) Bile-acid-induced cell injury and protection. *World J Gastroenterol* **15**:1677-1689.

Phanish MK, Wahab NA, Colville-Nash P, Hendry BM and Dockrell ME (2006) The differential role of Smad2 and Smad3 in the regulation of pro-fibrotic TGFbeta1 responses in human proximal-tubule epithelial cells. *Biochem J* **393**:601-607.

Pihusch R, Rank A, Gohring P, Pihusch M, Hiller E and Beuers U (2002) Platelet function rather than plasmatic coagulation explains hypercoagulable state in cholestatic liver disease. *J Hepatol* **37**:548-555.

Plaa GL and Priestly BG (1976) Intrahepatic cholestasis induced by drugs and chemicals. *Pharmacol Rev* **28**:207-273.

Pohl JF, Melin-Aldana H, Sabla G, Degen JL and Bezerra JA (2001) Plasminogen deficiency leads to impaired lobular reorganization and matrix accumulation after chronic liver injury. *Am J Pathol* **159**:2179-2186.

Popov Y, Patsenker E, Stickel F, Zaks J, Bhaskar KR, Niedobitek G, Kolb A, Friess H and Schuppan D (2008) Integrin alphavbeta6 is a marker of the progression of biliary and portal liver fibrosis and a novel target for antifibrotic therapies. *J Hepatol* **48**:453-464.

Quinton TM, Kim S, Derian CK, Jin J and Kunapuli SP (2004) Plasmin-mediated activation of platelets occurs by cleavage of protease-activated receptor 4. *J Biol Chem* **279**:18434-18439.

Rabes HM (1976) Kinetics of hepatocellular proliferation after partial resection of the liver. *Prog Liver Dis* **5**:83-99.

Rake MO, Flute PT, Pannell G, Shilkin KB and Williams R (1973) Experimental hepatic necrosis: studies on coagulation abnormalities, plasma clearance, and organ distribution of 125I-labelled fibrinogen. *Gut* **14**:574-580.

Raucy JL, Kraner JC and Lasker JM (1993) Bioactivation of halogenated hydrocarbons by cytochrome P4502E1. *Crit Rev Toxicol* **23**:1-20.

Recknagel RO (1967) Carbon tetrachloride hepatotoxicity. *Pharmacol Rev* **19**:145-208.

Reilly TP, Bourdi M, Brady JN, Pise-Masison CA, Radonovich MF, George JW and Pohl LR (2001) Expression profiling of acetaminophen liver toxicity in mice using microarray technology. *Biochem Biophys Res Commun* **282**:321-328.

Reinehr R, Graf D and Haussinger D (2003) Bile salt-induced hepatocyte apoptosis involves epidermal growth factor receptor-dependent CD95 tyrosine phosphorylation. *Gastroenterology* **125**:839-853.

Romagnuolo J, Sadowski DC, Lalor E, Jewell L and Thomson AB (1998) Cholestatic hepatocellular injury with azathioprine: a case report and review of the mechanisms of hepatotoxicity. *Can J Gastroenterol* **12**:479-483.

Rondeau E, Vigneau C and Berrou J (2001) Role of thrombin receptors in the kidney: lessons from PAR1 knock-out mice. *Nephrol Dial Transplant* **16**:1529-1531.

Roth RA and Dahm LJ (1997) Neutrophil- and glutathione-mediated hepatotoxicity of alpha-naphthylisothiocyanate. *Drug Metab Rev* **29**:153-165.

Rothmeier AS and Ruf W (2012) Protease-activated receptor 2 signaling in inflammation. *Semin Immunopathol* **34**:133-149.

Rullier A, Gillibert-Duplantier J, Costet P, Cubel G, Haurie V, Petibois C, Taras D, Dugot-Senant N, Deleris G, Bioulac-Sage P and Rosenbaum J (2008) Protease-activated receptor 1 knockout reduces experimentally induced liver fibrosis. *Am J Physiol Gastrointest Liver Physiol* **294**:G226-235.

Rullier A, Senant N, Kisiel W, Bioulac-Sage P, Balabaud C, Le Bail B and Rosenbaum J (2006) Expression of protease-activated receptors and tissue factor in human liver. *Virchows Arch* **448**:46-51.

Russmann S, Zimmermann A, Krahenbuhl S, Kern B and Reichen J (2001) Veno-occlusive disease, nodular regenerative hyperplasia and hepatocellular carcinoma after azathioprine treatment in a patient with ulcerative colitis. *Eur J Gastroenterol Hepatol* **13**:287-290.

Sambrano GR, Huang W, Faruqi T, Mahrus S, Craik C and Coughlin SR (2000) Cathepsin G activates protease-activated receptor-4 in human platelets. *J Biol Chem* **275**:6819-6823.

Sambrano GR, Weiss EJ, Zheng YW, Huang W and Coughlin SR (2001) Role of thrombin signalling in platelets in haemostasis and thrombosis. *Nature* **413**:74-78.

Samyn M, Hadzic N, Davenport M, Verma A, Karani J, Portmann B and Mieli-Vergani G (2004) Peliosis hepatis in childhood: case report and review of the literature. *J Pediatr Gastroenterol Nutr* **39**:431-434.

Santa Cruz V, Liu H, Kaphalia L and Kanz MF (2007) Effects of methylenedianiline on tight junction permeability of biliary epithelial cells in vivo and in vitro. *Toxicol Lett* **169**:13-25.

Schaller J and Gerber SS (2011) The plasmin-antiplasmin system: structural and functional aspects. *Cell Mol Life Sci* **68**:785-801.

Schnabl B, Kweon YO, Frederick JP, Wang XF, Rippe RA and Brenner DA (2001) The role of Smad3 in mediating mouse hepatic stellate cell activation. *Hepatology* **34**:89-100.

Schwertz H, Tolley ND, Foulks JM, Denis MM, Risenmay BW, Buerke M, Tilley RE, Rondina MT, Harris EM, Kraiss LW, Mackman N, Zimmerman GA and Weyrich AS (2006) Signal-dependent splicing of tissue factor pre-mRNA modulates the thrombogenicity of human platelets. *J Exp Med* **203**:2433-2440.

Scott GB and Howell RM (1964) Acute Hepatic Necrosis and Blood Coagulation. An in Vivo Approach. *Br J Exp Pathol* **45**:95-101.

Sedlaczek N, Jia JD, Bauer M, Herbst H, Ruehl M, Hahn EG and Schuppan D (2001) Proliferating bile duct epithelial cells are a major source of connective tissue growth factor in rat biliary fibrosis. *Am J Pathol* **158**:1239-1244.

Segal H, Cottam S, Potter D and Hunt BJ (1997) Coagulation and fibrinolysis in primary biliary cirrhosis compared with other liver disease and during orthotopic liver transplantation. *Hepatology* **25**:683-688.

Seki E, de Minicis S, Inokuchi S, Taura K, Miyai K, van Rooijen N, Schwabe RF and Brenner DA (2009) CCR2 promotes hepatic fibrosis in mice. *Hepatology* **50**:185-197.

Selvamurugan N, Kwok S and Partridge NC (2004) Smad3 interacts with JunB and Cbfa1/Runx2 for transforming growth factor-beta1-stimulated collagenase-3 expression in human breast cancer cells. *J Biol Chem* **279**:27764-27773.

Shackel NA, McGuinness PH, Abbott CA, Gorrell MD and McCaughan GW (2001) Identification of novel molecules and pathogenic pathways in primary biliary cirrhosis: cDNA array analysis of intrahepatic differential gene expression. *Gut* **49**:565-576.

Shanmukhappa K, Sabla GE, Degen JL and Bezerra JA (2006) Urokinase-type plasminogen activator supports liver repair independent of its cellular receptor. *BMC Gastroenterol* **6**:40.

Shanware NP, Williams LM, Bowler MJ and Tibbetts RS (2009) Non-specific in vivo inhibition of CK1 by the pyridinyl imidazole p38 inhibitors SB 203580 and SB 202190. *BMB Rep* **42**:142-147.

Shaulian E and Karin M (2001) AP-1 in cell proliferation and survival. *Oncogene* **20**:2390-2400.

Shimizu M, Hara A, Okuno M, Matsuno H, Okada K, Ueshima S, Matsuo O, Niwa M, Akita K, Yamada Y, Yoshimi N, Uematsu T, Kojima S, Friedman SL, Moriwaki H and Mori H (2001) Mechanism of retarded liver regeneration in plasminogen activator-deficient mice: impaired activation of hepatocyte growth factor after Fas-mediated massive hepatic apoptosis. *Hepatology* **33**:569-576.

Shimizu S, Gabazza EC, Hayashi T, Ido M, Adachi Y and Suzuki K (2000) Thrombin stimulates the expression of PDGF in lung epithelial cells. *Am J Physiol Lung Cell Mol Physiol* **279**:L503-510.

Skokan JD, Hewlett JS and Hoffman GC (1973) Thrombocytopenic purpura associated with ingestion of acetaminophen (Tylenol). *Cleve Clin Q* **40**:89-91.

Slofstra SH, Bijlsma MF, Groot AP, Reitsma PH, Lindhout T, ten Cate H and Spek CA (2007) Protease-activated receptor-4 inhibition protects from multiorgan failure in a murine model of systemic inflammation. *Blood* **110**:3176-3182.

Soff GA (2012) A new generation of oral direct anticoagulants. *Arterioscler Thromb Vasc Biol* **32**:569-574.

Stang-Voss C and Appell HJ (1981) Structural alterations of liver parenchyma induced by anabolic steroids. *Int J Sports Med* **2**:101-105.

Stephenne X, Vosters O, Najimi M, Beuneu C, Dung KN, Wijns W, Goldman M and Sokal EM (2007) Tissue factor-dependent procoagulant activity of isolated human hepatocytes: relevance to liver cell transplantation. *Liver Transpl* **13**:599-606.

Suh TT, Holmback K, Jensen NJ, Daugherty CC, Small K, Simon DI, Potter S and Degen JL (1995) Resolution of spontaneous bleeding events but failure of pregnancy in fibrinogen-deficient mice. *Genes Dev* **9**:2020-2033.

Sullivan BP, Wang R, Tawfik O and Luyendyk JP (2010a) Protective and damaging effects of platelets in acute cholestatic liver injury revealed by depletion and inhibition strategies. *Toxicol Sci* **115**:286-294.

Sullivan BP, Weinreb PH, Violette SM and Luyendyk JP (2010b) The coagulation system contributes to alphaVbeta6 integrin expression and liver fibrosis induced by cholestasis. *The American Journal of Pathology* **177**:2837-2849.

Takano A, Hirata A, Inomata Y, Kawaji T, Nakagawa K, Nagata S and Tanihara H (2005) Intravitreal plasmin injection activates endogenous matrix metalloproteinase-2 in rabbit and human vitreous. *Am J Ophthalmol* **140**:654-660.

Tjandra K, Sharkey KA and Swain MG (2000) Progressive development of a Th1-type hepatic cytokine profile in rats with experimental cholangitis. *Hepatology* **31**:280-290.

Trejo J, Connolly AJ and Coughlin SR (1996) The cloned thrombin receptor is necessary and sufficient for activation of mitogen-activated protein kinase and mitogenesis in mouse lung fibroblasts. Loss of responses in fibroblasts from receptor knockout mice. *J Biol Chem* **271**:21536-21541.

Tsirigotis P, Sella T, Shapira MY, Bitan M, Bloom A, Kiselgoff D, Levin M, Libster D, Abdul Hai A, Gesundheit B, Or R, Slavin S and Resnick I (2007) Peliosis hepatis following treatment with androgen-steroids in patients with bone marrow failure syndromes. *Haematologica* **92**:e106-110.

Tsokos M and Erbersdobler A (2005) Pathology of peliosis. *Forensic Sci Int* **149**:25-33.

Tzirogiannis KN, Papadimas GK, Kondyli VG, Kourentzi KT, Demonakou MD, Kyriakou LG, Mykoniatis MG, Hereti RI and Panoutsopoulos GI (2006) Peliosis hepatis: microscopic and macroscopic type, time pattern, and correlation with liver cell apoptosis in a model of toxic liver injury. *Dig Dis Sci* **51**:1998-2006.

Uzonyi B, Lotzer K, Jahn S, Kramer C, Hildner M, Bretschneider E, Radke D, Beer M, Vollandt R, Evans JF, Funk CD and Habenicht AJ (2006) Cysteinyl leukotriene 2 receptor and protease-activated receptor 1 activate strongly correlated early genes in human endothelial cells. *Proc Natl Acad Sci U S A* **103**:6326-6331.

Van Aarsen LA, Leone DR, Ho S, Dolinski BM, McCoon PE, LePage DJ, Kelly R, Heaney G, Rayhorn P, Reid C, Simon KJ, Horan GS, Tao N, Gardner HA, Skelly MM, Gown AM, Thomas GJ, Weinreb PH, Fawell SE and Violette SM (2008) Antibody-mediated blockade of integrin alpha v beta 6 inhibits tumor progression in vivo by a transforming growth factor-beta-regulated mechanism. *Cancer Res* **68**:561-570.

Verrecchia F, Vindevoghel L, Lechleider RJ, Uitto J, Roberts AB and Mauviel A (2001) Smad3/AP-1 interactions control transcriptional responses to TGF-beta in a promoter-specific manner. *Oncogene* **20**:3332-3340.

Verstraete M (2000) Third-generation thrombolytic drugs. *Am J Med* **109**:52-58.

von Montfort C, Beier JI, Kaiser JP, Guo L, Joshi-Barve S, Pritchard MT, States JC and Arteel GE (2010) PAI-1 plays a protective role in CCl4-induced hepatic fibrosis in mice: role of hepatocyte division. *Am J Physiol Gastrointest Liver Physiol* **298**:G657-666.

Wagner M, Zollner G and Trauner M (2010) Nuclear receptor regulation of the adaptive response of bile acid transporters in cholestasis. *Semin Liver Dis* **30**:160-177.

Wang B, Dolinski BM, Kikuchi N, Leone DR, Peters MG, Weinreb PH, Violette SM and Bissell DM (2007a) Role of alphavbeta6 integrin in acute biliary fibrosis. *Hepatology* **46**:1404-1412.

Wang H, Zhang Y and Heuckeroth RO (2007b) PAI-1 deficiency reduces liver fibrosis after bile duct ligation in mice through activation of tPA. *FEBS Lett* **581**:3098-3104.

Wang H, Zhang Y and Heuckeroth RO (2007c) Tissue-type plasminogen activator deficiency exacerbates cholestatic liver injury in mice. *Hepatology* **45**:1527-1537.

Weinreb PH, Simon KJ, Rayhorn P, Yang WJ, Leone DR, Dolinski BM, Pearse BR, Yokota Y, Kawakatsu H, Atakilit A, Sheppard D and Violette SM (2004) Function-blocking integrin

alphavbeta6 monoclonal antibodies: distinct ligand-mimetic and nonligand-mimetic classes. *J Biol Chem* **279**:17875-17887.

Williams AM, Langley PG, Osei-Hwediah J, Wendon JA and Hughes RD (2003) Hyaluronic acid and endothelial damage due to paracetamol-induced hepatotoxicity. *Liver Int* **23**:110-115.

Williams CD, Antoine DJ, Shaw PJ, Benson C, Farhood A, Williams DP, Kanneganti TD, Park BK and Jaeschke H (2011) Role of the Nalp3 inflammasome in acetaminophen-induced sterile inflammation and liver injury. *Toxicol Appl Pharmacol* **252**:289-297.

Williams MJ, Du X, Loftus JC and Ginsberg MH (1995) Platelet adhesion receptors. *Semin Cell Biol* **6**:305-314.

Xu J, Lee G, Wang H, Vierling JM and Maher JJ (2004) Limited role for CXC chemokines in the pathogenesis of alpha-naphthylisothiocyanate-induced liver injury. *Am J Physiol Gastrointest Liver Physiol* **287**:G734-741.

Yadav SS, Howell DN, Steeber DA, Harland RC, Tedder TF and Clavien PA (1999) P-Selectin mediates reperfusion injury through neutrophil and platelet sequestration in the warm ischemic mouse liver. *Hepatology* **29**:1494-1502.

Yamamura Y, Hua X, Bergelson S and Lodish HF (2000) Critical role of Smads and AP-1 complex in transforming growth factor-beta -dependent apoptosis. *J Biol Chem* **275**:36295-36302.

Yamashita K, Matsuoka H, Ochiai T, Matsushita R, Kubuki Y, Suzuki M and Tsubouchi H (2000) Hepatocyte growth factor/scatter factor enhances the thrombopoietin mRNA expression in rat hepatocytes and cirrhotic rat livers. *J Gastroenterol Hepatol* **15**:83-90.

Yan HM, Ramachandran A, Bajt ML, Lemasters JJ and Jaeschke H (2010) The oxygen tension modulates acetaminophen-induced mitochondrial oxidant stress and cell injury in cultured hepatocytes. *Toxicol Sci* **117**:515-523.

Yee SB, Hanumegowda UM, Copple BL, Shibuya M, Ganey PE and Roth RA (2003) Endothelial cell injury and coagulation system activation during synergistic hepatotoxicity from monocrotaline and bacterial lipopolysaccharide coexposure. *Toxicol Sci* **74**:203-214.

Yoshidome H, Miyazaki M, Shimizu H, Ito H, Nakagawa K, Ambiru S, Nakajima N, Edwards MJ and Lentsch AB (2000) Obstructive jaundice impairs hepatic sinusoidal endothelial cell function and renders liver susceptible to hepatic ischemia/reperfusion. *J Hepatol* **33**:59-67.

Zarbock A, Polanowska-Grabowska RK and Ley K (2007) Platelet-neutrophil-interactions: linking hemostasis and inflammation. *Blood Rev* **21**:99-111.

Zareh M, Davis A and Henderson S (2011) Reversal of warfarin-induced hemorrhage in the emergency department. *West J Emerg Med* **12**:386-392.

Zhang Y, Feng X, We R and Derynck R (1996) Receptor-associated Mad homologues synergize as effectors of the TGF-beta response. *Nature* **383**:168-172.

Zhao J, Shi W, Wang YL, Chen H, Bringas P, Jr., Datto MB, Frederick JP, Wang XF and Warburton D (2002) Smad3 deficiency attenuates bleomycin-induced pulmonary fibrosis in mice. *Am J Physiol Lung Cell Mol Physiol* **282**:L585-593.

Zheng DM, Kitamura T, Ikejima K, Enomoto N, Yamashina S, Suzuki S, Takei Y and Sato N (2006) Sphingosine 1-phosphate protects rat liver sinusoidal endothelial cells from ethanol-induced apoptosis: Role of intracellular calcium and nitric oxide. *Hepatology* **44**:1278-1287.